# *Food biomolecule engineering by unconventional technological strategies*

A Ph.D. dissertation presented by

*Agnese Panozzo*

to the

University of Udine

for the degree of Ph.D. in Food Science

(Cycle XXVI)

Department of Food Science

UNIVERSITY OF UDINE

Italy

March 2014

| | |
|---|---|
| **Supervisor:** | Lara Manzocco, PhD<br>Department of Food Science<br>University of Udine, Italy |
| **Coordinator:** | Mara Lucia Stecchini, Professor<br>Department of Food Science<br>University of Udine, Italy |
| **Reviewers:** | Marc Hendrickx, Professor<br>Laboratory of Food Technology and Leuven Science and Nutrition Research Centre (LFoRCE)<br>Katholieke Universiteit Leuven, Belgium |
| | Carla Severini, Professor<br>Department of Food Science<br>University of Foggia, Italy |

## *Ringraziamenti*

Questa tesi è il risultato del percorso professionale e personale intrapreso tre anni fa. Durante questi anni ho avuto la fortuna di collaborare con molte persone senza le quali questo lavoro di dottorato e questa esperienza non sarebbero stati possibili.

Un ringraziamento particolare va alla Dott.ssa Lara Manzocco che mi ha guidato, seguito, scoraggiato e incoraggiato nel corso di questo lavoro di dottorato nel suo fondamentale ruolo di *supervisor*. Grazie per aver discusso i risultati *con* me e non *per* me, per il tempo speso a scrivere insieme nonostante io rendessi il procedere della scrittura estremamente lento, per aver sempre ascoltato e considerato la mia opinione anche quando era molto lontana dalla sua, per i "pensieri notturni" e le metafore che non sempre ho capito. Potrei andare avanti ancora molto, ma il punto è che ho imparato tantissimo. Grazie!

Probabilmente non avrei intrapreso questo percorso se non avessi avuto il suo appoggio, pertanto desidero ringraziare la Prof.ssa Maria Cristina Nicoli per aver creduto nelle mie capacità e avermi offerto l'opportunità di far parte del suo gruppo.

Vorrei quindi ringraziare la Prof.ssa Monica Anese e la Dott.ssa Sonia Calligaris, per i loro consigli e suggerimenti e per aver condiviso con me parte del loro e del mio lavoro.

I would also like to thank Prof. Marc Hendrickx and Prof. Ann Van Loey for giving me the opportunity to join their group during my visiting period at the Laboratory of Food Technology of the Katholieke Universiteit Leuven (Belgium). I really appreciate their guidance and interesting suggestions.

Special thanks also goes to Dr. Lien Lemmens who supervised my experimental work in Leuven. It was very nice and stimulating working with her.

Ringrazio inoltre la Prof.ssa Giovanna Lippe per il suo contributo scientifico nello svolgimento e interpretazione dei risultati dell'analisi di elettroforesi (SDS-PAGE). Ringrazio anche la Dott.ssa Astrid Fabbro per il suo supporto tecnico durante le analisi.

Un doveroso ringraziamento va alla Dott.ssa Marina Munari per il suo fondamentale aiuto e supporto in laboratorio.

Vorrei inoltre ringraziare gli studenti che ho seguito nell'ambito (e non) del dottorato: Alvise, Krystel, Selena, Francesca, Anita, Anna, Elisa, Francine. Ho imparato qualcosa da ognuno di loro e spero che possano dire lo stesso di me.

Finally, I would very much like to thank all my colleagues: Martina, Eva, Annalisa, Jean Carlo, Carlo, Laura, Paolo, Alexandra, Elena, Maria Luisa, Giorgio, Alberto, Paola, Zahra, Tina. Thank you for sharing time, coffees, cigarettes, work, problems, ideas, and successes with me, and for listening whenever needed.

Grazie a tutti!

Agnese

## *Table of contents*

# List of notations

## *List of abbreviations*

| | |
|---|---|
| 2-ME | *β*-mercaptoethanol |
| Abs | Absorbance |
| BAc | Bioaccessibility |
| BHT | Butylated hydroxytoluene |
| DAD | Diode array detection |
| Dopa | Dopamine (or 3,4-dihydroxyphenethylamine) |
| DTNB | 5'5'-Dithiobis(2-nitrobenzoic acid) |
| EDTA | Ethylenediaminetetraacetic acid |
| FA | Foam ability |
| FS | Foam stability |
| HMW | High molecular weight |
| HPH | High pressure homogenisation |
| HPLC | High-performance liquid chromatography |
| LMW | Low molecular weight |
| MW | Molecular weight |
| OD | Optical density |
| PL | Pulsed light |
| PPO | Polyphenoloxidase |
| PSD | Particle size distribution |
| SD | Standard deviation |
| SDS | Sodium dodecyl sulphate |
| SDS-PAGE | Sodium dodecyl sulphate polyacrylamide gel electrophoresis |
| SH | Sulfhydryl |
| UV | Ultraviolet light |
| UV-C | Short-length ultraviolet light |

## *List of symbols*

| | |
|---|---|
| $F_{50}$ | Fluence required to reduce the enzyme activity by 50% (photostability) |
| $C_0$ | Carotenoid content in tomato pulps |
| $C_m$ | Carotenoid content in the micelles |
| $C_d$ | Carotenoid content in the digest |
| ø | Diameter of suspended particles or bubbles in foams |

# Preface

In the past consumer demand was focused on microbiologically safe and stable food products. Nowadays consumers are also looking for higher quality products with enhanced fresh-like characteristics, fewer additives, improved sensory and nutritional quality. In other words, consumers seek foods that contribute to their health and wellness. Nevertheless, product convenience, affordability, and ethical production are more and more gaining importance. In this context, due to the reversing of the food chain, today it is the consumers who tell the producers what they want to eat (*from fork to farm*). The recent development of unconventional non-thermal technologies, such as high pressure, pulsed electric fields, ultrasounds, cold plasma, dense phase carbon dioxide, and ultraviolet light processing, addresses these new consumer needs towards safe, high quality, and fresh-like foods. As food structure and functions are the result of the status of food constituents, the structural modification of food constituents can lead to new product characteristics or improved functionalities. To this regard, different driving forces, such as mechanical or electromagnetic energy, were shown to effectively affect the structure of food proteins or polysaccharides. Taking advantage of specific potentials and opportunities of these unconventional technologies by focusing on the complex process-structure-function relationship, offers the exiting possibility for the development of fresh-like, healthy, tailor made foods. It is evident that this goal can only be reached by clearly understand the effects of the process on biomolecule structure and thus functions.

In this context, this PhD thesis aimed to investigate whether and how unconventional technologies, such as light processing and high pressure homogenisation, can be exploited to modify biomolecule structure inducing changes in their own functions as well as in the functions of other bioactives present in the matrix (Fig. A). To this aim, the thesis was divided in two parts. In the first part, the effect of UV-C and pulsed light on the structure and functions of selected proteins, including polyphenoloxidase, gluten, and egg white was investigated. In the second part, the effect of high pressure homogenisation on egg white proteins structure and functions as well as on microstructure and carotenoid bioaccessibility (BAc) of tomato pulps was studied.

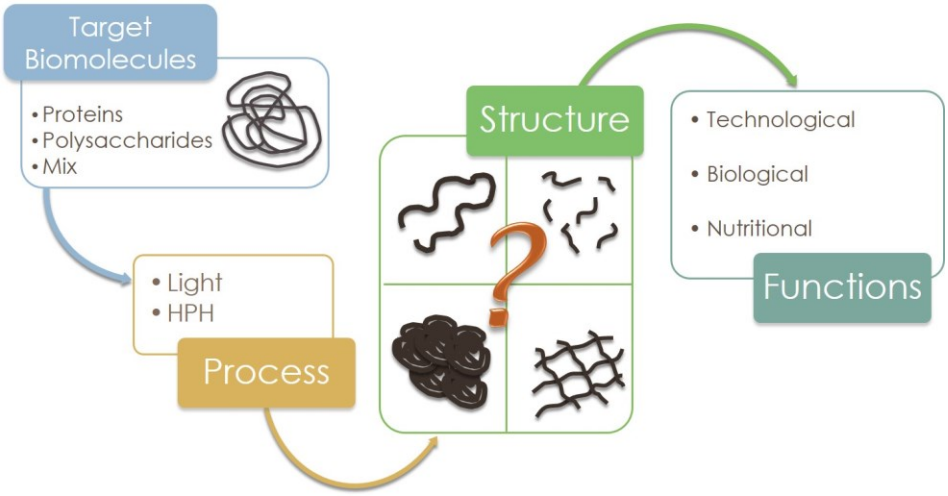


**Figure A** Overall research strategy of this PhD thesis.

# *Chapter 1 Introduction*

## 1.1 UV-C and pulsed light processing

Ultraviolet (UV) light processing indicates the use of the electromagnetic radiation that occupies the non-ionizing region of the spectrum between 200 nm (X-rays) and 400 nm (visible light). The UV spectrum can be further divided into three regions: short-length UV light (UV-C) from 200 to 280 nm, medium-length UV light (UV-B) from 280 to 320 nm, and full-length UV light (UV-A) from 320 to 400 nm (Bintsis, Litopoulou-Tzanetaki, & Robinson, 2000; Falguera, Pagán, Garza, Garvín, & Ibarz, 2011). UV radiation, in particular short-length UV light (UV-C), is nowadays recognised as an efficient technology to non-thermally inactivate a wide range of microorganisms, easy to use and characterized by favourable costs of equipment, energy and maintenance (Barbosa-Canovas, Pothakamury, Palou, & Swanson, 1998; Bintsis et al., 2000; Falguera et al., 2011). Practical UV disinfection systems are based on the exploitation of UV radiation under both continuous and pulsed conditions. In both the cases, the intensity of UV radiation is expressed as irradiance or intensity flux (W $m^{-2}$), while the dose, which is a function of the intensity and time of exposure, is expressed as radiant exposure or fluence (J $m^{-2}$) (Bintsis et al., 2000). Continuous UV-C processing exploits mercury lamps as the source of germicidal radiation. Mercury lamps are considered to provide almost monochromatic radiation at 254 nm, which is absorbed by microbial cell DNA, causing thymine dimers in the same DNA strand (photochemical effect). The resulting effect is that the DNA transcription and replication are blocked, compromising cellular functions and eventually leading to cell death (Bolton & Linden, 2003; Koutchma, 2009). On the other hand, pulsed light (PL) treatment is based on the repetition of consecutive short, high power light pulses. The latter are emitted by flash xenon lamps. Contrary to mercury lamps, xenon lamps emit radiation with a broad spectrum similar to that of the sun (170-2600 nm), including UV, visible and infrared light (Falguera et al., 2011). Similarly to continuous UV-C light, the germicidal effect of PL is primarily mediated by its UV component, thus consisting in the above-mentioned photochemical effect (Wang, Macgregor, Anderson, & Woolsey, 2005). Furthermore, after very intense PL treatments localized heating of bacteria can occur, which leads to cell death (photothermal effect) (Fine & Gervais, 2004; Wekhof, 2000). Finally, because of constant disturbance caused by the high-energy pulses, structural damages to bacterial cell may also be observed (photophysical effect) (Krishnamurthy, Tewari, Irudayaraj, & Demirci, 2008;

Takeshita et al., 2003). Due to its high peak power, PL may provide some practical advantages over continuous UV-C in those situations where rapid disinfection is required. In fact, the intense pulses of light, which typically last a few hundred microseconds, can result in the application of lethal UV dose levels that would require continuous UV sources to operate over a much longer time period. The latter can account for an increase in temperature that leads to degradation of the food components (Elmnasser et al., 2007; Krishnamurthy, Demirci, & Irudayaraj, 2004).

Both continuous and pulsed ultraviolet light is successfully used for sterilisation of packaging materials, working surfaces, utensils, air and drinkable water (Bintsis et al., 2000; Koutchma, Keller, Chirtel, & Parisi, 2004; Wright, Sumner, Hackney, Pierson, & Zoecklein, 2000). Moreover, it has been proposed to decontaminate the surface of shell eggs, fresh-cut vegetables and ready-to-eat meat products, as well as for killing microorganisms in liquids, such as milk, fruit juices and infant food (Caminiti et al., 2011; Choi, Cheigh, Jeong, Shin, & Chung, 2010; Hierro et al., 2011; Hierro, Manzano, Ordóñez, de la Hoz, & Fernández, 2009; Marquenie, Michiels, Van Impe, Schrevens, & Nicolaï, 2003; Pataro et al., 2011; Ramos-Villarroel, Martín-Belloso, & Soliva-Fortuny, 2011).

Ultraviolet light processing can be a viable non-thermal alternative in liquid and solid foods for eliminating or reducing the levels of most types of undesirable microorganisms. However, little is known about the interaction of UV light with food components, both in model systems and in a complex food matrix (Koutchma, 2009).

## 2.1 High pressure homogenisation

High pressure homogenisation (HPH) is obtained by forcing a fluid through a very small orifice, the valve gap of few micrometres in width, by means of a positive displacement pump. During this process the fluid undergoes several physical phenomena successively and/or simultaneously involved before, through, and at the outlet of the high pressure valve gap. In particular, the initial pressure build-up and drop generates intense mechanical forces and elongational stress in laminar flow at the valve entrance and in the valve gap, followed by turbulence, cavitation and impacts with solid surfaces at the gap outlet. The fluid travelling through the high pressure valve gap is accompanied by short-life heating phenomena (Floury, Bellettre, Legrand, & Desrumaux, 2004; Floury, Legrand, & Desrumaux, 2004; Middelberg, 1995; Paquin, 1999). The increase in temperature of the fluid must be measured and controlled by efficient cooling systems to avoid over-processing of heat-sensitive biomolecules (Cortés-Muñoz, Chevalier-Lucia,

& Dumay, 2009; Picart et al., 2006; Thiebaud, Dumay, Picart, Guiraud, & Cheftel, 2003).

The mechanical stresses, that take place during HPH, can be exploited to disrupt microorganism cells, thus leading to microbial decontamination of the food product (Middelberg, 1995). Despite several hypotheses (Diels, De Taeye, & Michiels, 2005; Diels & Michiels, 2006), the exact mechanism of how HPH inactivates microorganisms has not yet been fully elucidated. High pressure and velocity gradients, shear stresses, turbulence, shocks and cavitation phenomena occurring through the high pressure valve could induce mechanical disruption and/or at least alteration of cell membranes (Gogate & Pandit, 2008; Kleinig & Middelberg, 1998; Middelberg, 1995). The efficiency of HPH for microbial inactivation depends on different parameters, such as pressure level, extent of recycling through the homogeniser, physiological properties of the microorganism, as well as characteristic of the food matrix (Diels, Callewaert, Wuytack, Masschalck, & Michiels, 2005; Donsì, Ferrari, Lenza, & Maresca, 2009; Maresca, Donsì, & Ferrari, 2011; Pedras & Pinho, 2012; Picart et al., 2006; Thiebaud et al., 2003). Several studies showed HPH to be a continuous process that offers the advantage of notably reducing the microbial load at a level equivalent at least to pasteurisation in different foods, such as milk and dairy products, and fruit juices (Calligaris, Foschia, Bartolomeoli, Maifreni, & Manzocco, 2012; Cruz et al., 2007; Maresca et al., 2011; Pereda, Ferragut, Quevedo, Guamis, & Trujillo, 2007; Poliseli-Scopel, Hernández-Herrero, Guamis, & Ferragut, 2012; Suárez-Jacobo et al., 2012). In addition to microbial inactivation, HPH is widely used in the food, biotechnology, cosmetic and pharmaceutical areas to fragment particles in dispersions or emulsions, to produce fine and stable emulsions, to modify the viscous properties of fluids due to the particle size reduction, to facilitate metabolite extraction (Dumay et al., 2013; Floury, Bellettre, et al., 2004; Floury, Legrand, et al., 2004). Despite the potential of sanitisation of food, use of HPH in food industry is limited by the high cost of the equipment, the availability of cheaper alternative technologies, such as high-temperature short-time processing, and the lack of predictive tools for microbial inactivation (Diels & Michiels, 2006; Donsì, Annunziata, & Ferrari, 2013). However, HPH has the great advantage that this technology can be also used for obtaining food systems having different rheological and microstructural properties than those obtained from row materials (Vannini, Lanciotti, Baldi, & Guerzoni, 2004). Therefore, HPH represent a promising technology for obtaining safe and tailor-made foods.

## 3.1 Biomolecule engineering by unconventional processes

The development of emerging technologies in food processing addresses new consumer needs toward safe, healthy, convenient, and minimally processed foods, as well as environmental friendly and sustainable food manufacturing techniques with low energy requirements and reduced water use (Aguilera & Lillford, 2008; Toepfl, Mathys, Heinz, & Knorr, 2006). Hitherto, the main purpose of unconventional processing has been to obtain safe foods without the detrimental effects of thermal treatments. However, any processes used to eliminate pathogenic and/or food spoilage microorganisms will inevitably affect the structure of the food product (Heldman, Lund, & Husain, 2008).

Food matrix is composed of different components, such as protein and polysaccharides. As the structure and functions of food biomolecules are closely interlinked, structural changes of food constituents can lead to new product characteristics or improved functionalities (Aguilera, 2005, 2006; Fischer & Windhab, 2011; Norton, Moore, & Fryer, 2007). Taking advantage of specific potentials and opportunities of non thermal unconventional processes, including the understanding and control of the complex process-structure-function relationships, offers the possibility for the development of foods with unique properties (tailor-made foods) (Hermansson, 2002; Knorr et al., 2011). To this regard, both UV processing and HPH may provide, besides microbial inactivation, additional advantages. In fact, the same driving forces that induce microbial inactivation, can affect food biomolecules, inducing changes in their structure and functions.

In the case of the UV processing, the energy of the UV radiation is captured by the chromophore, and transferred throughout the molecule as chemical energy. The latter induces changes in the conformation, size and architecture of the polymer, leading to modifications in its properties (Davies & Truscott, 2001; Wondraczek, Kotiaho, Fardim, & Heinze, 2011). Proteins are major targets for photoreactions due to the abundance of endogenous chromophores within their structure. Both amino acid side-chains (e.g., thriptophan, tyrosine, phenylalanine, cysteine) and bound prosthetic groups (e.g., flavins, heme) may act as efficient chromophores. Proteins have the additional ability to bind exogenous chromophores, and rapidly react with other excited state species. The result is the development of side-chain oxidation, backbone fragmentation, and/or formation of cross-links and aggregates (Davies & Truscott, 2001; Davies, 2003; Pattison, Rahmanto, & Davies, 2012). Ultraviolet treatments were reported to increase tensile strength of gluten, zein, and albumin films (Rhim, Gennadios, Fu, Weller,

& Hanna, 1999). Photocrosslinking of egg white protein and sodium caseinate was associated to improved emulsifying and foaming properties (Kuan, Bhat, & Karim, 2011).

Similarly to UV processing, also pulsed light treatments were demonstrated to cause milk protein aggregation by disulphide bonds without further significant changes in protein components (Elmnasser et al., 2008). Fernández et al. (2012) showed that pulsed light induced conformational changes in β-lactoglobulin, enhancing its absorption rate at the air/water interface. In addition, β-lactoglobulin solutions treated with pulsed light formed highly elastic interfaces, resulting in more stable foams. As regards protein biologic activity, ultraviolet and pulsed light processing was demonstrated to reduce the catalytic activity of different enzymes and the immunoreactivity of allergenic proteins (Chung, Yang, & Krishnamurthy, 2008; Dunn, Clark, & Asmus, 1989; Guerrero-Beltrán & Barbosa-Cánovas, 2006; Manzocco, Dri, & Quarta, 2009; Manzocco & Nicoli, 2012; Manzocco, Quarta, & Dri, 2009; Shriver & Yang, 2011; Yang et al., 2010)

On the other hand, intense mechanical stresses induced by HPH have been shown to affect the structure of food proteins and polysaccharides, resulting in changes in their functional properties. Recently, Patrignani et al. (2013) showed that inactivation of *Salmonella enterica* in liquid whole egg by HPH at 100 MPa for up to 5 passes was accompanied by minor impact on product viscosity as well as an increase in foam capacity and stability. These modifications in the technological performances of liquid whole egg were attributed to unfolding and increased exposure of hydrophobic regions of egg proteins as a consequence of HPH treatment. At similar pressure levels, the typical egg lipoprotein matrix was maintained and no proteolysis was detected in high pressure homogenised whole egg (Marco-Molés & Hernando, 2009). Denaturation and/or aggregation of globular proteins, such as whey proteins, can be induced by HPH processing depending on the intensity of mechanical forces and/or the temperature of the sample. For instance, HPH treatment up to 140 MPa did not produce changes in the secondary structure of β-lactoglobulin but promoted slight interactions among particles (Subirade, Loupil, Allain, & Paquin, 1998). When whey proteins were treated, dissociation of large aggregates was observed resulting in an increase of surface hydrophobicity (Bouaouina, Desrumaux, Loisel, & Legrand, 2006). Upon homogenisation at higher pressures (>250 MPa), whey protein aggregation was also observed (Grácia-Juliá, René, & Cortés-Muñoz, 2008). Similarly, soybean 11S globulins were reported to denature upon HPH leading to the formation of a gel-like architecture (Floury, Desrumaux, & Legrand, 2002). HPH (200-600 MPa) also induced an initial increase and subsequent decrease in free SH content of soy

protein isolate. These structural modifications led to changes in emulsifying and gelling properties of soy protein isolates (Wang et al., 2008). With regard to protein biologic activity, changes in enzymatic activity of several enzymes were observed as a consequence of HPH induced protein conformational changes. In particular, inactivation of pectate lyase in banana juice, and polyphenoloxidase and pectin methyl esterase in apple juice was observed upon HPH at pressure higher than 200 MPa (Calligaris, et al., 2012; Suárez-Jacobo et al., 2012). By contrast, HPH up to 130 MPa was found to enhance the antimicrobial activity of lysozyme and lactoperoxidase (Vannini et al., 2004). Despite the abundance of literature evidences, the effect of high pressure homogenisation on protein structure and functions is still contradictory.

HPH has been also shown to affect polysaccharides in fruit- and vegetable-based products. In this case, homogenisation has been shown to modify not only the particle size of plant fibre suspensions but also the particle interactions, thus affecting rheological properties such as the viscosity (Bayod, Månsson, Innings, Bergenståhl, & Tornberg, 2007). For instance, HPH has been shown to decrease the viscosity of carrot and broccoli puree (Christiaens et al., 2012; Lopez-Sanchez, Nijsse, et al., 2011). By contrast, HPH of tomato puree resulted in an increase in product viscosity (Colle, Van Buggenhout, Van Loey, & Hendrickx, 2010; Lopez-Sanchez, Nijsse, et al., 2011). The latter was attributed to the formation and strengthening of a fibre network as a consequence of mechanical stresses induced by HPH treatment (Bayod et al., 2007; Beresovsky, Kopelman, & Mizrahi, 1995; Lopez-Sanchez, Svelander, Bialek, Schumm, & Langton, 2011; Lopez-Sanchez, Nijsse, et al., 2011). It has been suggested that such structural modifications may affect the release and bioaccessibility of micronutrients, such as carotenoids, from the food matrix (Parada & Aguilera, 2007; van het Hof et al., 2000).

Based on these evidences, light processing and HPH could be exploited to modify the structure of food biomolecules, thus obtaining food systems with well-defined functional properties and biologic activity.

## 4.1 Aim and outline of this PhD thesis

The aim of this PhD thesis was to investigate the potentials of unconventional processes, such as light processing and high pressure homogenisation, to modify the structure of selected food biomolecules, and thus their functions as well as the functions of other bioactives present in the matrix, in order to obtain tailor-made foods. To this aim, different matrices were considered (Fig. B). In particular, as an example of a globular protein, the enzyme polyphenoloxidase (PPO) was

selected and the effect of PL on structure and activity of PPO in model solutions was investigated. As an example of a mix of globular proteins, egg white was chosen and the effect of either UV-C, or PL, or HPH treatment on its structure and technological performances and immunoreactivity was studied. In addition, as an example of a mix of globular and fibrous proteins, gluten was selected and the effect of PL on its structure and immunoreactivity was evaluated. Besides proteins, different polysaccharides were also considered. In this context, as an example of a semi-crystalline polysaccharide included in granules, wheat starch was selected and the effect of PL on its structure and technological performances was studied. On the other hand, differently coloured tomatoes were considered as a food matrix containing fibrous polysaccharides, and the effect of HPH on their structure and technological performances as well as carotenoid bioaccessibility was investigated. Finally, as a mix of proteins and polysaccharides wheat flour was considered and the effect of PL on its structure and immunoreactivity was studied. Depending on the matrix, different analytical methodologies were chosen to assess structural changes induced by unconventional processing.

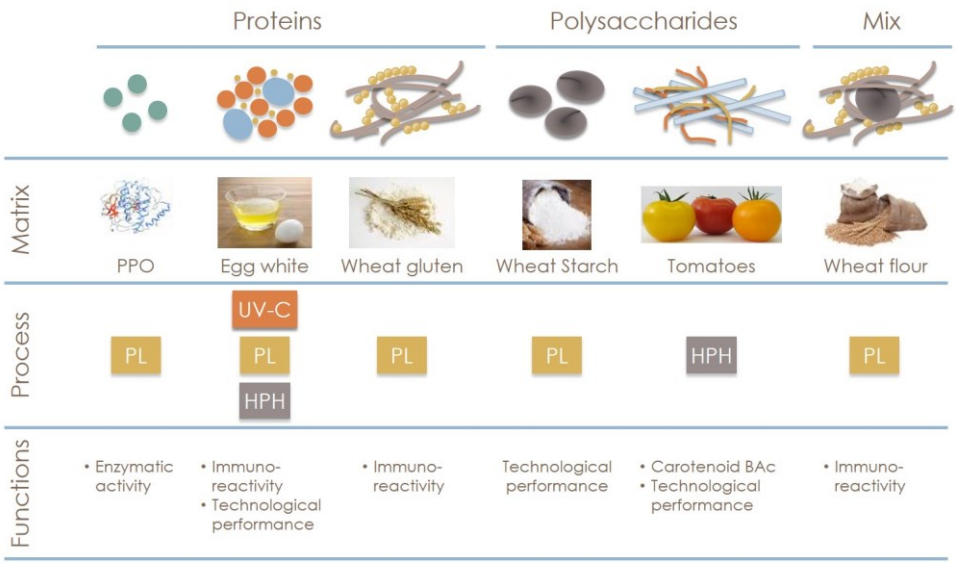


**Figure B** Aim of this PhD thesis.

The results of this PhD research project will be discussed considering first the effect of light processing on PPO, egg white, wheat gluten, starch, and wheat flour. In the second part, the effect of HPH on egg white proteins and tomato pulps will be considered.

# *Chapter 2 Materials and Methods*

## 2.1 Sample preparation

### Polyphenoloxidase

Mushroom tyrosinase (PPO) (3933 U $mg^{-1}$, Sigma, St. Louis, MO, USA) was used. PPO solutions were prepared by diluting increasing amounts of the enzyme in 0.1 M potassium phosphate buffer pH 7.0 (Sigma, St. Louis, MO, USA). The initial activities of the different PPO solutions on $1.5 \cdot 10^{-3}$ M Dopa (Sigma, St. Louis, MO, USA) in 0.1 M potassium phosphate buffer pH 7.0 were 0.0040, 0.0065, 0.01, 0.015, 0.026, 0.046 and 2.000 Abs $min^{-1}$. Aliquots of 100 µL PPO solutions were introduced into transparent plastic pouches (polycoupled Combiflex PA/PE 090, 20/70, Savonitti, Codroipo, Italy) of 2 x 3 cm, allowing 80% of the UV radiation to reach the sample, as declared by the producer. The pouches were hermetically sealed (Easy Packer EP400, Orved, VM-16, Musile di Piave, Italy) and submitted to pulsed light treatment.

### Egg white

Organic eggs were obtained from a local supermarket. The egg white was manually separated from the egg yolk and the chalazae were removed. The albumen was manually gently mixed. Egg white pH was 8.6±0.3. Egg white was immediately either treated by high pressure homogenisation, or introduced (1.5 g egg white) into transparent plastic pouches (polycoupled Combiflex PA/PE 090, 20/70, Savonitti, Codroipo, Italy) of 3.5 x 6.0 cm. The pouches were hermetically sealed (Easy Packer EP400, Orved, VM-16, Musile di Piave, Italy) and submitted to either UV-C light or PL treatment.

### Wheat gluten and flour

Wheat gluten (80% purity grade, Sigma-Aldrich, Milan, Itlay), and wheat flour obtained from a local supermarket were suspended in 0.05 M sodium phosphate buffer containing 0.5% SDS (w/v) (pH 6.9) in concentration equal to 1% (w/v). 2 mL of gluten or flour suspension was introduced into 2 x 3 cm plastic pouches (Polycoupled Combiflex PA/PE 090, 20/70, Savonitti, Codroipo, Italy). Additional samples were prepared introducing 0.5 g wheat gluten, starch, or flour into the pouches. The pouches were hermetically sealed (Easy Packer EP400, Orved, VM-16, Musile di Piave, Italy) and submitted to PL treatment. After pulsed light treatments, gluten, and flour powder was suspended in 0.5% (w/v)

SDS-0.05 M sodium phosphate buffer (pH 6.9) solution in concentration equal to 1% (w/v) and analysed.

**Starch**

Wheat starch (Sigma-Aldrich, Milan, Itlay) was suspendend in distilled water in concentration equal to 1% (w/v). 2 mL of starch suspension was introduced into 2 x 3 cm plastic pouches (Polycoupled Combiflex PA/PE 090, 20/70, Savonitti, Codroipo, Italy). The pouches were hermetically sealed (Easy Packer EP400, Orved, VM-16, Musile di Piave, Italy) and submitted to PL treatment.

**Tomato pulps**

Red, orange and yellow ripe tomatoes (*Solanum lycopersicum* L.) of the cultivars Admiro, Bolzano and Lorenzo respectively, were purchased at a local greengrocer. They were washed, wiped, manually quartered with a sharp knife, frozen in liquid nitrogen and stored at −40 °C until use. The same batch of each tomato was used for the preparation of all samples. The frozen tomato quarters were thawed, peeled, mixed (3 times for 5 s) (Büchi Mixer B-400, Flawil, Switzerland) and sieved (pore size 1.0 mm) in order to remove the seeds. Tomato pulps were immediately treated by HPH and analysed within 24 h.

## 2.2 Unconventional processing

**UV-C light treatment**

Egg white samples were exposed for increasing time (5, 30 min) to UV-C light (15 W, OF, OSRAM, GmbH HNS, Munich, Germany, maximum emission 253.7 nm) in a thermostated cell (Climacell 222, MMM Medcenter, Einrichtungen GmbH, Graefelfing, Germany) at 8 °C. The distance between the samples and the lamp was 2.5 cm and the irradiance incident on the samples was 35.4 W $m^{-2}$. Irradiance was measured using a portable luminometer (HD-2102.2 Delta Ohm, Padova, Italy) equipped with a UV-C light probe (LP471 UVC, Padova, Italy). The luminometer sensor was placed in the thermostated cell at 2.5 cm distance from the UV-C lamp and irradiance value recorded.

The dose received by the samples exposed to the light for 5 and 30 min was 1.06 and 6.37 J $cm^{-2}$ respectively. The lamp was allowed to stabilise by turning it on at least 15 min before use. Analogous samples kept under dark were prepared as control. No temperature changes were observed as a consequence of lighting in all samples.

**Pulsed light treatments**

Pulsed light treatments were carried out at room temperature by using a pulsed light mobile decontamination unit (Claranor, Rouaine, France) equipped with 4 xenon lamps with emission in the range 200-1000 nm (200-400 nm: 41%; 400-700 nm: 51%; 700-1000 nm: 8%). Lamps were positioned at each side of a quartz plaque held in the centre of the cube shaped chamber. According to the manufacturer's instructions, PPO, egg white, gluten, starch, and flour samples were placed on the quartz plaque and lamps set at distances allowing the sample to be exposed to increasing light fluence from 0 to 1.75 J $cm^{-2}$ $pulse^{-1}$. Exposure to higher fluence up to 31.5 J $cm^{-2}$ was obtained by delivering to the sample increasing number of pulses (0-18), each having a fluence of 1.75 J $cm^{-2}$. Pulse duration was 50 μs and repetition rate was 0.5 Hz.

**High pressure homogenisation**

Egg white was homogenised using a two stage high pressure homogeniser (Panda PLUS 2000, Gea Niro Soavi, Parma, Italy) provided with cylindrical tungsten carbide homogenising valves. The first valve, which is the actual homogenisation stage, was set at 150 MPa and the second one at 5 MPa. Aliquots of 250 mL egg white were homogenised *via* multiple passes up to 17 at 10.8 L $h^{-1}$ flow rate. The homogeniser inlet and outlet were connected to a heat exchanger (Julabo F70, Seelbach, Germany) set at 4 °C. Additional samples were obtained by homogenising the egg white with the first valve set at 0 MPa. Untreated egg white was considered as control. All the samples were kept at 4 °C until analysis. All the samples were analysed within 24 h after the homogenisation process.

Tomato pulps were homogenised *via* a single pass at 20, 50 and 100 MPa using a high pressure homogeniser (Panda 2K; Gea Niro Soavi, Mechelen, Belgium) with inlet and outlet connected to a heat exchanger at a pre-set temperature of 4 °C. Non homogenised pulps were considered as control samples. All the samples were kept in the dark at 4 °C until analysis.

## 2.3 Temperature measurements

Sample temperature was measured by a copper-constantan thermocouple probe (Ellab, Denmark) connected to a portable data logger (mod. 502A1, Tersid, Milano, Italy). In samples subjected to UV-C and PL treatment, measurements were performed within 10 s from the end of the treatment. In samples subjected to HPH, measurements were performed just before and immediately after homogenization.

## 2.4 Determination of PPO structure and function

### HPLC-gel permeation analysis

HPLC-gel permeation analysis was performed in duplicate by a HPLC system Jasco (model 880-02, Japan Spectroscopic Co., Tokyo, Japan) equipped with a UV-Vis detector as reported by Manzocco et al. (2009). Two columns were used: BioSep-SEC-S 3000, 30 cm length, 7.80 mm internal diameter and BioSep-SEC-S 2000 30 cm length, 7.80 mm internal diameter, 5 μm granulometry, 125 Å porosity, with separation range among 5 and 150 kDa. Injection volume was 20 μL and the mobile phase, delivered at a flow rate of 0.6 mL min-1, was 0.1 M potassium phosphate buffer pH 7.0 in isocratic conditions. The detection wavelength was 220 nm. Bovine Serum Albumin (67 kDa), α-Lactalbumin (15 kDa) and β-Lactoglobulin (18 kDa) albumin (44.29 kDa) from Sigma (St. Louis, MO, USA) were used as calibration standards. Peaks integration was performed by CHROM-CARD for Windows software (1.19 version).

### Polyphenoloxidase activity

The PPO activity was assayed spectrophotometrically (Shimadzu UV-2501PC, UV-Vis recording spectrophotometer, Shimadzu Corporation, Kyoto, Japan) at 25 °C according to the methodology of Kahn (1985), based on the absorption at 420 nm of the brown polymers formed when L-Dopa is oxidized in the presence of PPO. The reaction was started by the addition of 20 μL of PPO solution to 2 mL of medium containing 0.1 M potassium phosphate buffer pH 7.0 and $1.5 \cdot 10^{-3}$ M L-Dopa as substrate. The absorbance at 420 nm was monitored each minute for 15 min. The changes in absorbance per minute were calculated by linear regression applying the pseudo zero order kinetic model. The eventual final stationary phase was excluded from regression data. One unit of PPO was defined as the amount of enzyme which produces an increase in absorbance at 420 nm of 0.001 per minute under the testing conditions. PPO activity was calculated as the percentage ratio between enzymatic activity of the pulsed light treated solution and of the untreated one.

Linear regression of enzymatic activity as a function of pulsed light fluence was also performed considering the linear part of the curve. The photostability of PPO was calculated as the fluence required to reduce the original PPO activity by 50% ($F_{50}$) and expressed as J $cm^{-2}$.

**Data analysis**

At least five independently treated samples were assessed for enzymatic activity. Coefficients of variations, expressed as percentage ratio between standard deviation and mean value were lower than 9. HPLC gel permeation analyses were carried out in duplicate. Linear regression analysis was performed using Microsoft Office Excel 2003. Goodness-of-fit was evaluated by means of the determination coefficients (R2) and the corresponding p values.

## 2.5 Determination of egg white protein structure and functions

**Absorbance**

The absorption spectroscopy measurements at 280, 380, and 680 nm were performed by a UV-Vis spectrophotometer (UV-2501 PC, Shimadzu Kyoto, Japan) at 25 °C with a 1 cm path-length cuvette. Egg white was diluted 1:100 (v/v) with 0.05 M tris-HCl buffer pH 9.0 containing 0.4 M NaCl.

**Dynamic light scattering**

Light scattering measures were made using a Particle Sizer NICOMP$^{TM}$ 380 ZLS (PSS NICOMP Particle Sizing System, Santa Barbara, California, USA). Egg white samples were diluted either 1:1000 (v/v) with 0.05 M tris-HCl buffer pH 9.0 containing 0.4 M NaCl, or 1:50 with deionized water. The angle of observation was 90°. The refractive index of the solution was set at 1.333 and the viscosity was approximated to that of pure water at 25 °C. Hydrodynamic radius refers to the corresponding volume distribution calculated by NICOMP Distribution Analysis.

**Determination of free sulfhydryl content**

The concentration of free sulfhydryl groups (SH) of the egg white samples was determined using Ellman's reagent (5',5-dithiobis (2-nitrobenzoic acid), DTNB) (Sigma Aldrich. Milan, Italy). Changes in free sulfhydryl groups were measured in duplicate as reported by Beveridge, Toma, & Nakai (1974). Briefly, egg white (1.5 g) was diluted to 10 mL with 1% (p/v) NaCl in Tris-glycine buffer (10.4 g Tris, 6.9 g glycine, 1.2 g EDTA per liter, pH 8.0) (Sigma Aldrich, Milan, Italy). A volume of 2.9 mL of 0.5% SDS in Tris-Glycine buffer was added to 0.1 mL of diluted egg white and 0.02 mL of Ellman's reagent (4 mg mL-1 DTNB in Tris-glycine buffer) to develop colour. After 15 min, absorbance was measured at 412 nm by a UV-Vis spectrophotometer (UV-2501 PC, Shimadzu Kyoto, Japan).

Concentration of free sulfhydryl groups (μM $g^{-1}$) was calculated from the following equation:

$$SH = \frac{73.53 \cdot A_{412} \cdot D}{C} \quad (1)$$

where $A_{412}$ is the absorbance at 412 nm; $C$ is gluten concentration (mg $mL^{-1}$); $D$=5.02 is the dilution factor; and 73.53 is derived from $\frac{10^6}{1.36 \cdot 10^{-4}}$; $1.36 \cdot 10^4$ is the molar absorptivity (Ellman, 1959).

**HPLC gel-permeation analysis**

Egg white was diluted 1:50 (w/v) with 0.05 M tris-HCl buffer pH 9.0 containing 0.4 M NaCl (Sigma Aldrich, Milan, Italy). The solution was filtered on 0.20 μm pore size filters (Econofilters, Agilent Technologies, Cernusco sul Naviglio, Italy). Samples were analysed using a HPLC system Jasco (model 880-02, Japan Spectroscopic Co., Tokyo, Japan) equipped with a UV-Vis detector. Two columns were used: BioSep-SEC-S 3000, 30 cm length, 7.80 mm internal diameter and BioSep-SEC-S 2000 30 cm length, 7.80 mm internal diameter, 5 μm granulometry, 125 Å porosity, with separation range among 5 and 150 kDa. Injection volume was 20 μL and the mobile phase, delivered at a flow rate of 0.6 mL $min^{-1}$, was 0.05 M tris-HCl buffer pH 9.0 containing 0.4 M NaCl in isocratic conditions. Detection wavelength was 220 nm. Bovine serum albumin (67 kDa), α-lactalbumin (14 kDa), β-lactoglobulin (18 kDa), albumin (44.29 kDa) (Sigma, St. Louis, MO, USA), and insulin (5.7 kDa) (Roche Diagnostic GmbH, Mannheim, Germany) were used as calibration standards. A linear relation ($R^2$=0.92) was found between retention time and molecular weight of standard proteins, expressed in logarithmic values. Peaks integration was performed by CHROM-CARD for Windows software (1.19 version).

**SDS-polyacrylamide gel electrophoresis**

Sodium dodecyl sulphate polyacrylamide gel electrophoresis (SDS-PAGE) was performed according to Laemmli (1970). Egg white was diluted 1:4 with 0.05 M tris-HCl buffer pH 8.8 containing 0.4 M NaCl. The egg white solution was then further diluted 1:4 with sample buffer (Bromophenol blue 0.01%, 120 mM Tris-HCl, pH 6.8, 4% (w/v) SDS, 20% (v/v) glycerol). 5 μL of sample (15 μg protein) were loaded on a 15% (w/v) polyacrylamide separating gel containing bis-acrylamide cross linker, mounted on a Mini 2-D (Bio-Rad, Richmond, California, USA) vertical electrophoresis cell. The egg white electrophoretic patterns were

obtained by running the samples at 15 mA with standard proteins of known molecular weight (Precision Plus Protein™ Dual Color Standards, Bio-Rad, Segrate, Italy). The gels were subsequently stained in NOVEX ® Colloidal Blue Staining Kit (Invitrogen, Carlsbad, California, USA) for one night and then destained in bi-distilled water. Gels were scanned and analysed with the ImageQuant TL Image Analysis Software (Amersham Bioscience Inc., Piscataway, New Jersey, USA) to determine the molecular weight of each band.

**Immunoreactive egg white proteins**

The quantitative determination of immunoreactive egg white was performed at room temperature by the enzyme immunoassay RIDASCREEN® Fast Ei/Egg Protein (R-Biopharm AG, Darmstadt, Germany) according to the manufacturer's recommendations. Analyses were performed on samples diluted to $8\times10^{-10}$ g $L^{-1}$ with the 0.05 M Tris-HCl pH 8.8 buffer containing 0.4 M NaCl. Absorbance at 450 nm was measured by using a microplate reader (Sunrise, Tecan Group, Männedorf, Switzerland). Concentration of immunoreactive egg white was determined according to the calibration curve obtained using the standard solutions provided with the immunoassay kit.

**Apparent viscosity**

Viscosity at 20 °C was measured by a Stresstech Rheometer (Reologia Instruments AB, Lund, Sweden) with a parallel plate geometry of 40 mm diameter, and a gap of 2 mm. The system was thermostated by a Jumo Dicon cell (Sm M.K. Juccheim GMBM & Co, Fulda, Germany). The measurements were performed at shear rate from 1.093 and 159.4 $s^{-1}$. Apparent viscosity was calculated at shear rate equal to 5.17 $s^{-1}$.

**Gel firmness**

Aliquots of 3.5 g of egg white were introduced in 10 mL capacity vials, hermetically sealed with butyl septa and metallic caps. Samples were heated in a water thermostated bath (YELLOW line, IKA-Werke, Germany) at 90 °C for 5 min. Firmness was measured by a puncture test using an Instron 4301 (Instron LTD, High Wycombe, UK) according to the methodology of Manzocco et al. (2009) with minor modifications. The instrumental settings and operations were accomplished using the software Automated Materials Testing System (version 5, Series IX, Instron LTD, High Wycombe, UK). Samples were punctured with a 1.5 mm cylindrical probe. Crosshead speed was set at 10 cm $min^{-1}$. Force-distance curves were obtained from the puncture tests and firmness was taken as the force

(N) required to puncture the gel 0.5 cm. For each sample 6 measures were performed.

**Gelling temperature**

Gelling temperature was determined by a rotational rheometer (Stresstech Rheometer, Reologia Instruments AB, Lund, Sweden) equipped with a 40 mm diameter cone-plate geometry. As reported by Raikos, Campbell, Stephen, & Euston, (2007), a temperature sweep was conducted from 60 to 75 °C at a heating rate of 1.0 °C $min^{-1}$ using a frequency of 1 Hz and a strain of 0.008. These conditions were chosen within the linear viscoelastic region of the samples. The outer edges of the plates were covered with a thin layer of mineral oil (d= 0.84 g $mL^{-1}$, Sigma Aldrich, Milan, Italy) to minimize water loss during measurements.

**Foam ability and stability**

Foams were obtained by whipping 5 mL of egg white for 3 min at 20 °C in a 50 mL cylinder by a high speed mixer (Ika-Werke, DI 25 basic, Staufen, Germany) operating at 9500 rpm. The volume of the foam and of the drained liquid was assessed just after whipping and during holding up to 30 min at 20 °C. Percentage foam ability (FA) and stability (FS) were calculated as follows:

$$FA\ (\%) = (Vf\text{-}Vl_0)/Vl_0 \times 100 \quad (2)$$

$$FS\ (\%) = Vf_{30}/Vf \times 100 \quad (3)$$

where Vf is the foam volume, $Vl_0$ is the initial volume of the liquid egg white and $Vf_{30}$ is the foam volume after 30 min observation.

**Microscopy**

Just whipped foams and foams held for 30 min at 20 °C were placed onto a microscope slide. Pictures of foam bubbles were acquired as quickly as possible using a digital camera (Leica EC3, Solms, Germany) mounted on a Leica™ microscope (Leica DM 2000, Solms, Germany), magnification 100x.

**Image analysis**

Images were submitted to analysis using Image-Pro Plus (ver. 6.3, Media Cybernetics, Inc., Bethesda, MD, U.S.A.). In particular, images were converted to grey scale (8 bit). Because of the low contrast between the bubbles and the surrounding medium, the boundaries of the air bubbles were selected by a semi

automatic procedure. The maximum diameter of the bubbles was measured. Bubbles in each image were subdivided into three classes, depending on their average diameter: the first class (small bubbles) consisted of bubbles with average diameter lower than 0.05 mm; the second class (medium bubbles) included bubbles with average diameter from 0.05 to 0.1 mm; the third class (large bubbles) consisted of bubbles with average diameter higher than 0.1 mm. The percentage ratio between the number of bubbles belonging to each class and the total number of bubbles in the image was calculated.

**Data analysis**

Results are expressed as mean of three replicates ± standard deviation. Means were compared using one-way analysis of variance (ANOVA) ($P$<0.05) followed by Tukey test. Least squares linear regression analyses were also performed (Statistica 6.0, StatSoft inc., Tulsa, USA).

## 2.6 Determination of gluten proteins structure and function

**Absorbance**

The absorption spectroscopy measurements at 280 and 320 nm were performed by a UV-Vis spectrophotometer (UV-2501 PC, Shimadzu Kyoto, Japan) at 25 °C with a 1 cm path-length cuvette. Gluten and flour samples were diluted with 0.5% (w/v) SDS-0.05 M sodium phosphate buffer solution (pH 6.9) to obtain absorbance signals on scale.

**Microscopy analysis**

Micrographs of gluten (100x), and flour samples (40x) were taken using a digital camera (Leica EC3, Solms, Germany) mounted on a light microscope (Leica DM 2000, Solms, Germany).

**Dynamic light scattering**

Light scattering measures were made using a Particle Sizer NICOMP™ 380 ZLS (PSS NICOMP Particle Sizing System, Santa Barbara, California, USA). The angle of observation was 90°. The refractive index of the solution was set at 1.333 and the viscosity was approximated to that of pure water at 25 °C. Hydrodynamic radius refers to the corresponding volume distribution calculated by NICOMP Distribution Analysis.

**Determination of free sulfhydryl content**

The concentration of free sulfhydryl groups (SH) of gluten and wheat flour samples was determined using Ellman's reagent (5',5-dithiobis (2-nitrobenzoic acid), DTNB) (Sigma Aldrich, Milan, Italy). The procedure described by Stathopoulos, Tsiami, David Schofield, & Dobraszczyk (2008), based on the method of Beveridge et al. (1974), was followed. Briefly, a Tris–glycine–EDTA (TGE) buffer was prepared by dissolving Tris (10.4 g), glycine (6.9 g) and EDTA (sodium salt) (1.2 g) (Sigma Aldrich. Milan, Italy) in 800 mL distilled water. The pH was adjusted to 8.0 using concentrated hydrochloric acid and the volume was then made up to 1 L. Ellman's reagent was prepared by dissolving 20 mg of DTNB in 5 mL of dimethylformamide (4 mg $mL^{-1}$ solution) (Sigma Aldrich, Milan, Italy) and stored in the dark at room temperature. A working SDS–TGE solution was freshly prepared each time by mixing 45 mL of TGE stock solution with 5 mL SDS stock solution (25%, w/v). The working solution was degassed in an ultrasonic bath for 30 min, and flushed with nitrogen during stirring for 15 min. 10 mg gluten and 100 mg flour was suspended in 3 mL TGE–SDS buffer at 20 °C and vortexed every 10 min for 30 min. 0.06 mL Ellman's reagent was added to the suspension and the mix was held at 20 °C for 15 min. This was followed by centrifugation at 3,000 *g* for 15 min at 4 °C. The supernatant was then centrifuged at 20,000*g* for 15 min at 4 °C. The absorbance of the supernatant was measured at 412 nm by a UV-Vis spectrophotometer (UV-2501 PC, Shimadzu Kyoto, Japan). Both reagent and sample blanks were used.

Concentration of free sulfhydryl groups (μM $g^{-1}$) was calculated from the following equation:

$$SH = \frac{73.53 \cdot A_{412} \cdot D}{C} \quad (1)$$

where $A_{412}$ is the absorbance at 412 nm; $C$ is gluten concentration (mg $mL^{-1}$); $D$=5.02 is the dilution factor; and 73.53 is derived from $\frac{10^6}{1.36 \cdot 10^{-4}}$; $1.36 \cdot 10^4$ is the molar absorptivity (Ellman, 1959).

**HPLC gel-permeation analysis**

Gluten proteins were analysed by HPLC gel-permeation according to the procedure described by Gupta, Khan, & Macritchie (1993), with minor modifications. Before HPLC analysis gluten and flour samples were submitted to protein extraction. The samples were heated at 40 °C for 5 min and subsequently stirred at room temperature for 20 h to assure dissolution. The samples were

centrifuged at 10,000 *g* for 30 min. The supernatant was collected and filtered (Whatman PVDF syringe filter, 0.45 µm pore size-25 mm diameter). Analyses were performed on a HPLC system Jasco (model 880-02, Japan Spectroscopic Co., Tokyo, Japan) equipped with a UV-Vis detector. Two columns were used: BioSep-SEC-S 3000, 30 cm length, 7.80 mm internal diameter and BioSep-SEC-S 2000 30 cm length, 7.80 mm internal diameter, 5 µm granulometry, 125 Å porosity, with separation range among 5 and 150 kDa. The eluent consisted of 50% (v/v) acetonitrile (Sigma) and 50% (v/v) MilliQ water, containing 0.1% (v/v) trifluoroacetic acid (Sigma). The injection volume was 10 µl. Flow rate was set at 0.5 ml $min^{-1}$ and the detection wavelength was 210 nm. Bovine serum albumin (67 kDa), α-lactalbumin (14 kDa), β-lactoglobulin (18 kDa), albumin (44.29 kDa) (Sigma Aldrich, Milan, Italy) were used as calibration standards. Peak retention times were estimated by CHROM-CARD for Windows software (1.19 version). A linear relation ($R^2$=0.99) was found between retention time and molecular weight of standard proteins, expressed in logarithmic values.

**SDS-polyacrylamide gel electrophoresis**

Sodium dodecyl sulphate polyacrylamide gel electrophoresis (SDS-PAGE) was performed according to Laemmli (1970). 63 µL gluten samples were diluted with 37 µL sample buffer (bromophenol blue 0.01%, 120 mM Tris-HCl, pH 6.8, 4% (w/v) SDS, 20% (v/v) glycerol). Flour samples were submitted to protein extraction procedure, as explained for HPLC analysis, 80 µL supernatant were diluted with 20 µL sample buffer (bromophenol blue 0.2%, 0.5 M Tris-HCl, pH 6.8, 10% (w/v) SDS, 50% (v/v) glycerol). 5 µL of gluten sample (25 µg protein), and 20 µL flour protein extract (12.8 µg protein) were loaded on a 13% (w/v) polyacrylamide separating gel containing bis-acrylamide cross linker, mounted on a Mini 2-D (Bio-Rad, Richmond, California, USA) vertical electrophoresis cell. The electrophoretic patterns of gluten proteins were obtained by running the samples at 15 mA with standard proteins of known molecular weight (Precision Plus Protein™ Dual Color Standards, Bio-Rad, Segrate, Italy). The gels were subsequently stained in NOVEX ® Colloidal Blue Staining Kit (Invitrogen, Carlsbad, California, USA) for one night and then destained in bi-distilled water. Gels were scanned and analysed with the ImageQuant TL Image Analysis Software (Amersham Bioscience Inc., Piscataway, New Jersey, USA) to determine the molecular weight of each band.

### Immunoreactive gliadin

The quantitative determination of immunoreactive gliadin was performed at 25 °C by the enzyme immunoassay RIDASCREEN® Fast Gliadin (R-Biopharm AG, Darmstadt, Germany) according to the manufacturer's recommendations. Analyses were performed on light treated gluten samples and light treated wheat flour samples diluted to 2 mg $L^{-1}$ with 0.5% (w/v) SDS-0.05 M sodium phosphate buffer solution (pH 6.9). Absorbance at 450 nm was measured by using a microplate reader (Sunrise, Tecan Group, Männedorf, Switzerland). Concentration of immunoreactive gliadin was determined according to the calibration curve obtained using the standard solutions provided with the immunoassay kit.

### Data analysis

The results are averages of at least three measurements taken from different samples and are reported as means ± SD. Analyses of variance (ANOVA) was performed with significance level set to $P<0.05$ (Statistica for Windows, ver. 5.1, Statsoft Inc. Tulsa, USA, 1997). The Tukey procedure was used to test for differences between means.

## 2.7 Determination of starch structure and function

### Absorbance

The absorption spectroscopy measurements at 280 and 320 nm were performed by a UV-Vis spectrophotometer (UV-2501 PC, Shimadzu Kyoto, Japan) at 25 °C with a 1 cm path-length cuvette. Starch samples were diluted with distilled water to obtain absorbance signals on scale.

### Turbidity

The optical density at 680 nm of starch samples was measured each minute during 15 min by a UV-Vis spectrophotometer (UV-2501 PC, Shimadzu Kyoto, Japan) at 25 °C with a 1 cm path-length cuvette.

### Dynamic light scattering

Light scattering measures were made using a Particle Sizer NICOMP™ 380 ZLS (PSS NICOMP Particle Sizing System, Santa Barbara, California, USA). The angle of observation was 90°. The refractive index of the solution was set at 1.333 and the viscosity was approximated to that of pure water at 25 °C. Hydrodynamic

radius refers to the corresponding volume distribution calculated by NICOMP Distribution Analysis.

**Gelatinisation**

5 mL of starch suspension were introduced in 10 mL capacity vials, hermetically sealed with butyl septa and metallic caps. Starch samples were heated in a water thermostated bath (YELLOW line, IKA-Werke, Germany) at 100 °C for 30 min.

**Microscopy analysis**

Micrographs of starch granules (200x), and gelatinised starch granules (100x) were taken using a digital camera (Leica EC3, Solms, Germany) mounted on a light microscope (Leica DM 2000, Solms, Germany).

**Data analysis**

The results are averages of at least three measurements taken from different samples and are reported as means ± SD. Analyses of variance (ANOVA) was performed with significance level set to $P<0.05$ (Statistica for Windows, ver. 5.1, Statsoft Inc. Tulsa, USA, 1997). The Tukey procedure was used to test for differences between means.

## 2.8 Determination of tomato pulps microstructure and functions

(This experimental work was performed at the Laboratory of Food Technology of the *Katholieke Universiteit Leuven*, Belgium).

**Light microscopy**

Micrographs of tomato pulps were taken using a digital camera mounted on a light microscope (Olympus BX-41, Optical Co. Ltd., Tokyo, Japan). To visualize the microstructure of the tomato pulps, the samples were diluted 1:10 (v/v) with 0.1 % toluidine blue aqueous solution. The presence of starch was also evaluated by diluting 1:4 (v/v) tomato pulp with a iodine staining solution (0.2% iodine, 2% potassium iodide aqueous solution). Few droplets of the mixtures were placed on microscopic slides, covered with cover glasses and studied using a 10x magnification. To visualize the tomato chromoplasts, one droplet of tomato pulp was placed on a microscopic slide, covered with a cover glass and analysed using a 100x magnification.

**Particle size distribution (PSD)**

The PSD of tomato pulps was measured by laser diffraction using a Malvern Mastersizer S long bench instrument (Malvern Instrument Ltd., Worcestershire, UK). Tomato pulp was poured into a stirred tank filled with water until a laser obscuration of 20% was achieved. The diluted sample was pumped into the measuring cell, which was located in the optical path of the laser beam. The laser beam (He–Ne laser, wavelength 633 nm), collimated at 18 mm, was scattered to detector units (42 element composite solid state detector array), which detected particles in the range of 0.05 to 880 μm. Volumetric PSDs were calculated from the intensity distribution of the scattered light using the Mie theory by use of the instrument software.

**Bostwick consistency**

The consistency of tomato pulps was measured using a Bostwick consistometer. This empirical test was conducted allowing the sample to flow under its own weight along a sloped stainless steel tray for 30 s at room temperature (23 °C). The distance the pulps flowed was recorded as the Bostwick consistency index (cm). High values correspond to a low consistency pulp with low resistance to flow, while lower values are associated with high consistency pulps resistant to flow. Measurements were done in triplicate.

**In vitro bioaccessibility**

The lycopene, ζ-carotene and lutein *in vitro* bioaccessibility was measured immediately after processing the tomato pulp by simulating human digestion in the stomach and small intestine *in vitro*. The procedure described by Moelants et al. (2012), based on Hedrén, Diaz, & Svanberg (2002), was followed. In particular, 5 g tomato pulp was weighted into a 50 mL capacity brown falcon tube. The sample was diluted with 5 mL NaCl/ ascorbic acid solution (0.9% NaCl, 1% ascorbic acid in water), 5 mL stomach electrolyte solution (0.30% NaCl, 0.11% KCl, 0.15% $CaCl_2 \cdot 2H_2O$, 0.05% $KHPO_4$, 0.07% $MgCl_2 \cdot 6H_2O$ in water) and 10 mL of freshly prepared oil emulsion. The latter was obtained by suspending 1% (w/v) L-α-phosphatidylcholine from egg yolk (Sigma) in water. 5% (v/v) extra virgin olive oil was then added and the mixture was homogenized (UltraTurrax® T25, IKA® - Werke GMBH & CO.KG, Staufen, Germany) at 9500 rpm during 10 min. A second homogenization was performed at 100 MPa for one cycle using the high pressure homogeniser described above.

To simulate the first phase of gastric digestion, the pH of the mixture was adjusted to 4±0.05 with 1 M HCl or 1 M $NaHCO_3$ and 5 mL pepsin solution

(0.52% porcine pepsin, from Sigma, in electrolyte solution) was added. After flushing the headspace of the samples with nitrogen for 20 s, the mixture was incubated at 37 °C for 30 min while shaking end-over-end. The pH of the mixture was then acidified to 2±0.05 to mimic the drop of the gastric pH after the intake of a meal (Tyssandier *et al*., 2003). The headspace of the samples was flushed again with nitrogen for 20 s and the incubation at 37 °C continued for another 30 min. To imitate the passage through the small intestine, the pH of the partially digested tomato pulp was raised to 6.9±0.05 and 3 mL pancreatin/bile salts solution (0.4% porcine pancreatin, 2.5% bile extract, 0.5% pyrogallol, and 1% $\alpha$-tocopherol, from Sigma, in water) was added. Finally, the headspace of the sample was flushed with nitrogen for 20 s and incubated for 2 h at 37 °C. The digest was centrifuged (L7 Ultracentrifuge, Beckman, Palo Alto, CA, USA) at 165,000 *g* during 65 min at 4 °C to separate the micelles. The supernatant was collected, filtered (Chromafil PET filters, 0.20 μm pore size-25 mm diameter) and analyzed for carotenoid content ($C_m$). The *in vitro* bioaccessibility of the carotenoids was defined as the percentage ratio between the carotenoid content in the micelles ($C_m$) and in the digest of the control sample (i.e. non homogenised tomato pulp) ($C_d$). The latter sample was obtained immediately after digestion (no ultracentrifugation).

**Carotenoid content**

The extraction of lycopene, $\zeta$-carotene and lutein was performed following the procedure of Sadler, Davis, & Dezman (1990), with minor modifications. The analysis was performed under subdued light to prevent carotenoid degradation and isomerisation. 0.5 g NaCl and 50 mL extraction solution (50% hexane, 25% acetone, 25% ethanol, 0.1% butylated hydroxytoluene) were added to 2 g freshly prepared tomato pulp, to the digest of non homogenised tomato pulp or to the micellar fraction. The mixture was stirred at 4 °C for 20 min. Reagent grade water (15 mL) was added and stirring was continued for 10 min. The apolar phase was then separated from the aqueous phase using a separation funnel. The apolar phase, containing the carotenoids, was collected, filtered (Chromafil PET filters, 0.20 μm pore size-25 mm diameter) and transferred to an amber HPLC vial. When necessary, the apolar phase was concentrated under vacuum at 30 °C for 35 min using a rotary evaporator. The concentrated carotenoid extracts were redissolved in hexane:dichloromethane (4:1 v/v) and transferred to an amber HPLC vial. The concentration factor was calculated by adding a known amount of $\beta$-apo-8'-carotenal prior to the evaporation of the apolar solvent.

The HPLC analyses were performed on an Agilent 1200 series system equipped with a diode array detector (Agilent Technolgies 1200 Series, Diegem, Belgium), according to Colle *et al.* (2010) with some modifications. Carotenoids were separated at 25 °C on a reversed phase $C_{30}$ column (3 μm×150 mm×4.6 mm, YMC Europe, Dinslaken, Germany) coupled to its guard column. A mobile phase of reagent grade water (A), methanol (B) and methyl-t-butyl-ether (C) was used. The gradient elution was as follows: 0 min: 4% (A), 96% (B); 6-9 min: 4% (A), 81% (B), 15% (C); 21-24 min: 4% (A), 41% (B), 55% (C); 32 min: 4% (A), 31% (B), 65% (C); 34-38 min: 4% (A), 26% (B), 70% (C); 38-48 min: 4% (A), 96% (B). Lycopene, ζ-carotene and lutein were identified based on retention times and spectral characteristics compared to the standards (data not shown). To quantify the carotenoids, HPLC-DAD peak responses were measured at 472 nm for lycopene, and at 450 nm for ζ-carotene and lutein. The carotenoid content was calculated based on their calibration curve and expressed as μg/g tomato pulp.

**Data analysis**

Results obtained are expressed as mean of three replicates ± standard deviation. Means were compared using one-way analysis of variance (ANOVA) followed by Tukey test ($P$<0.05) (Statistica 6.0, StatSoft inc., 2001). Least squares linear regression analyses were performed by using Statistica for Windows (ver. 4.5, 1993, Stat Soft Inc., Tulsa, USA).

# PART I Effect of light processing on food biomolecules

The aim of the first part of this PhD research was to investigate the effects of light processing on selected food proteins focusing on the process-structure-function relationship. To this aim different types of proteins, which serve important functionality in foods, were chosen. The following chapters will discuss the effect of PL on the structure and enzymatic activity of PPO in model solution, the effect of UV-C light and PL on the structure and technological performances (viscosity, gelling and foaming properties) as well as immunoreactivity of egg white proteins, the effect of PL on wheat gluten structure and immunoreactivity, the effect of PL on wheat starch structure and gelatinization, and the effect of PL on wheat flour microstructure and immunoreactivity.

## *Chapter 3 Effect of pulsed light on polyphenoloxidase*

### Aim of the study

In this chapter the effect of PL treatment on a globular protein exerting enzymatic activity was studied. In particular, polyphenoloxidase (PPO) was chosen as an example. This enzyme is known to be composed of monomers that undergo association determining the formation of dimers and tetramers. The tetramer structure is normally the main form of PPO (Jolley, Nelson, & Robb, 1969). PPO is one of the most important enzymes involved in food spoilage. It is well known to cause browning in cut fruits and vegetables leading to less attractive appearance and loss in nutritional quality. Therefore, PPO inactivation is highly desirable for increasing the stability and quality properties in fresh-cut products. Usually enzyme inactivation is obtained by thermal treatment (conventional blanching) and by the use of antioxidants and/or enzyme inhibitors (Almeida & Nogueira, 1995). However, conventional blanching usually results in a substantial loss of both technological and nutritional quality-related properties of fresh-cut products. In contrast, PL treatments could represent not only an easy disinfection technique but also a novel approach to non-thermally inactivate undesired enzymes limiting the overall quality depletion associated to conventional inactivation methods. As protein enzymatic activity is closely related to its

structure, structure modifications potentially induced by light exposure can reasonably modify the enzyme activity. There is much circumstantial evidence indicating that protein enzymatic activity could be strongly affected by PL treatment. Although food scientists have largely investigated the possibility to exploit PL to inactivate PPO in fruits and vegetables, still contradictory results are available in the literature. In 1989, Dunn et al. suggested that pulsed light could inhibit PPO in potato slices and alkaline phosphatase in model systems. More recently, Oms-Oliu, Martín-Belloso, & Soliva-Fortuny (2010) showed that pulsed light promoted an increase in PPO activity in fresh-cut mushrooms. On the other hand, Ramos-Villarroel et al. (2011) observed that PL, combined with antibrowning agents, can prevent enzymatic browning in fresh-cut avocado. Whilst, Charles, Vidal, Olive, Filgueiras, & Sallanon (2013) demonstrated the increase in PPO activity in fresh-cut mango submitted to pulsed light treatment. Given these apparently contradicting evidences, investigations on model systems could provide useful insights into the effects of PL on structure and activity of PPO. To this aim, the effect of PL on the structure and enzymatic activity of PPO in model solution was investigated.

**Results and discussion**

Aqueous solutions containing considerably different amounts of PPO (4.0 or 30.0 U), which mimic the actual amount of this enzyme in real foods, were prepared. The solutions were exposed to PL with increasing fluence up to 15.75 J $cm^{-2}$. Upon these intense treatments, a slight increase in temperature was detected. However, sample temperature never exceeded 36.0±0.7 °C, suggesting minor effects of temperature increase on PPO inactivation. The effect of pulsed light on PPO structure and function was assessed by evaluating molecular changes by HPLC gel-permeation and enzymatic activity. Table 3.1 shows the evolution of the areas of the peaks detected in the chromatograms of the aqueous solutions containing 4.0 U of enzyme as a function of the light fluence received during the pulsed light treatment.

**Table 3.1** Peak areas (±SD) relevant to HPLC-gel permeation analysis of a 4.0 U polyphenoloxidase solution as a function of the pulsed light fluence.

| Fluence (J cm$^{-2}$) | Peak area (arbitrary units x 1000) | | | | | | |
|---|---|---|---|---|---|---|---|
| | Peak 1 (rt=16.8) | Peak 2 (rt=23.7) | Peak 3 (rt=26.4) | Peak 4 (rt=27.9) | Peak 5 (rt=32.4) | Peak 6 (rt=34.2) | Peak 7 (rt=36.6) |
| 0.00 | 2.6 ± 0.4 | 32.3 ± 3.1 | 24.5 ± 4.1 | 8.9 ± 1.1 | 19.5 ± 2.8 | 17.1 ± 2.1 | 8.1 ± 0.3 |
| 0.40 | 2.2 ± 0.9 | 33.8 ± 1.4 | 23.5 ± 0.6 | 5.7 ± 1.0 | 19.1 ± 3.2 | 19.6 ± 2.3 | 9.7 ± 0.6 |
| 1.75 | 2.3 ± 0.7 | 28.8 ± 0.8 | 11.6 ± 3.4 | 3.0 ± 1.6 | 20.3 ± 2.2 | 19.8 ± 1.5 | 11.2 ± 1.1 |
| 5.25 | 5.0 ± 1.3 | 22.3 ± 1.1 | 9.1 ± 1.7 | 2.7 ± 1.2 | 22.1 ± 2.7 | 22.9 ± 2.0 | 11.7 ± 0.9 |
| 8.75 | 5.6 ± 0.9 | 14.1 ± 3.7 | 6.1 ± 1.3 | 0.4 ± 0.1 | 31.2 ± 3.8 | 34.4 ± 2.7 | 18.3 ± 1.6 |
| 12.25 | 2.2 ± 0.8 | 8.0 ± 3.0 | 4.1 ± 1.6 | 0.1 ± 0.1 | 29.3 ± 1.4 | 35.5 ± 3.1 | 15.8 ± 1.5 |
| 15.75 | n.d. | 6.9 ± 1.7 | 4.6 ± 1.5 | n.d. | 20.9 ± 3.9 | 32.3 ± 2.4 | 13.8 ± 1.3 |

n.d.: Not detectable; rt: retention time

Seven peaks (peak 1, 2, 3, 4, 5, 6 and 7), having retention times 16.8, 23.7, 26.4, 27.9, 32.4, 34.2, and 36.6 min, were observed. Apparent molecular weights of proteins eluted in peaks 2, 3 and 4 were recognised as the tetrameric, dimeric and monomeric forms of the quaternary structure of PPO, which have molecular weights of 130.0, 65.0, and 32.5 kDa, respectively (Martinez & Whitaker, 1995). It can be noted that the areas of peaks 2, 3, and 4 progressively decreased with the increase in the pulsed light fluence. Exposure of PPO to pulsed light also resulted in the modification of the area of peak 1. Such peak was associated to a molecule, whose short retention time could account for protein unfolding/aggregation. A certain amount of denatured protein was actually present also in the untreated solution, probably as a consequence of enzyme extraction operations. However, exposure to PL resulted in the increase of the peak area relevant to this protein fraction, which reached a maximum value upon 8.75 J cm$^{-2}$ treatment. On further pulsing, a decrease in the area of this peak was then observed, so that peak 1 became not detectable in the 15.75 J cm$^{-2}$ treated sample. A similar evolution, although with a maximum value at slightly different fluence, was also observed for the areas of peaks 5, 6, and 7. The latter are relevant to molecular species with longer retention time and apparent molecular weight around 5 kDa. The peak areas of these protein fragments reached a maximum value in the samples treated at about 10 J cm$^{-2}$ fluence. Also in this case, a further increase in PL intensity promoted the degradation of the protein fragments eluted in these peaks.

As already mentioned in Chapter 1.3, photo-degradation of proteins proceeds through aggregation and cleavage phenomena. The former are the result of cross-linking reactions involving aminoacid residues. In fact, upon photo-oxidation, His can easily react with other aminoacid residues to give cross-links (Shen, Spikes, Smith, & Kopeček, 2000). Besides, light can affect the structure of proteins via

photo-excitation of Trp, Tyr, Phe, Met and Cys groups inducing the reduction of disulphide (S-S) bonds (Davies & Truscott, 2001). The breakage of disulphide bonds would directly disturb the protein structure causing a loss in its biologic activity. However, the new generated thiol groups can further react to form either intermolecular S-S bonds responsible for aggregation (Wu, Sheng, Xie, & Wang, 2008), or protein radicals that are potential progenitors of backbone fragmentation (Davies & Truscott, 2001).

The results acquired by HPLC-gel permeation analysis (Table 3.1) suggest PL to promote modifications of the structure of PPO by inducing both unfolding/aggregation phenomena and protein backbone cleavage. However, denatured proteins (peak 1) as well as their fragments (peaks 5, 6 and 7) can react on further light pulsing. In other words, high fluence treatments could lead to the degradation of the unfolded and cleaved proteins produced at lower fluences. Protein unfolding and aggregation have been previously reported for PPO exposed to continuous UV light (Manzocco, Quarta, et al., 2009). However, in that case, no degradation of the newly formed large protein was detected. It is thus possible that pulsed light could promote PPO degradation *via* reaction pathways other than those characterising UV treatments. Conversely, it is also possible that similar mechanisms are involved but fluence strongly affect the overall extent of protein degradation.

HPLC-gel permeation analysis were also performed on the aqueous solutions containing 30.0 U of enzyme and exposed to pulsed light (Table 3.2).

**Table 3.2** Peak areas (±SD) relevant to HPLC-gel permeation analysis of a 30.0 U polyphenoloxidase solution as a function of the pulsed light fluence.

| Fluence ($J\ cm^{-2}$) | Peak area (arbitrary units x 1000) | | | | | | |
|---|---|---|---|---|---|---|---|
| | Peak 1 (rt=16.8) | Peak 2 (rt=23.7) | Peak 3 (rt=26.4) | Peak 4 (rt=27.9) | Peak 5 (rt=32.4) | Peak 6 (rt=34.2) | Peak 7 (rt=36.6) |
| 0.00 | 31.6 ± 1.8 | 304.1 ± 6.6 | 404.4 ± 1.5 | 41.6 ± 1.5 | 12.2 ± 0.2 | 10.3 ± 1.8 | n.d. |
| 0.40 | 30.3 ± 3.3 | 303.5 ± 10.4 | 392.8 ± 9.2 | 46.9 ± 3.5 | 16.8 ± 1.3 | 10.2 ± 0.2 | n.d. |
| 1.75 | 34.7 ± 3.8 | 261.4 ± 3.8 | 116.0 ± 5.1 | 37.4 ± 0.8 | 14.4 ± 1.1 | 11.8 ± 0.5 | 2.4 ± 0.9 |
| 5.25 | 30.6 ± 2.7 | 201.0 ± 2.2 | 58.4 ± 2.6 | 21.3 ± 0.3 | 12.3 ± 0.2 | 16.9 ± 2.8 | 4.6 ± 0.9 |
| 8.75 | 24.2 ± 1.9 | 155.2 ± 3.4 | 56.3 ± 1.3 | 15.9 ± 0.3 | 10.2 ± 07 | 17.4 ± 0.2 | 4.7 ± 1.8 |
| 12.25 | 24.2 ± 2.3 | 84.1 ± 2.9 | 57.0 ± 2.1 | 13.8 ± 0.5 | 17.6 ± 1.1 | 34.2 ± 0.5 | 9.9 ± 0.1 |
| 15.75 | 27.8 ± 2.6 | 45.4 ± 0.7 | 54.7 ± 2.4 | 7.9 ± 0.6 | 17.7 ± 1.3 | 34.4 ± 1.5 | 10.1 ± 0.1 |

n.d.: not detectable; rt: retention time

By comparing the peak areas of the untreated samples (0 $J\ cm^{-2}$) containing 30.0 or 4.0 U of PPO (Table 3.2 and 3.1, respectively), a marked difference in the relative abundance of the protein eluted in the different peaks can be observed. In

fact, while the tetrameric structure of PPO (peak 2) was the most abundant in the 4.0 U sample, the dimeric one (peak 3) was favoured in the 30.0 U sample. The latter, despite its almost ten-fold higher concentration, also showed a lower amount of small proteins (peaks 5, 6 and 7) than that observed in the solution containing 4.0 U of enzyme (Table 3.1). It was hypothesised that self crowding of proteins promotes specific conformational structures, which are reasonably those allowing the excluded volume to be reduced. In other words, crowding conditions would favour compact protein structures, while hindering dissociation phenomena. In the crowded environment of the 30.0 U samples, photo-degradation of aggregates eluted in peak 1 was limited and protein fragments moderately increased upon light exposure. It can be inferred that, in this condition, polyphenoloxidase photo-degradation mainly occurred through intramolecular reactions with minor contribution of cross-linking among vicinal proteins. However, it is not excluded that in crowded conditions, shadowing effects could play a critical role on protein photosensitivity. In fact, the effect of light is known to be reduced by any body between target object and light source. For instance, microorganisms can be protected from the germicidal effect of light by other cells, as occurs when biofilms are formed (Sommers, Sites, & Musgrove, 2010). Analogously, proteins could protect each other from light according to local shadowing effects. In this way, molecules placed at the surface of the sample would represent a physical screen for the internal ones, preventing their photoreaction.

To understand the effect of PL induced structure modification on protein function, enzymatic activity of the solutions containing 4.0 and 30.0 U of PPO was measured. PPO activity was assessed by regression analysis of changes in absorbance at 420 nm as a function of time ($R^2$>0.98; P<0.05). Results are reported in table 3.3.

**Table 3.3** Residual activity (±SD) of 4.0 or 30.0 U polyphenoloxidase solution as a function of the pulsed light fluence.

| Fluence (J cm$^{-2}$) | Activity (%) | |
|---|---|---|
| | 4.0 U | 30.0 U |
| 0.00 | 100±1.4 | 100±3.2 |
| 0.40 | 45.1±4.0 | 63.2±0.8 |
| 1.75 | 7.6±0.6 | 23.4±1.6 |
| 5.25 | 2.5±2.1 | 8.2±0.9 |
| 8.75 | n.d. | n.d. |
| 12.25 | n.d. | n.d. |
| 15.75 | n.d. | n.d. |

n.d.: not detectable

Table 3.3 shows that PPO activity decreased with the increase in PL fluence. In addition, no residual activity was detected in samples exposed to fluence equal or higher than 8.75 J $cm^{-2}$. These results are consistent with the decrease in the peaks relevant to tetrameric, dimeric, and monomeric PPO fractions (peaks 2, 3, and 4) observed by HPLC gel permeation analysis (Tables 3.1 and 3.2). In fact these protein fractions are generally recognised as those having enzymatic activity (Martinez & Whitaker, 1995). Samples showing no residual activity were also stored for one week at 4 °C and reassessed for enzyme activity. Data not shown indicate that the enzyme was unable to recover its activity. These results confirm that intense pulsed light treatments can irreversibly and completely inactivate PPO in model solutions.

To better understand the effect of crowding on PPO photosensitivity, aqueous solutions containing increasing units of enzyme (from 4.0 to 46.0 U) were prepared and exposed to one pulse of light with different fluence at room temperature (22.1±0.4 °C). In this case, lower PL fluence values were chosen to better appreciate the inactivation effect of processing on PPO. The temperature of the samples was measured just after the treatment and did not exceed 23.4 ± 0.7 °C. Based on this evidence, PPO inactivation should be mainly attributed to the effect of light exposure. As expected, the activity of PPO progressively decreased as the fluence of the light pulse increased (Fig. 3.1).

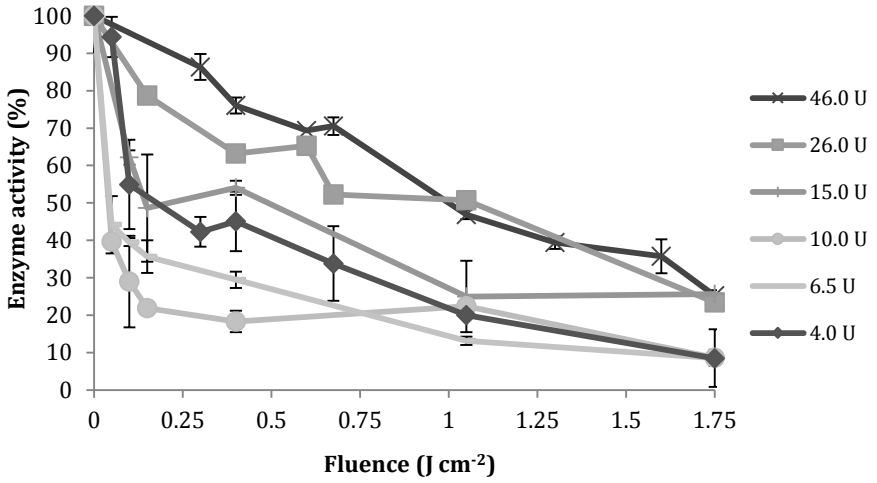


**Figure 3.1** Residual activity of solutions containing different PPO units as a function of PL fluence. Bars represent standard deviation of residual activity value.

The effect of pulsed light on PPO activity strongly depended on the initial amount of the enzyme in the solution. For instance, the activity of the solution containing 10.0 U of PPO quickly decreased by exposure to low fluence pulses, and reached an almost constant value on further increase in the pulse fluence. By contrast, the solutions containing 26.0 or 46.0 U of PPO showed a progressive activity decrease according to a straight line in the entire tested fluence range.

In order to evidence the relation between the inactivation effect of pulsed light and the amount of enzyme in the aqueous solution, the photostability of PPO was calculated. To this aim, regression analysis of enzymatic activity data reported in Fig. 3.1 was performed as a function of pulsed light fluence considering data relevant to the linear part of the curve.

Regression coefficients data were used to calculate the photostability of PPO ($F_{50}$, J $cm^{-2}$). A low value of $F_{50}$ indicates PPO to be easily denatured by pulsed light. By contrast, higher values of $F_{50}$ account for intense resistance of the enzyme to pulsed light. Fig. 3.2 shows the $F_{50}$ values of PPO in aqueous solutions containing increasing units of enzyme.

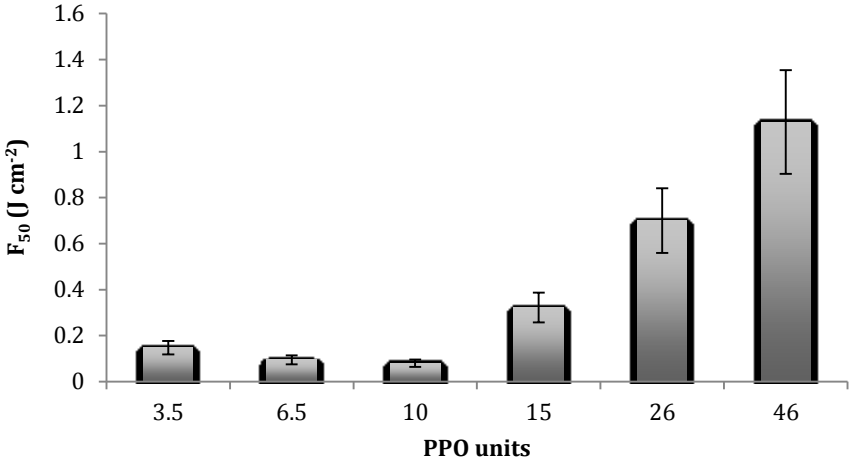


**Figure 3.2** Photostability, expressed as fluence required to reduce the original PPO activity by 50% ($F_{50}$), of solutions containing different PPO units.

PPO solutions containing 4.0, 6.5 and 10.0 U of enzyme resulted particularly sensitive to pulsed light. In other words, these samples lost 50% of their activity upon exposure to a light fluence approaching 0.1 J $cm^{-2}$. On the contrary, samples containing higher (15.0, 26.0 or 46.0 U) amounts of enzyme presented higher photostability. In fact, a fluence higher than 0.30 J $cm^{-2}$ was required to produce a 50% decrease in PPO activity. The dependence of PPO photostability on the

amount of the enzyme in the solution is in accordance with previous literature data showing that protein concentration can strongly affect their photosensitivity (Manzocco & Nicoli, 2012). For instance, no photodegradation of egg white was reported in systems having concentration higher than the critical concentration C* which accounts for the quantity of proteins that can be accommodated in a given volume of solution without mutual perturbation (Lapasin & Pricl, 1995). Beyond this specific concentration, the system can be considered crowded. According to the literature (Ellis & Minton, 2006; Minton, Karmin, Hahn, & Minton, 1982; van den Berg, Ellis, & Dobson, 1999; van den Berg, Wain, Dobson, & Ellis, 2000), crowding of proteins in water solutions could control protein structure modifications by accelerating their folding and aggregation. It is thus possible that macromolecular crowding could favour specific protein conformations, potentially modifying their sensitivity to structural modifications caused by physical stresses. Based on these considerations, it can be inferred that self crowding of PPO, and thus protein vicinity in the aqueous solution, could increase their photostability. However, as stated before, shadowing effects of protein in crowded environment cannot be completed neglected.

**Conclusions**

Present results demonstrate that PL allows the inactivation of PPO in model solution as a consequence of protein structure modifications. The PPO sensitivity to PL strongly depended, not only on PL intensity, but also on the enzyme concentration. The vicinity of the enzyme molecules in the solution favours specific protein conformations. At concentrations up to 10 U, PPO would be easily inactivated because proteins could undergo both intramolecular modification and photoreaction with surrounding molecules. By contrast, at higher concentrations, protein vicinity could favour conformations having lower photosensitivity, probably because less prone to intermolecular rearrangements. These results suggest that the intensity of PL treatment is not the only factor determining the extent of protein modification. In fact, environmental factors, such as protein vicinity, can also play an important role on the reactions of protein upon PL exposure.

# *Chapter 4 Effect of light processing on egg white*

## 4.1 Effect of UV-C on egg white proteins

### Aim of the study

This chapter is focused on the effect of UV-C light processing on egg white, which was chosen as a matrix composed of a mix of globular proteins. Egg white is extensively used as a food ingredient in a variety of food formulations, due to its multifunctional properties. In fact, egg white is mainly composed of globular proteins, which are characterised by excellent foaming and gelling properties, in addition to their high nutritional value (Mine, 1995). Unfortunately, beside these outstanding technological performances, egg white proteins are also responsible for allergenic reaction, mostly in children (Mine & Yang, 2008).

Since egg white is highly susceptible to microbial contamination, liquid egg white must be processed to guarantee its safety. Normally, heat pasteurization is required to control spoilage microorganisms and pathogens. *Salmonella*, mainly the egg-associated serotype Enteritidis, is the pathogen of concern (USDA-ARS 74-48, 1969; European Regulation CEE 1441/2007; Code of Federal Reulations, 2010). Despite pasteurisation of egg white is performed at temperatures which allow protein coagulation to be prevented, heat treatment can easily impair protein functional properties. In this context, UV-C light treatments can represent an attractive non-thermal alternative to conventional thermal processing for microbial inactivation (de Souza & Fernández, 2011; Geveke & Torres, 2013; Geveke, 2008; Unluturk, Atilgan, Baysal, & Unluturk, 2010; Unluturk, Atilgan, Handan Baysal, & Tari, 2008). Besides the sanitisation effect, UV-C light processing is particularly interesting thanks to its potential ability to alter the structure of proteins with consequent modification of their functions. For instance, UV-C treatments were reported to increase the tensile strength of gluten, zein, and albumin films, as a consequence of photocrosslinking (Rhim et al., 1999). Irradiated fish gelatin exhibited higher gel strength, marked reduction in viscosity, and significant changes in melting temperatures (Bhat & Karim, 2009). Photocrosslinking of egg white protein and sodium caseinate was associated to improved emulsifying and foaming properties (Kuan et al., 2011). With regard to protein biologic activity, ultraviolet exposure was demonstrated to reduce the catalytic activity of different enzymes and the immunoreactivity of allergenic proteins by promoting protein aggregation and/or backbone fragmentation (Guerrero-Beltrán & Barbosa-Cánovas, 2006; Manzocco, Dri, et al., 2009;

Manzocco & Nicoli, 2012; Manzocco, Quarta, et al., 2009). The aim of the present study was thus to investigate the effects of UV-C processing on egg white protein structure and selected functional properties.

**Results and discussion**

Egg white was exposed to UV-C light with increasing fluence in a thermostated chamber at 8 °C. Structure characteristics of untreated and UV-C treated samples were then analyzed. In Table 4.1.1 results relevant to absorbance at 280, 380 and 680 nm, hydrodynamic radius and percentage of particles, as well as free sulfhydryl groups concentration are reported.

**Table 4.1.1** Absorbance at 280, 380 and 680 nm, hydrodynamic radius, percentage of the main particle fraction, and concentration of free sulfhydryl groups in egg white exposed to increasing UV-C light fluence (0, 1.06, 6.37 J $cm^{-2}$) at 8 °C.

| | | Fluence (J $cm^{-2}$) | | |
|---|---|---|---|---|
| | | 0 | 1.06 | 6.37 |
| Absorbance | 280 nm | 1.089 ± 0.002 $^{c}$ | 1.096 ± 0.003 $^{b}$ | 1.184 ± 0.011 $^{a}$ |
| | 380 nm | 0.008 ± 0.001 $^{c}$ | 0.011 ± 0.001 $^{b}$ | 0.032 ± 0.008 $^{a}$ |
| | 680 nm | 0.194 ± 0.002 $^{c}$ | 0.201± 0.002 $^{b}$ | 0.293 ± 0.012 $^{a}$ |
| Hydrodynamic radius (nm) | | 5.7 ± 0.1 $^{c}$ | 9.9 ± 1.8 $^{b}$ | 13.9 ± 3.5 $^{a}$ |
| Particles (%) | | 99.8 ± 0.1 $^{a}$ | 98.8 ± 0.7 $^{b}$ | 95.9 ± 1.5 $^{c}$ |
| Free SH groups (μM $g^{-1}$) | | 40.5 ± 2.1 $^{b}$ | 30.4 ± 3.8 $^{c}$ | 52.7 ± 1.1 $^{a}$ |

$^{a,b,c}$ for each property, means indicated by the same letter are not significantly different ($P$>0.05).

Egg white showed a progressive increase in absorbance at 280 nm with UV-C fluence. This result apparently contradicts literature evidences indicating that intense UV irradiation of protein solutions can cause a decrease in absorbance at this wavelength as a consequence of oxidation of Trp chromophores (Wu et al., 2008). It can be hypothesized that the bleaching of Trp residues in light treated egg white was probably counterbalanced by the occurrence of other reactions. The increase in absorbance at 280 nm could be actually attributed to the formation of early non enzymatic browning reaction products (Rizzi, 1994). This hypothesis is supported by the concomitant increase in absorbance at 380 nm, which is consistent with the formation of brown melanoidins (Rizzi, 1994). Literature data actually indicates that UV irradiation of model systems containing aminoacids and reducing sugars is associated to the formation of a number of different Maillard reaction products (Sheldon, Jones, & Shibamoto, 1988).

Egg white exposed to UV light appeared more turbid as shown by the increase in absorbance at 680 nm as well as by the dimension of protein particles (Table 4.1.1). Dynamic light scattering analysis of fresh egg white showed the

prevalence of protein particles with average hydrodynamic radius equal to 5.7 nm. Upon light exposure, the size of this class of protein particles increased up to 13.9 nm. However the percentage of these particles decreased due to the presence of a novel class of particles with hydrodynamic radius higher than 100 nm. The latter were found to approach 4% of the overall particles after 6.37 J $cm^{-2}$ UV processing. The presence of high size particles, in combination with the increase in turbid appearance, validates the formation of protein aggregates as a consequence of structural modifications of egg white proteins upon light treatment. To investigate the nature of these structural modifications, samples were analysed for the concentration of free sulfhydryl groups (SH). In fact, based on literature data, the decrease in free SH could indicate protein cross-linking, while their increase generally accounts for both protein unfolding and backbone fragmentation (Beveridge et al., 1974). In the case of UV treated egg white (Table 4.1.1), the concentration of free SH decreased after exposure to 1.06 J $cm^{-2}$ and increased upon exposure to 6.37 J $cm^{-2}$. These data suggest that the structural modification induced by UV radiation may be rather complex, potentially involving more than one mechanism of denaturation. According to several authors (Davies & Truscott, 2001; Wu, Sheng, Xie, & Wang, 2008), and similarly to what observed for PL-treated PPO (Chapter 3, Tables 3.1 and 3.2), light exposure can induce protein structure modifications by means of both unfolding/aggregation phenomena and cleavage. On the basis of these considerations, it can be inferred that the decrease in free SH concentration of egg white exposed to 1.06 J $cm^{-2}$ UV-C light (Table 4.1.1) could be attributed to partial unfolding and subsequent formation of S-S bonds. However, disulphides have also been reported to further dissociate, in a reversible reaction, to give free SH groups (Davies & Truscott, 2001). Consequently, the energy received by egg white upon exposure to 6.37 J $cm^{-2}$ UV-C light could be sufficient to cleave native and light-induced S-S bonds, giving reason to the increase in free SH groups reported in Table 4.1.1.

In order to confirm this hypothesis, specific information about the light-induced structural modifications of egg white proteins were obtained by HPLC-gel permeation analysis. The chromatogram relevant to the freshly prepared egg white showed the presence of five main peaks with retention time of 20.08, 24.8, 27.3, 31.0 and 37.0 min. By comparison of molecular weight, they were attributed to ovomucin (peak 1), ovotransferrin (peak 2), ovalbumin (peak 3), ovomucoid (peak 4) and lysozyme (peak 5) respectively (Awadé & Efstathiou, 1999; Mine, 1995). Table 4.1.2 shows the evolution of the area of the peaks detected in the chromatograms of egg white proteins as a function of their exposure time to UV radiation.

**Table 4.1.2** Peak areas relevant to HPLC-gel permeation analysis of egg white exposed to increasing UV-C light fluence (0, 1.06, 6.37 J $cm^{-2}$) at 8 °C.

| Peak | Retention time (min) | Protein | Peak area (arbitrary units x 1000) | | |
|---|---|---|---|---|---|
| | | | 0 J $cm^{-2}$ | 1.06 J $cm^{-2}$ | 6.37 J $cm^{-2}$ |
| 1 | 20.1 | Ovomucin | $691.4 \pm 301.3^{ab}$ | $303.8 \pm 175.9^{b}$ | $888.1 \pm 283.1^{a}$ |
| 2 | 24.8 | Ovotransferrin | $416.8 \pm 84.9^{c}$ | $937.4 \pm 376.7^{b}$ | $2344.8 \pm 742^{a}$ |
| 3 | 27.3 | Ovalbumin | $22007.6 \pm 161.9^{a}$ | $22048.8 \pm 2901.7^{a}$ | $22553.7 \pm 3372.2^{a}$ |
| 4 | 31.0 | Ovomucoid | $20.3 \pm 16^{a}$ | $15.1 \pm 2.8^{b}$ | $16.4 \pm 2.2^{b}$ |
| 5 | 37.0 | Lysozyme | $1252.2 \pm 142.1^{a}$ | $722.3 \pm 16.5^{b}$ | $287.4 \pm 25.8^{c}$ |
| 6 | 18.2 | Protein 1 | n.d. | $374.3 \pm 98.4^{b}$ | $1158.2 \pm 451.4^{a}$ |
| 7 | 35.1 | Protein 2 | $7.6 \pm 1.1^{b}$ | $15.3 \pm 1.5^{a}$ | $11.9 \pm 2.5^{a}$ |
| 8 | 41.9 | Protein 3 | n.d. | n.d. | $7.2 \pm 10.2^{a}$ |

$^{a,b,c}$ for each peak, means indicated by the same letter are not significantly different ($P>0.05$).
n.d. not detected.

Upon light exposure, peak areas of ovalbumin, ovomucin and ovomucoid did not show marked changes. Light exposure significantly affected only the areas of peaks relevant to lysozyme and ovotransferrin. In particular, the peak area of lysozyme progressively decreased while that associated to ovotransferrin increased. These data indicate that egg white proteins are not similarly sensitive to light exposure. Lysozyme seems particularly susceptible to structural modifications caused by light exposure. As regards the increase in the peak area of ovotransferrin, it is hardly believable that the presence of this protein could increase as a consequence of light treatment. Rather molecules having apparent molecular weight similar to ovotransferrin could occur due to unfolding or aggregation of other proteins. Exposure of egg white to UV light was actually associated to the appearance of a novel peak with very short retention time as compared to that of all other proteins detected in the untreated sample (Peak 6). Such peak was associated to a molecule, whose short retention time could be attributed to protein aggregation/unfolding. Actually its apparent molecular weight could be roughly estimated to be around 600 kDa. The presence of this peak is consistent with the occurrence of particles with hydrodynamic radius higher than 100 nm as well as with the decrease of free SH groups after 5 min of exposure (Table 4.1.1). The peak area of two additional peaks (peak 7 and peak 8), relevant to molecular species with longer retention time, and thus lower apparent molecular weight, was also found to increase with exposure time. These species were not detected by light scattering analysis, probably because they were masked by the bigger ones. These results confirm that UV-C radiation promotes

egg white protein modification inducing not only unfolding/aggregation phenomena but also protein backbone cleavage.

As observed by many authors, the modification of protein structure and the formation of Maillard reaction products could affect protein allergenicity (Chen & Phillips, 2005; Gruber, Vieths, Wangorsch, Nerkamp, & Hofmann, 2004; Taheri-Kafrani et al., 2009). Anugu, Yang, Shriver, Chung, & Percival (2010) reported that pulsed UV light treatment allowed the allergenicity of isolated egg white proteins to be reduced. Based on these considerations, egg white samples submitted to UV light treatment were analysed for immunoreactivity by an ELISA method. No differences in immunoreactivity were observed between egg white exposed to UV light and the untreated one (data not shown). This suggests that light-induced structural modifications do not affect the conformation of the protein epitopes. Actually, ovalbumin and ovomucoid, which are known to be the major allergens of egg white (Hoffman, 1983; Langeland, 1982; Mine & Yang, 2008), resulted to be scarcely sensitive to UV radiation (Table 4.1.2).

To understand whether the changes in egg white protein structure upon light exposure could be associated also to modifications in their technological performances, samples exposed to UV light were also analysed for apparent viscosity, gelling and foaming properties (Table 4.1.3).

**Table 4.1.3** Gelling temperature, gel firmness, apparent viscosity, foam volume and foam stability in egg white exposed to increasing UV-C light fluence (0, 1.06, 6.37 J $cm^{-2}$) at 8 °C.

| | Fluence (J $cm^{-2}$) | | |
|---|---|---|---|
| | 0 | 1. 06 | 6.37 |
| Gelling temperature (°C) | 70.6±1.2[a] | 68.3±0.7[a] | 69.4±0.6[a] |
| Gel firmness (N) | 0.084 ± 0.010[a] | 0.081 ± 0.010[a] | 0.082 ±0.006[a] |
| Apparent viscosity (Pa s) | 0.21±0.02[b] | 0.43±0.03[a] | 0.24±0.04[b] |
| Foam volume (mL) | 16.5 ± 2.1[b] | 19.5 ± 0.7[a] | 14.0 ± 1.4[b] |
| Foam stability (%) | 87.5 ± 0.7[b] | 94.9 ± 0.8[a] | 93.3 ± 0.8[a] |

[a,b] for each property, means indicated by the same letter are not significantly different ($P$>0.05).

Gelling temperature and gel firmness were not affected by light exposure. By contrast, apparent viscosity, taken as an indicator of the rheological behaviour of egg white, was found to significantly increase after exposure to 1.06 J $cm^{-2}$ UV-C light. A decrease in this property was detected on further exposure so that the sample treated at 6.37 J $cm^{-2}$ presented apparent viscosity similar to the control. It can be hypothesized that light modified proteins could interact resulting in a weak and unstable protein network, justifying the increase in apparent viscosity at intermediate electromagnetic energy levels. The structural continuity of this weak

network would be probably interrupted by the presence of large protein clusters and small fragments formed upon exposure to higher UV-C light fluence (6.37 J $cm^{-2}$). Table 4.1.3 also shows that 1.06 J $cm^{-2}$ UV-C light exposure increased the volume of the foam produced by egg white whipping. A more intense treatment was associated to a foam volume similar to that produced by the untreated egg white. Changes in the white colour of the foams could not be observed with the naked eye. However, foam prepared from egg white exposed to both 1.06 and 6.37 J $cm^{-2}$ UV light appeared moist and creamy, contrasting with the brittle and dry appearance of those prepared from untreated egg white. Micrographs of just prepared foams and of foams held for 30 min at 20 °C are shown in Fig 4.1.1.

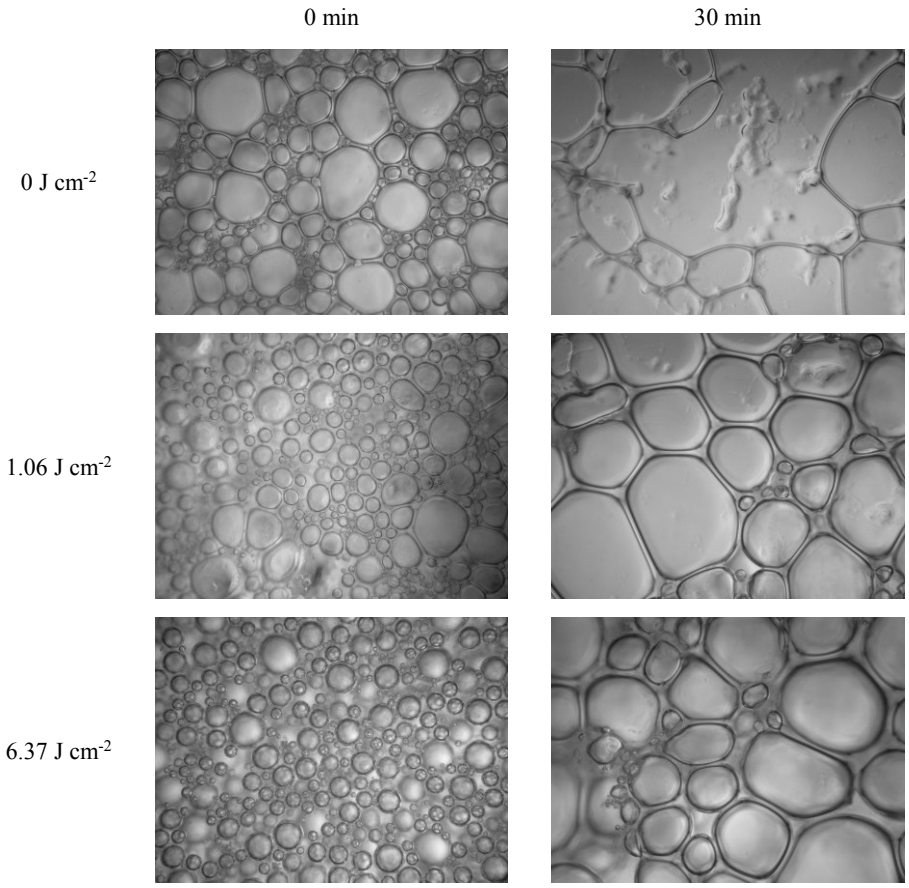


**Figure 4.1.1** Micrographs (100x) of just prepared and 30 min held foams obtained from egg white exposed to increasing UV-C light fluence (0, 1.06, 6.37 J $cm^{-2}$) at 8 °C.

Foam micrographs were analysed for bubble diameter. These data were used to cluster bubbles in three different categories according to their diameter: small (diameter lower than 0.05 mm), medium (diameter from 0.05 to 0.1 mm) and large (diameter higher than 0.1 mm) bubbles. Table 4.1.4 shows the percentage of small, medium and large bubbles in the foams obtained from untreated and UV-processed egg white, just after whipping and 30 min after whipping.

**Table 4.1.4** Percentage of small (diameter lower than 0.05 mm), medium (diameter from 0.05 to 0.1 mm) and large (diameter higher than 0.1 mm) bubbles in foams obtained from egg white exposed to increasing UV-C light fluence (0, 1.06, 6.37 J $cm^{-2}$) at 8 °C. Bubble percentage was calculated in just whipped foams and after 30 min from whipping.

| Fluence (J $cm^{-2}$) | Time after whipping (min) | Bubbles (%) | | |
|---|---|---|---|---|
| | | Small | Medium | Large |
| 0 | 0 | 45.84 | 20.83 | 33.33 |
| | 30 | 1.26 | 20.75 | 77.99 |
| 1.06 | 0 | 55.36 | 41.07 | 3.53 |
| | 30 | 9.53 | 28.57 | 61.90 |
| 6.37 | 0 | 75.34 | 20.55 | 4.11 |
| | 30 | 23.53 | 35.29 | 41.18 |

Foams obtained from UV treated egg white presented a remarkably lower percentage of large bubbles as compared to the control. Accordingly, a higher percentage of small bubbles was measured. The latter increased with the intensity of the ultraviolet treatment. As expected, after a 30 min rest at 20 °C, small bubbles decreased concomitantly with the increase in large bubbles in all foams. However, UV exposed egg white showed a lower tendency to bubble dismutation and coalescence, leading to a lower presence of large bubbles. Actually, foams obtained from UV treated egg white presented significantly higher stability (Table 4.1.3). The peculiar properties of the foams obtained from UV processed egg white could be reasonably explained based on two different mechanisms. Light modified proteins could form a better interfacial network during foaming. This effect would be particularly important in the sample exposed to 1.06 J $cm^{-2}$. In fact, the higher apparent viscosity of egg white could increase the viscoelasticity of the aqueous phase at the interface. Secondly, it can be inferred that high size protein aggregates, which are abundant after exposure to 6.37 J $cm^{-2}$ UV light (Table 4.1.2), could behave as surface-active solid particles begetting a pickering foam (Pickering, 1907). The latter would be stabilized not only by the surfactant native proteins but also by the solid protein aggregates. As suggested by Murray, Durga, Yusoff, & Stoyanov, (2011), native proteins and solid particles could

attract each others, increasing the particle jamming in the fluid interstices between bubbles. This would cause the formation of a firmer shell, positively affecting foaming properties.

**Conclusions**

Similarly to what previously observed for PL treated PPO, results obtained suggest that UV-C light processing performed under the tested experimental conditions can modify egg white protein structure by both backbone cleavage and aggregation phenomena. These structural modifications were not sufficient to induce changes in egg white gelling properties. By contrast, an improvement in egg white foaming properties was observed upon exposure to UV-C light. This effect was attributed to the modification of the viscoelastic behaviour of egg white. With regard to biological functions, no changes in egg white proteins immunoreactivity were observed upon UV-C light exposure. This result, in contrast with the inactivation of PPO observed upon PL exposure, can be explained by the higher concentration of proteins in egg white as compared to PPO in model solutions.

## 4.2 Effect of PL on egg white proteins

### Aim of the study

This chapter deals with the effect of PL processing on egg white protein structure and functions. Similarly to UV-C treatments, PL processing can also be regarded as an attractive non-thermal alternative to conventional thermal processing for microbial inactivation of different food products (Caminiti et al., 2011; Choi, Cheigh, Jeong, Shin, & Chung, 2010b; Hierro et al., 2011, 2009; Palgan et al., 2011; Ramos-Villarroel et al., 2011; Ramos-Villarroel, Aron-Maftei, Martín-Belloso, & Soliva-Fortuny, 2012; Wuytack et al., 2003). In addition to microbial inactivation PL treatments were demonstrated to modify the structure and thus potentially the functions of several proteins. As an example, PL was shown cause milk protein aggregation by disulphide bonds without further significant changes in protein components (Elmnasser et al., 2008). Fernández et al. (2012) showed that pulsed light induced conformational changes in β-lactoglobulin, enhancing its absorption rate at the air/water interface. In addition, β-lactoglobulin solutions treated with pulsed light formed highly elastic interfaces, resulting in more stable foams. With regard to protein biologic activity, exposure to pulsed light was shown to modify proteins that cause allergy. For instance, a decrease in the IgE binding capacity of liquid peanut butter, soybean extracts and egg white proteins was observed upon pulsed light treatment (Anugu et al., 2010; Chung et al., 2008; Yang et al., 2010). The loss of immunoreactivity was attributed to the formation of insoluble aggregates.

In addition, pulsed light was demonstrated to modify the catalytic activity of different enzymes (Charles et al., 2013; Oms-Oliu et al., 2010; Ramos-Villarroel et al., 2011). As discussed in Chapter 3, PL was found to reduce PPO enzymatic activity by inducing changes in protein structure. In particular, results acquired by HPLC-gel permeation analysis (Chapter 3, Table 3.1) suggest PL to promote modifications of the structure of PPO by inducing initially both unfolding/aggregation phenomena and protein backbone cleavage, and degradation of the unfolded and cleaved proteins produced at lower fluences on further pulsing. Protein unfolding and aggregation have been previously reported for PPO exposed to continuous UV light (Manzocco, Quarta, et al., 2009). However, in that case, no degradation of the newly formed large protein was detected. These results suggest that PL-induced and UV-C light-induced protein structure modifications proceed *via* different reaction pathways. Conversely, it is also possible that similar mechanisms are involved but light spectra and fluence

strongly affect the overall extent of protein degradation. For this reason, the effect of PL on egg white proteins was also investigated.

**Results and discussion**

Egg white was exposed to PL with increasing fluence, up to 31.50 J $cm^{-2}$, at room temperature. The untreated egg white was taken as control. Analogously to egg white samples exposed to UV-C light, PL-treated egg white samples were then analysed for structure characteristics.

Exposure to pulsed light was associated to significant changes in egg white absorbance at 280, 380 and 680 nm (Table 4.2.1).

**Table 4.2.1** Absorbance at 280, 380 and 680 nm of egg white exposed to pulsed light with increasing fluence.

| Fluence | Absorbance | | |
|---|---|---|---|
| (J $cm^{-2}$) | 280 nm | 380 nm | 680 nm |
| 0 | 1.099 $^{c}$ | 0.008 $^{f}$ | 0.194 $^{g}$ |
| 5.25 | 1.135 $^{b}$ | 0.029 $^{e}$ | 0.361 $^{f}$ |
| 10.50 | 1.205 $^{a}$ | 0.048 $^{c}$ | 0.608 $^{e}$ |
| 15.75 | 1.126 $^{b}$ | 0.053 $^{bc}$ | 0.991 $^{d}$ |
| 21.00 | 1.105 $^{c}$ | 0.056 $^{ab}$ | 1.002 $^{c}$ |
| 26.25 | 1.009 $^{d}$ | 0.060 $^{a}$ | 1.037 $^{b}$ |
| 31.50 | 0.944 $^{e}$ | 0.039 $^{d}$ | 1.203 $^{a}$ |

$^{a,b,c,d,e,f}$ for each property, means indicated by the same letter are not significantly different ($P$>0.05).

Independently on PL fluence, sample temperature never exceeded 40 °C for few seconds. With the samples being kept below this temperature, changes in absorbance should be attributed to the effect of pulsed light treatment solely. Sample absorbance was strongly affected by the PL fluence. In particular, an increase in egg white absorbance at 280 and 380 nm was detected up to 10.50 and 26.25 J $cm^{-2}$ respectively. The increase in absorbance at 280 nm can be attributed to the formation of early non-enzymatic browning reaction products. The latter would further react to produce brown melanoidins absorbing at 380 nm (Rizzi, 1994). Similarly to what observed for egg white exposed to UV-C light (Chapter 4.1, Table 4.1.1), it is likely that the UV component of pulsed light could contribute to induce the development of these reactions. However, the melanoidins formed by pulsed light treatment could be further degraded causing a maximum of absorbance at 380 nm in the sample exposed to 26.25 J $cm^{-2}$ PL (Table 4.2.1). This result is consistent with the well known capability of intense light to bleach pigments.

The decrease in absorbance at 280 nm of egg white exposed to PL with fluence higher than 10.50 J $cm^{-2}$ could also be explained based on oxidation of Trp

chromophores of proteins (Wu et al., 2008). The development of oxidative reactions could be directly involved in the occurrence of structural modifications of egg white proteins. This hypothesis is supported by the evidence that egg white exposed to pulsed light appeared more turbid, as shown by the progressive increase in absorbance at 680 nm (Table 4.2.1).

Dynamic light scattering analysis of fresh egg white showed the prevalence of protein particles with average hydrodynamic radius equal to 5.7 nm (Figure 4.2.1). Upon light exposure, the size of this class of protein particles increased up to 27.5 nm. However the percentage of these particles decreased due to the presence of a novel class of particles with hydrodynamic radius higher than 100 nm. The latter were found to approach 32% of the overall particles after exposure to 31.50 J $cm^{-2}$.

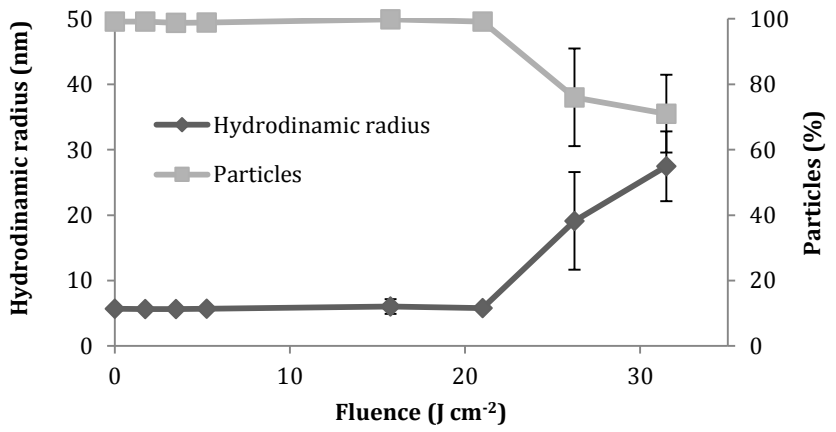


**Figure 4.2.1** Hydrodynamic radius and percentage of the main particle fraction in egg white exposed to pulsed light with increasing fluence.

The presence of high size particles, in combination with the increase in turbid appearance, validates the formation of protein aggregates as a consequence of structural modifications of egg white proteins exposed to pulsed light. To investigate the nature of these structure modifications, samples were analysed for concentration of free sulfhydryl groups (SH). In fact, based on literature data, the decrease in free SH could indicate protein cross-linking, while their increase generally accounts for both protein unfolding and backbone fragmentation (Beveridge et al., 1974). In the case of egg white exposed to pulsed light, the concentration of free SH increased up to 15.75 J $cm^{-2}$ (Figure 4.2.2).

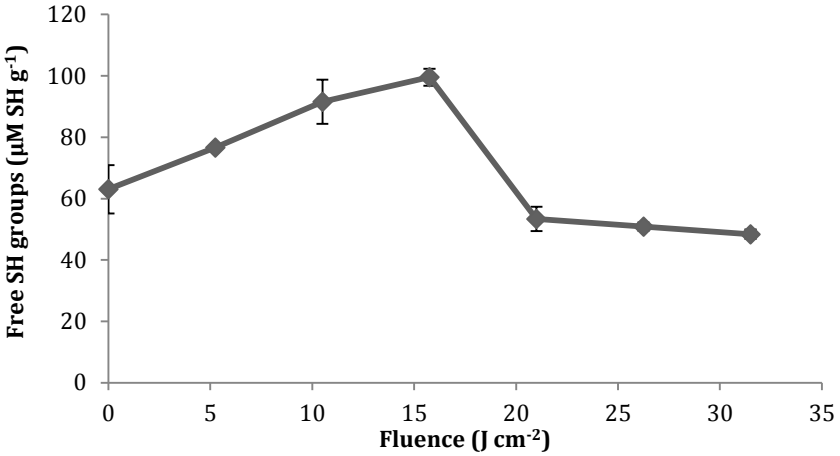


**Figure 4.2.2** Free sulfhydryl groups in egg white exposed to pulsed light with increasing fluence.

According to Wu et al. (2008), light would affect the structure of proteins inducing the reduction of disulphide (S-S) bonds and the formation of protein radicals. Based on these considerations, the initial increase in free SH groups could be attributed to the breakage of disulphide bonds, which would directly disturb the protein structure and promote its partial unfolding. On further pulsing, a decrease in free SH groups was observed. At these energy levels, pulsed light would favour the reaction between the new generated free thiol groups to form intermolecular S-S bonds as well as protein radicals (Wu et al., 2008). As previously observed considering the effect of PL and UV-C light on PPO and egg white, respectively, newly formed protein radicals could contribute to backbone fragmentation and/or formation of high molecular aggregates arising from radical termination reaction (Chapters 3, and 4.1, Tables 3.1, 3.2, and 4.1.1)

In order to confirm these hypotheses, specific information about the structural modifications induced by pulsed light treatment of egg white proteins was obtained by HPLC-gel permeation analysis. The chromatogram relevant to the freshly prepared egg white showed the presence of five main peaks with retention time of 20.1, 24.8, 27.3, 31.0 and 37.0 min. By comparison of molecular weight, they were attributed to ovomucin (peak 1), ovotransferrin (peak 2), ovalbumin (peak 3), ovomucoid (peak 4) and lysozyme (peak 5) respectively (Awadé & Efstathiou, 1999; Mine, 1995). Table 4.2.2 shows the evolution of the area of the peaks detected in the chromatograms of egg white proteins as a function of PL fluence.

**Table 4.2.2** Peak areas relevant to HPLC-gel permeation analysis of egg white exposed to pulsed light with increasing fluence (0, 5.25, 10.50, 15.75, 21.00, 26.25, 31.50 J $cm^{-2}$).

| Peak | R.t. (min) | Protein | Peak area (arbitrary units x 1000) | | | | | | |
|---|---|---|---|---|---|---|---|---|---|
| | | | 0 | 5.25 | 10.50 | 15.75 | 21.00 | 26.25 | 31.50 |
| 1 | 20.1 | Ovomucin | 691.4$^{a}$ | 184.8$^{b}$ | 209.1$^{b}$ | 184.7$^{b}$ | 3.7$^{c}$ | n.d. | n.d. |
| 2 | 24.8 | Ovotransferrin | 416.8$^{c}$ | 481.1$^{c}$ | 826.4$^{b}$ | 1044.3$^{a}$ | n.d. | n.d. | n.d. |
| 3 | 27.3 | Ovalbumin | 22007.6$^{a}$ | 23458.6$^{a}$ | 19820.2$^{a}$ | 17929.8$^{b}$ | 687.5$^{c}$ | 613.7$^{c}$ | 595.4$^{c}$ |
| 4 | 31.0 | Ovomucoid | 20.3$^{a}$ | 20.2$^{a}$ | 19.2$^{a}$ | 16.1$^{a}$ | n.d. | n.d. | n.d. |
| 5 | 37.0 | Lysozyme | 1252.2$^{a}$ | 1120.1$^{a}$ | 811.3$^{b}$ | 95.8$^{c}$ | 14.9$^{d}$ | 4.5$^{e}$ | n.d. |
| 6 | 18.2 | Protein 1 | n.d. | 966.0$^{a}$ | 350.4$^{b}$ | 213.4$^{b}$ | 38.2$^{c}$ | 21.0$^{d}$ | 19.4$^{d}$ |
| 7 | 35.1 | Protein 2 | 7.6$^{e}$ | 19.4$^{d}$ | 40.2$^{c}$ | 45.3$^{bc}$ | 46.2$^{ab}$ | 48.4$^{ab}$ | 52.0$^{a}$ |
| 8 | 41.9 | Protein 3 | n.d. | n.d. | n.d. | 5.4$^{c}$ | 6.8$^{c}$ | 19.8$^{b}$ | 52.0$^{a}$ |

$^{a,b,c,d,e}$ for each peak, means indicated by the same letter are not significantly different ($P$>0.05).
R.t.: retention time; n.d. not detected.

Upon pulsed light treatment, a decrease in the peak areas of ovomucin, ovalbumin, ovomucoid and lysozyme was observed. The increase in PL fluence was associated to a progressive decrease in the mean peak areas of lysozyme. By contrast, the peak areas of ovalbumin and ovomucoid showed an abrupt change between 15.75 and 21.00 J $cm^{-2}$. Similarly to what observed in the case of UV-C treatment (Chapter 4.1, Table 4.1.2), this result indicates that egg white proteins are not similarly sensitive to pulsed light. The area of the peak relevant to ovotransferrin was found to increase up to 15.75 J $cm^{-2}$ and became not detectable on further pulsing. It is hardly believable that the amount of this protein could increase as a consequence of pulsed light exposure. Rather unfolding or aggregation of other proteins could lead to molecules having apparent molecular weight similar to that of ovotransferrin.

The steep decrease in the peak areas relevant to the native egg white proteins could be the result of their light-induced interaction to form aggregates. This is consistent with the presence of particles with hydrodynamic radius higher than 100 nm (Figure 4.2.1), leading to a turbid appearance (Table 4.2.1), as well as with the decrease of free SH groups after 15.75 J $cm^{-2}$ (Figure 4.2.2). In addition, exposure of egg white to pulsed light was associated to the appearance of a novel peak with very short retention time as compared to that of all other proteins detected in the untreated sample (Peak 6). Such peak was probably the result of protein aggregation/unfolding. This protein appeared in the sample submitted to 5.25 J $cm^{-2}$ and its area progressively decreased by increasing PL fluence. In other words, the protein fraction eluted in peak 6 was particularly unstable, being intensely prone to photodegradation. The peak area of two additional peaks (peak 7 and peak 8), relevant to molecular species with longer retention time, and thus lower apparent molecular weight, was also found to increase with exposure to

pulsed light. These evidences show that PL treatments are able to promote the modification of egg white protein structure by favouring not only unfolding/aggregation phenomena but also protein backbone cleavage. However, the protein fragment with lower apparent molecular weight (peak 8) was detected only in samples exposed to PL fluences higher than 10.50 J $cm^{-2}$, indicating that severe protein fragmentation requires high energy levels.

As suggested by many authors, modification of protein structure and development of non enzymatic browning could affect protein allergenicity (Gruber, Vieths, Wangorsch, Nerkamp, & Hofmann, 2004; Chen & Phillips, 2005; Taheri-Kafrani et al, 2009). Egg white samples subjected to PL were then analysed for immunoreactivity by an ELISA method (Figure 4.2.3).

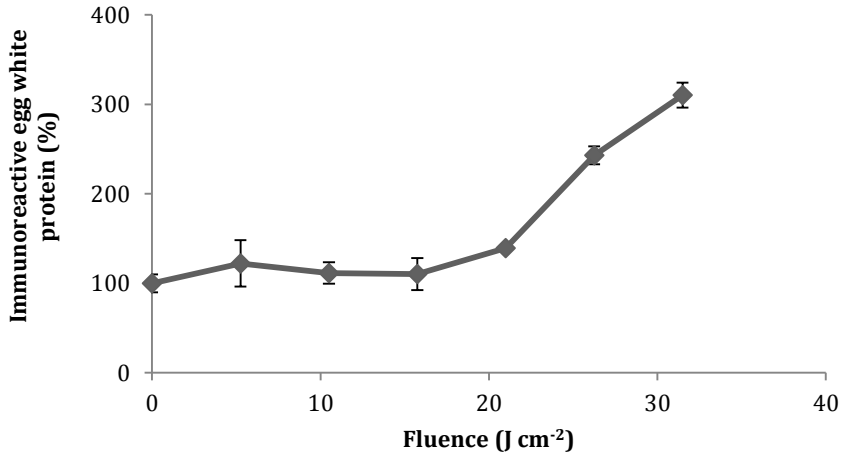


**Figure 4.2.3** Immunoreactive proteins in egg white exposed to pulsed light with increasing fluence.

No differences in immunoreactivity were observed between untreated egg white and egg white exposed to a number of light pulses up to 21.00 J $cm^{-2}$. These results are consistent to what observed considering the effect of UV-C light on egg white (Chapter 4.1). Also in that case no changes in egg white immunoreactivity were observed upon exposure to UV-C light up to 6.37 J $cm^{-2}$. By contrast, higher PL fluences were associated to a significant increase in egg white immunoreactivity. The latter occurred in correspondence to the increase of the area of peak 8 (Table 4.2.2), which was associated to the smallest protein fragments. Actually, egg white immunoreactivity resulted well correlated with the area of this peak ($R=0.95$, $p>0.05$). It can be hypothesized that protein

fragmentation caused by intense pulsed light treatment could lead to a higher exposure of the protein epitopes, giving reason for the marked increase in egg white immunoreactivity (Figure 4.2.3).

The increase in egg white immunoreactivity by intense pulsed light treatments apparently contradicts data reported by Anugu et al. (2010). These authors actually found that PL was effective in reducing egg allergens. However, it is noteworthy that this evidence was obtained by studying the effect of PL on isolated egg proteins in diluted conditions. These model systems are definitely far from the real egg white. In fact, as indicated by Manzocco & Nicoli (2012) and as observed for PL treatments of PPO in model solutions (Chapter 3), crowding effects could steer the sensitivity of egg white proteins to light exposure. Therefore, it seems reasonable to hypothesise that crowding could favour specific conformational changes in light treated egg white proteins, affecting immunoreactivity in a completely different way from that observed in model systems without crowding.

To understand whether, similarly to UV-C light (Chapter 4.1, Tables 4.1.3 and 4.1.4, Figure 4.1.1), also PL-induced changes in egg white protein structure could be associated to modifications in their technological performances, samples exposed to PL were also analysed for apparent viscosity, gelling and foaming properties.

Contrarily to what observed when egg white was subjected to UV-C light (Chapter 4.1, Table 4.1.3), no significant changes in apparent viscosity of egg white (0.21±0.02 Pa s) were found upon PL treatment. This is quite unexpected considering the intense structural changes of egg white protein exposed to PL. It is possible that the effects of protein aggregation and backbone cleavage counterbalanced each other, leading to negligible changes in the overall apparent viscosity of egg white.

By contrast, gelling temperature was found to progressively decrease with the increase in the number of pulses (Figure 4.2.4) but no significant differences in gel firmness (0.082±0.01 N) were detected. It is likely that unfolding/aggregation phenomena induced by pulsed light (Figure 4.2.1 and Table 4.2.2) could favour protein gelling, decreasing the temperature of gel formation but exerting no effects on the final strength of the gel.

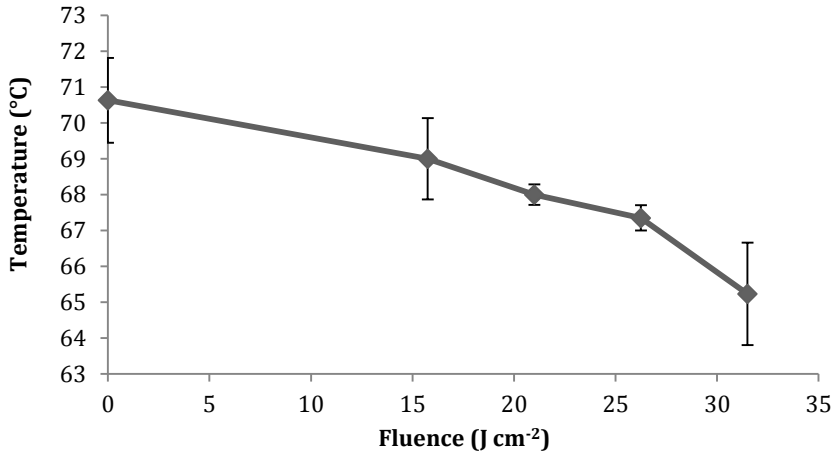


**Figure 4.2.4** Gelling temperature of egg white exposed to pulsed light with increasing fluence.

The foam volume obtained from pulsed egg white was similar to that produced by the untreated egg white (data not shown). However, as observed in the case of UV-C light treated egg white (Chapter 4.1, Fig. 4.1.1) foams prepared from light treated egg white appeared moist and creamy, contrasting with the brittle and dry appearance of those prepared from untreated egg white. Just prepared and 30 min rested foams obtained from egg white exposed to pulsed light were observed under a light microscope. Micrographs are shown in Figure 4.2.5.

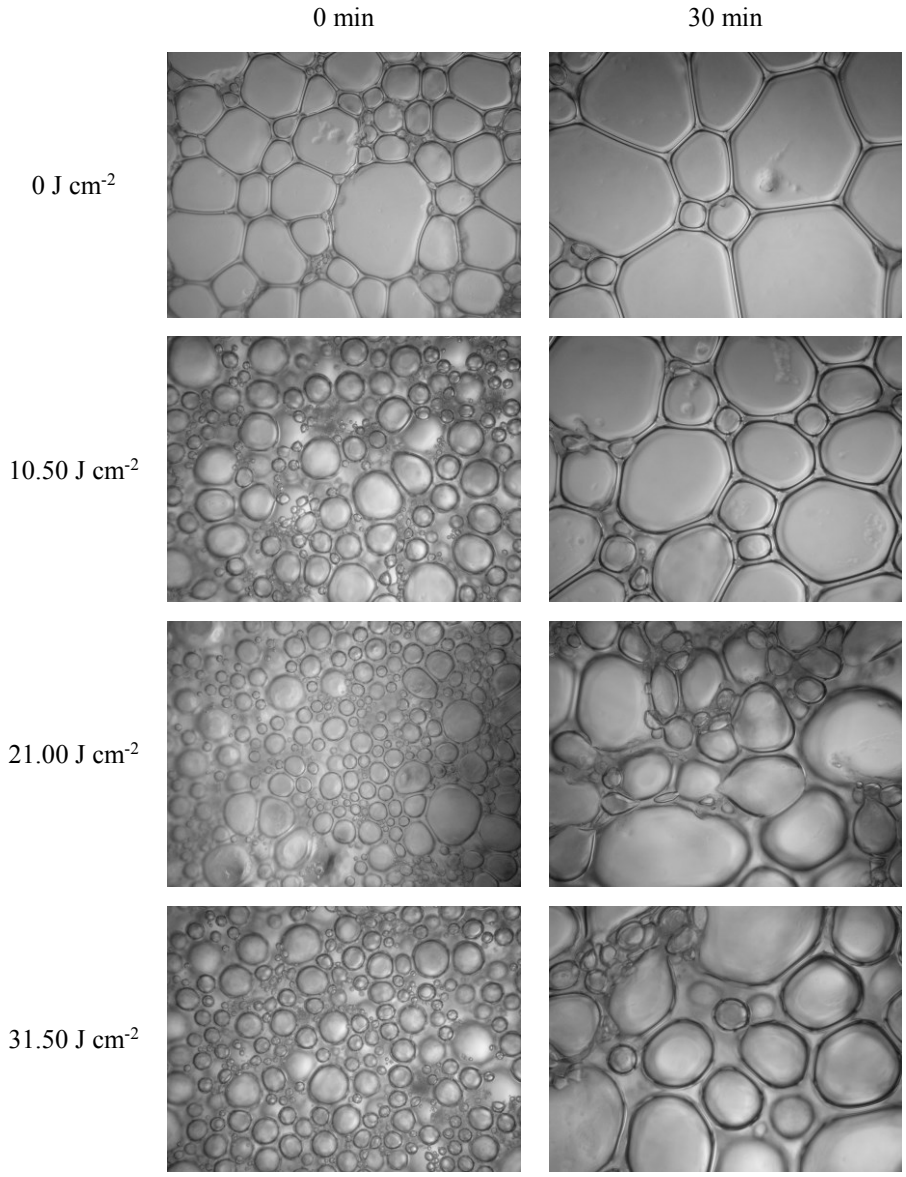


**Figure 4.2.5** Micrographs (100x) of just prepared and 30 min held foams obtained from egg white exposed to PL with increasing fluence (0, 10.50, 21.00, 31.50 J $cm^{-2}$).

Foams obtained from pulsed egg white presented a lower amount of large bubbles as compared to the control. In particular, the occurrence of large bubbles was not observed in egg white exposed to 31.50 J $cm^{-2}$. In addition, the higher the intensity of pulsed light treatment, the smaller the bubbles in foams. As expected,

after a 30 min rest at 20 °C, bubble size increased due to dismutation and coalescence. However, these phenomena were less evident in the light treated samples. The higher stability of the foams obtained from pulsed egg white was tentatively attributed to the presence of high size protein aggregates (Figure 4.2.2), which could behave as surface-active solid particles begetting a pickering foam (Pickering, 1907). The latter would be stabilized not only by the surfactant native proteins but also by the solid protein aggregates. As suggested by Murray et al. (2011), native proteins and solid particles could attract each others, increasing the particle jamming in the fluid interstices between bubbles. This would cause the formation of a firmer shell, positively affecting foaming properties.

**Conclusions**

Similarly to what observed in the case of UV-C light treatment, PL treatment induced structural modifications of egg white proteins by means of both backbone cleavage and aggregation phenomena. These observations suggest the photo-induced structural modification of proteins to occur *via* similar reaction pathways in the case of UV-C and PL light. However, in the case of PL processing the higher intensity of the process resulted in protein structural modification of a larger extent as compared to UV-C light.

The increase in immunoreactivity as well as the decrease in gelling temperature, which were not observed when egg white was subjected to UV-C light, can be attributed to the much intense structural modifications of egg white proteins. By contrast, similar improvement was observed in foaming properties of PL treated egg white as compared to UV-C light treated egg white.

These results suggest that when proteins are sitting in similar environmental conditions, the intensity of the light treatment is the major factor affecting their structure and thus their functions. Based on these results, both PL and UV-C light processing can be regarded as technologies allowing the functional properties of globular proteins (i.e. PPO, egg white proteins) to be modified.

## *Chapter 5 Effect of PL on Gluten proteins*

### Aim of the study

In this chapter the effect of PL on wheat gluten proteins will be discussed. Gluten was chosen as an example of a mix of globular and fibrous proteins. Gluten is a viscoelastic complex mixture of proteins, containing many, probably several hundred, polypeptides, about half of the protein being monomeric (gliadins) and the remaining being disulphide- cross linked polypeptides that form the polymeric glutenin fraction. The molecular weights (MWs) of native proteins range from around 30,000 to more than 10 million (Gianibelli, Larroque, MacRitchie, & Wrigley, 2001; Wieser, 2007; Wrigley, 1996). Glutenin forms a network of fibres in which globular gliadins are entrapped. In other words, gluten can be considered to be like a dough in which the diluting effect of starch is no longer present.

Traditionally the most common use of gluten proteins has been in baked products. However, due to its unique technological properties and favourable costs as compared to other proteins, the use of gluten as an ingredient has extended to a variety of food products (Day, Augustin, Batey, & Wrigley, 2006). With regard to their biological properties, gluten proteins are well known to cause allergenic response in people with coeliac disease. Coeliac disease is one of the most frequent food intolerances worldwide, and affected people can only avoid symptoms by maintaining a strict gluten-free diet for their entire life (van Eckert et al., 2010; Wieser & Koehler, 2008).

Literature evidences, as well as results presented in Chapters 3 and 4.2, show that PL can be efficiently exploited to modify protein structure, thus leading to modification of protein functionalities (Charles et al., 2013; Elmnasser et al., 2008; Fernández et al., 2012; Oms-Oliu et al., 2010; Ramos-Villarroel et al., 2011). However, it was suggested that globular and fibrous protein can react differently on light exposure (Delincée, 1983; Stewart, 2001). Therefore, the aim of the present study was to investigate the effects of PL on gluten protein structure and immunoreactivity.

### Results and discussion

Gluten powder was exposed to increasing pulsed light fluence at room temperature (22.1±0.4 °C). To assess the effect of hydration on gluten photoreactivity, aqueous suspensions containing 1% (w/v) gluten powder were also prepared and light treated. The temperature of the samples was measured just after the treatment and did not exceed 40 °C (Figure 5.1).

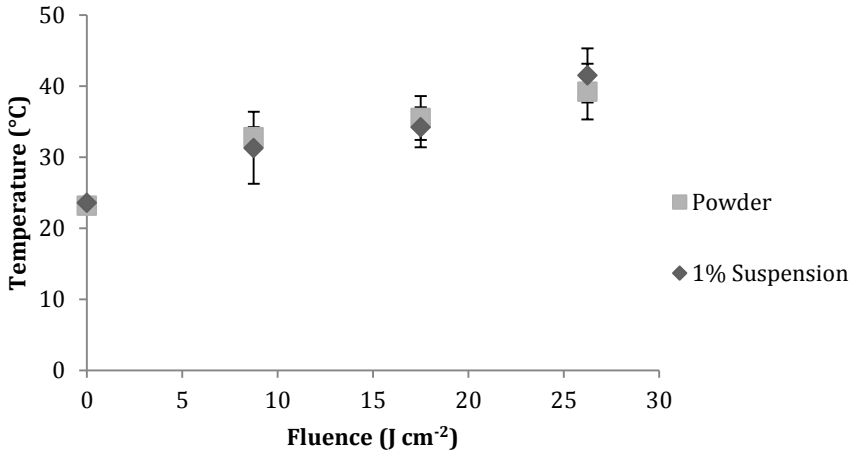


**Figure 5.1** Temperature of gluten powder and 1% (w/v) gluten suspension exposed to pulsed light with increasing fluence (0, 8.75, 17.50, 26.25 J $cm^{-2}$).

Being this temperature much lower than that associated to conformational modifications of gluten proteins (Guerrieri, Alberti, Lavelli, & Cerletti, 1996), any modifications of gluten proteins should be attributed to the sole effect of pulsed light. In order to investigate the effect of pulsed light on gluten protein structure, spectrophotometric analyses of gluten samples were performed. Upon exposure to pulsed light, a significant increase in gluten absorbance at 280 and 320 nm was observed as compared to the control untreated gluten (Table 5.1).

**Table 5.1** Absorbance at 280 and 320 nm of untreated gluten (Control), gluten powder and 1% (w/v) gluten suspension exposed to pulsed light with increasing fluence (0, 8.75, 17.50, 26.25 J $cm^{-2}$).

| | Powder | | 1% Suspension | |
|---|---|---|---|---|
| Fluence (J $cm^{-2}$) | Abs 280 nm | Abs 320 nm | Abs 280 nm | Abs 320 nm |
| 0 (Control) | 9.13±0.11 $^{d}$ | 3.65±0.06 $^{b}$ | 9.13±0.11 $^{b}$ | 3.65±0.06 $^{b}$ |
| 8.75 | 9.69±0.20 $^{c}$ | 3.89±0.18 $^{a}$ | 13.66±0.06 $^{a}$ | 5.71±0.08 $^{a}$ |
| 17.50 | 10.33±0.30 $^{b}$ | 4.28±0.18 $^{a}$ | 13.87±0.93 $^{a}$ | 5.81±0.47 $^{a}$ |
| 26.25 | 10.79±0.16 $^{a}$ | 4.38±0.09 $^{a}$ | 13.72±0.19 $^{a}$ | 6.14±0.11 $^{a}$ |

$^{a,b,c,d}$ Means on the same column indicated by the same letter are not statistically different ($P$>0.05).

When gluten powder was treated, the increase in light fluence was associated to a progressive increase in absorbance at both wavelengths. It is noteworthy that wheat gluten powder usually contains approximately 75% protein, up to 8% moisture, and varying amounts of starch, lipids and fibre. The starch and fibre are entrapped in the cohesive matrix of the protein (Day et al., 2006). Given the

intimate contact between proteins and polysaccharides in the sample, the increase in gluten absorbance at 280 nm could be the result of the formation of early non-enzymatic browning reaction products. The latter are highly reactive molecules, easily consumed to produce brown melanoidins absorbing at 320 nm (Table 5.1). The development of non-enzymatic browning in gluten exposed to pulsed light is supported by previous results indicating that this reaction can occur in egg white proteins upon exposure to both UV-C and PL (Chapters 4.1 and 4.2, Tables 4.1.1 and 4.2.1) as well as by literature evidences (Sheldon et al., 1988). Condensation reactions typical of non-enzymatic browning are well known to be favoured by hydration due to the increase in reactants mobility (Roos, 2003). For this reason, hydrated gluten resulted much more prone to photo-induced non-enzymatic browning than gluten powder (Table 5.1). With the increase in the number of pulses, the gluten suspension showed a progressive increase in brown melanoidins absorbing at 320 nm, while negligible changes in early non-enzymatic reaction products were detected. This result suggests that the expected increase in absorbance at 280 nm was probably counterbalanced by the development of other reactions affecting gluten spectrum. The UV component of pulsed light is actually reported to be absorbed by protein endogenous chromophores (e.g. Trp or Phe residues) causing oxidative reactions (Davies, 2003). The latter may not only decrease protein absorbance at 280 nm but also induce modifications in protein structure as previously observed in the case of egg white (Chapter 4.1 and 4.2, Tables 4.1.1 and 4.2.1). To this regard, photo induced structural changes have been previously reported also in different proteins, including lysozyme, ovalbumin, lactoglobulin (Fernández et al., 2012; Wu et al., 2008). The occurrence of structural modifications in gluten was thus assessed by microscopy analysis. The micrograph of untreated gluten showed the presence of starch granules embedded in the protein clusters (Figure 5.2). The latter are composed of high molecular weight (HMW) glutenins, low molecular weight (LMW) glutenins, and gliadins, which form a protein network by means of S-S bonds (Shewry, Halford, Belton, & Tatham, 2002). These protein clusters were not altered by pulsed light when gluten powder was treated (data not shown). Whereas, pulsed light treatment of gluten suspension led to the disruption of the protein clusters into small particles (Figure 5.2).

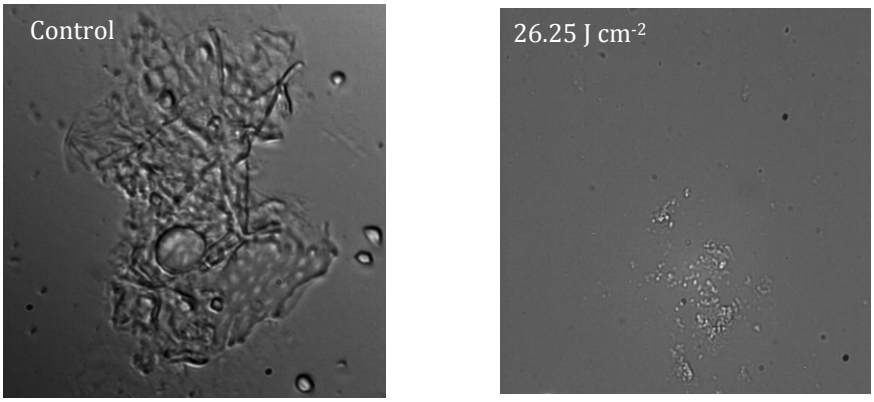


**Figure 5.2** Micrographs (100x) of untreated (control) gluten and 1% (w/v) gluten suspension exposed to 26.25 J $cm^{-2}$ of pulsed light.

Microscopy observations were supported by particle size analysis of the samples (Table 5.2).

**Table 5.2** Percentage distribution of small (ø < 50 nm), medium (100 < ø < 400 nm) and large (ø > 1000 nm) particle fractions in untreated gluten (control), gluten powder and 1% (w/v) gluten suspension exposed to pulsed light with increasing fluence (0, 8.75, 17.50, 26.25 J $cm^{-2}$).

| | Powder | | | 1% Suspension | | |
|---|---|---|---|---|---|---|
| Fluence | Particles (%) | | | Particles (%) | | |
| (J $cm^{-2}$) | Small | Medium | Large | Small | Medium | Large |
| 0 (Control) | 7.4 ± 1.1 [a] | 42.8 ± 7.8 [b] | 60.3 ± 11.5 [a] | 7.4 ± 1.1 [a] | 42.8 ± 7.8 [c] | 60.3 ± 11.5 [a] |
| 8.75 | 3.6 ± 0.6 [b] | 40.2 ± 7.3 [b] | 63.0 ± 11.9 [a] | 1.9 ± 0.2 [b] | 73.6 ± 12.8 [b] | 41.2 ± 6.8 [b] |
| 17.50 | 1.7 ± 0.2 [b] | 99.3 ± 18.9 [a] | n.d. | 1.9 ± 0.3 [b] | 95.7 ± 7.7 [a] | n.d |
| 26.25 | 1.1 ± 0.1 [c] | 90.7 ± 17.2 [a] | n.d. | 1.2 ± 0.2 [b] | 86.3 ± 13.9 [a] | n.d |

[a,b,c,d] Means on the same column indicated by the same letter are not statistically different ($P$>0.05). n.d.: not detected.

In the untreated control sample three classes of particles were observed: small, medium and large particles, having diameter lower than 50 nm, between 100 and 400 nm, and higher than 1000 nm, respectively. The relative distribution of these classes was significantly affected by light exposure. In particular, an increase in the percentage of medium size protein particles was detected to the detriment of the larger and smaller ones. In addition, changes in particle distribution resulted much more evident in the case of the gluten suspension as compared to the gluten powder. The changes in particle size distribution support the hypothesis of photo-induced modification of intra- and inter-molecular protein-protein interaction. To verify this hypothesis changes in free sulfhydryl (SH) groups were measured (Figure 5.3).

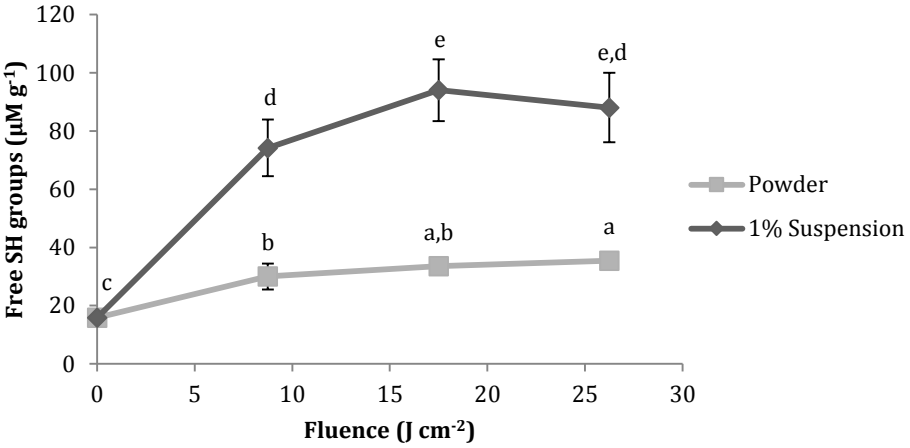


**Figure 5.3** Free sulfhydryl groups in gluten powder and 1% (w/v) gluten suspension exposed to pulsed light with increasing fluence (0, 8.75, 17.50, 26.25 J $cm^{-2}$). Means indicated by the same letter are not statistically different ($P$> 0.05).

Significant changes in free SH groups of gluten were observed upon light exposure (Figure 5.3). In particular, a slight and progressive increase in free SH groups was detected in the gluten powder. On the other hand, gluten suspension showed a marked increase in SH groups upon exposure to 8.75 J $cm^{-2}$ PL fluence and no significant changes in this parameter at higher fluences. In other words, in both the cases a saturation curve was obtained, however with different end levels depending on gluten hydration level. As reported in the literature (Wu et al., 2008), light would affect the structure of proteins inducing the reduction of disulphide (S-S) bonds. The location of inter- and intramolecular S-S bonds is crucial for the state of aggregation of HMW glutenins with LMW glutenins as well as with gliadins. Therefore, the S-S/SH exchange would directly disturb the structure of the protein matrix, possibly leading to its disruption and rearrangement, as suggested also by microscopy and particle size data (Figure 5.2 and Table 5.2). Further information about protein structural modifications induced by pulsed light treatment were obtained by HPLC-gel permeation analysis (Figure 5.4).

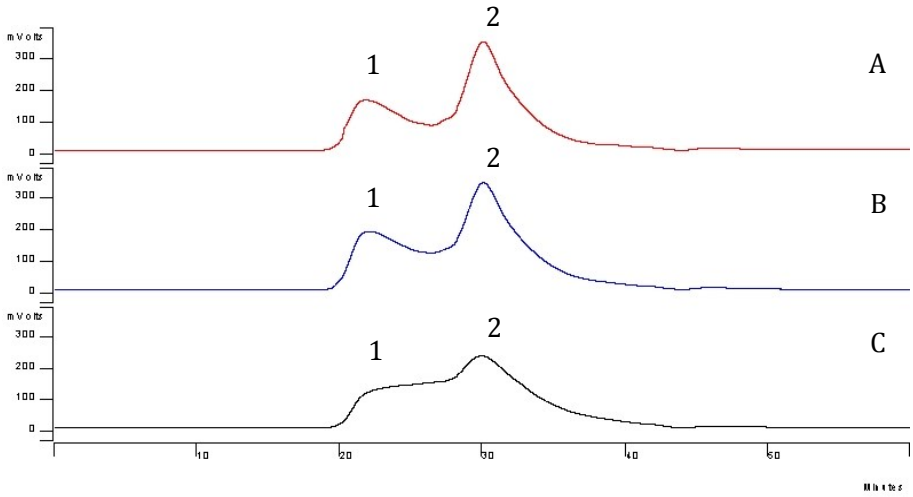


**Figure 5.4** Chromatograms relevant to untreated gluten (A), gluten powder (B) and 1% gluten suspension (C) exposed to 26.25 J $cm^{-2}$ PL fluence.

The chromatogram relevant to the untreated gluten showed the presence of two broad peaks with retention times of 21.8 (peak 1) and 30.0 min (peak 2). Apparent molecular weight of proteins eluted in these peaks were roughly estimated to be 84.2 and 14.7 kDa respectively. By comparison of apparent molecular weight with literature data, peak 1 was attributed to large polymer protein fractions whilst peak 2 was ascribed to small monomer protein fractions (van der Zalm, van der Goot, & Boom, 2011). Upon exposure of gluten to pulsed light, the signal intensity of peaks 1 and 2 progressively decreased with concomitant appearance of a large band between them (Figure 5.4). This effect resulted much more intense in the case of gluten suspension as compared to gluten powder and is consistent with the increase in medium size particles observed by dynamic light scattering (Table 5.2). To better understand the nature of photo-induced gluten modification, samples were analysed by SDS-PAGE. Samples reduced by using β-mercaptoethanol as a reducing agent were also considered (Figure 5.5).

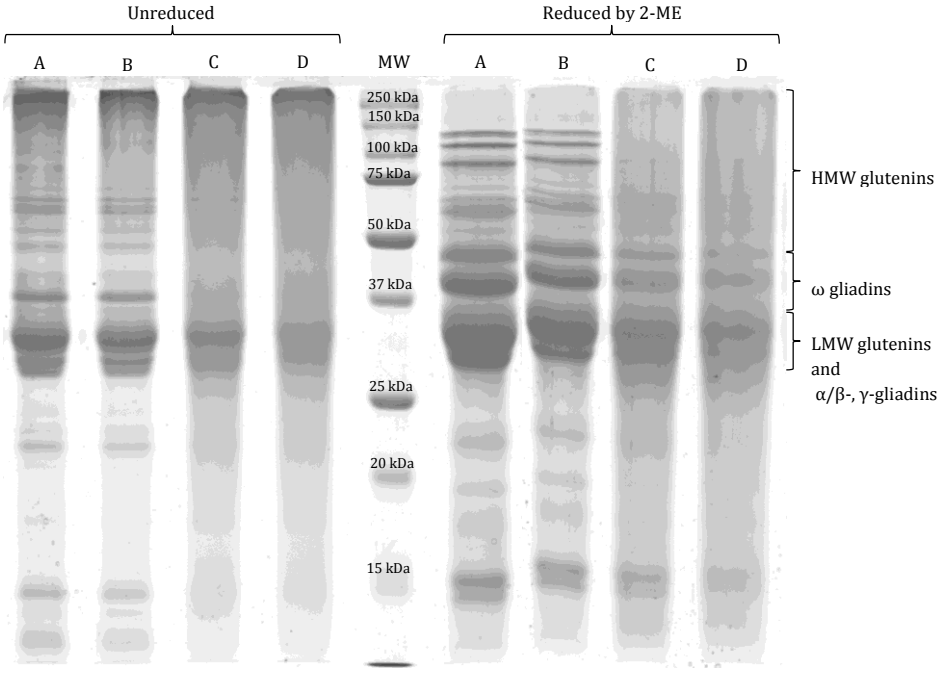


**Figure 5.5** SDS PAGE of untreated gluten (A), gluten powder exposed to 26.25 J $cm^{-2}$ (B), and 1% (w/v) gluten suspension exposed to 8.75 J $cm^{-2}$ (C) and 17.50 J $cm^{-2}$ (D) unreduced (Unreduced) and reduced with β-mercaptoethanol (Reduced by 2-ME). (MW: standard molecular weights).

Gluten protein fractions were identified by comparison of molecular weight and literature data (Belitz, Kieffer, Seilmeier, & Wieser, 1986; Shewry & Tatham, 1997; Wieser, 2007; Zilić, Barać, Pešić, Dodig, & Ignjatović-Micić, 2011). In particular, unreduced gluten not exposed to PL (A, Unreduced) showed several bands relevant to HMW-glutenins (66-150 kDa), few intense bands relevant to ω-gliadins (46-65 kDa), as well as few thick bands associated to LMW-glutenins, α/β- and γ-gliadins (28-43 kDa). In addition, the high intensity and the smearing of the band at the top of the lane suggested the presence in the untreated gluten of high molecular weight protein fractions unable to enter the gel. As known, SDS is an anionic surfactant able to disrupt non covalent bonds, such as hydrogen bonds, hydrophobic and electrostatic interactions among proteins. Therefore, the protein fractions unable to enter the gel probably account for the protein clusters based on S-S bonds. SDS-PAGE of untreated gluten suspension under reducing conditions confirmed this hypothesis. In fact, sample reduction by β-mercaptoethanol increased the mobility of these large protein fractions, leading to the appearance of a higher number of sharp bands in the HMW-glutenins as well as broad intense

bands in the LMW-glutenins, α/β- and γ-gliadins regions. The thick intense bands in the region of ω-gliadins probably account for other protein fractions with similar molecular weight. In fact, being ω-gliadins poor in sulphur residues, it is hardly believable this protein fraction was affected by reducing conditions. No changes in the electrophoretic pattern of gluten powder exposed to PL were observed (Figure 5.5, B). By contrast, marked modifications were detected for gluten suspensions (Figure 5.5, C and D). The electrophoretic pattern of the unreduced gluten exposed to PL lacked the sharp bands relevant to HMW-glutenins and, in their place, diffuse background coloration was observed. When samples were reduced by β-mercaptoethanol a higher mobility of the large protein fractions was observed. These results were attributed to photo-induced partial depolymerisation of HMW glutenins by means of S-S/SH exchange. The progressive decrease in intensity of the bands corresponding to ω-gliadins as well as to LMW-glutenins, α/β- and γ-gliadins suggested pulsed light to induce the modification of these protein fractions as well. With regard to ω-gliadins, this protein fraction is regarded to be poor in cysteine residues, but rich in aromatic residues (Lutz, Wieser, & Koehler, 2012; Wieser, Antes, & Seilmeier, 1998; Wieser, 2007). The latter could absorb the electromagnetic energy relevant to the UV fraction of PL, leading to protein structure modification (Wu et al., 2008). On the other hand, LMW-glutenins, α/β- and γ-gliadins are rich in cysteine residues and are known to form both intra- and inter-molecular crosslinks by means of disulphide bonds (Lutz et al., 2012; Wieser et al., 1998; Wieser, 2007). It can be inferred that PL induced SS/SH exchange would affect the structure of these protein fractions leading to both depolymerisation of oligomeric fractions and unfolding of monomeric fractions. In addition, it is not excluded that unfolded and depolymerised proteins would further interact leading to form protein species characterised by a broad range of molecular weights. This hypothesis is supported by the smearing of the upper part of the lanes of PL treated gluten suspension, as well as by the presence of few and more distinct bands in the lanes relevant to the reduced gluten samples.

As observed by many authors as well as in the case of egg white (Chapter 4.2, Figure 4.2.3), the modification of protein structure and the development of non enzymatic browning could affect protein allergenicity (Gruber et al., 2004; Taheri-Kafrani et al., 2009). Based on this consideration, gluten samples were also analysed for immunoreactivity by an ELISA method (Figure 5.6).

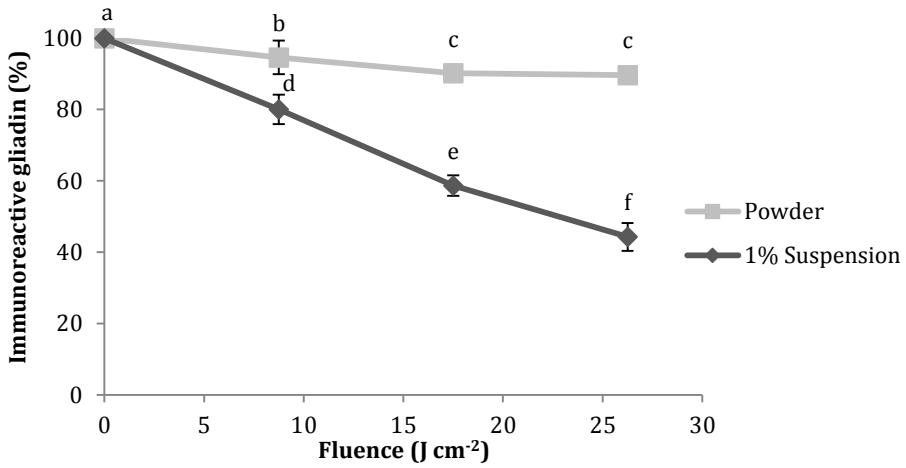


**Figure 5.6** Immunoreactive gliadin in gluten powder and 1% (w/v) gluten suspension exposed to pulsed light with increasing fluence (0, 8.75, 17.50, 26.25 J $cm^{-2}$). Means indicated by the same letter are not statistically different ($P$> 0.05).

A slight decrease in immunoreactive gliadin was detected upon treatment of gluten powder. In the gluten suspension, immunoreactive gliadin decreased by 50% upon 15 light pulses. It is likely that structural changes caused by pulsed light could lead to a lower exposure of gliadin epitopes or to their degradation, giving reason for the marked decrease in gluten immunoreactivity. The decrease in immunoractive gliadin by PL is in agreement with literature data suggesting that this technology may promote the decrease in food allergenicity (Anugu, Yang, Shriver, Chung, & Percival, 2010). However, opposite results were obtained considering egg white proteins exposed to pulsed light (Chapter 4.2). These results suggest that the effect of pulsed light on allergens is strictly dependent not only on protein nature but also on processing conditions and hydration level. To this regard, it has been hypothesised that protein photoreactivity would only occur at concentrations lower than the critical concentration for macromolecular crowding (Manzocco & Nicoli, 2012). As observed in the case of PPO and egg white exposed to PL (Chapters 3 and 4.1), at higher concentrations, proteins could be fully photo-resistant since their vicinity in the suspension would favour conformations that are less prone to structural rearrangements induced by light exposure.

**Conclusions**

Results obtained suggest that PL could be efficiently exploited to decrease gluten immunoreactivity as a consequence of gluten structure modification. However, similarly to what observed in the case of PPO (Chapter 3), the sensitivity of gluten to pulsed light was strongly affected by hydration. While gluten powder was highly resistant to photo-induced structure modification, pulsed light induced partial depolymerisation of oligomeric fractions and unfolding of monomeric fractions of hydrated gluten by promoting S-S/SH group exchange. The latter would also favour further structural rearrangement of unfolded and depolymerised proteins, leading to protein species having a broad range of molecular weights.

If in the case of both PPO and egg white proteins (Chapters 3, 4.1, and 4.2) light processing accounted for modification of both protein conformation and secondary structure, in the case of gluten protein only conformational changes could be observed. This can be attributed to the different nature of proteins. In fact, both PPO and egg white proteins are globular proteins, which are probably free enough to unfold, interact with other vicinal proteins, and even break upon intense light exposure. By contrast gluten proteins, structured in a network of fibrous glutenin entrapping globular gliadins, are probably spatially hampered to react upon light exposure.

## *Chapter 6 Effect of PL on starch*

### Aim of the study

Wheat starch was chosen as a polysaccharide matrix. Starch is an important biopolymer in foods. It is a major storage product in plants and one of the most important carbohydrate sources for human nutrition. It is composed of a mixture amylose and amylopectin and occurs in form of granules (Belitz, Grosch, & Schieberle, 2001). Starch is semi-crystalline and birefringent as can be observed under polarised light. Starch is important in many food applications because of its unique ability to modify the texture of different food matrices such as extruded breakfast cereals and snacks (Chanvrier, Uthayakumaran, & Lillford, 2007; Dogan, McCarthy, & Powell, 2005). All these food products are obtained by means of a thermal treatment, which defines their final quality characteristics. Upon heating, starch undergoes gelatinisation, and loss of birefringence. Gelatinisation is regarded as the hydration and irreversible swelling of the granule, the destruction of molecular order within the starch granule and the melting of starch crystals (Zobel, 1988). Gelatinization is a major step to exhibit featured characteristics of starch (Li & Yeh, 2001). Tester & Morrison (1990) suggested swelling to be a property of amylopectin. Crosslinking was found to enhance the molecular interactions by covalent bonding and reduce the swelling volume of corn starch (Ziegler, Thompson, & Casasnovas, 1993). Photocrosslinking of starch by means of UV exposure has been suggested to improve the performances of starch-based films. Based on these considerations, light processing could be exploited to modify starch structure and thus functions. To this aim wheat starch suspension was exposed to PL (26.25 J $cm^{-2}$), and analysed for structure and function characteristics.

### Results and discussion

Wheat starch suspension (1% w/v) was exposed to 26.25 J/$cm^{-2}$ PL fluence. PL treatments were performed at room temperature (22.4±0.8 °C). The temperature of the samples was measured just after the treatment and did not exceed 40 °C (36.9±3.1 °C). Therefore, gelatinisation of starch during the treatment can be excluded and any modifications of starch samples should be attributed to the sole effect of PL. In order to investigate the effect of PL on starch structure, spectrophotometric analyses of starch samples were performed (Table 6.1).

**Table 6.1** Absorbance at 280 and 320 nm of untreated starch (Control), and 1% (w/v) starch suspension exposed to pulsed light with 26.25 J $cm^{-2}$ fluence.

| Fluence (J $cm^{-2}$) | Abs 280 nm | Abs 320 nm |
|---|---|---|
| 0 (Control) | 2.07±0.09 [a] | 2.23±0.05 [a] |
| 26.25 | 2.07±0.11 [a] | 2.21±0.09 [a] |

[a] Means on the same column indicated by the same letter are not statistically different ($P$>0.05).

Contrarily to what observed in egg white and gluten samples (Chapters 4.1, 4.2 and 5, Tables 4.1.1, 4.2.1, and 5.1), PL did not induce any changes in starch absorbance at both 280 and 320 nm. This result suggests PL not to induce the formation of compounds absorbing at these wavelengths.

The occurrence of structural modifications in starch samples was further investigated by measuring the sample optical density at 640 nm during 15 min taken as an index of turbidity. Results are shown in figure 6.1.

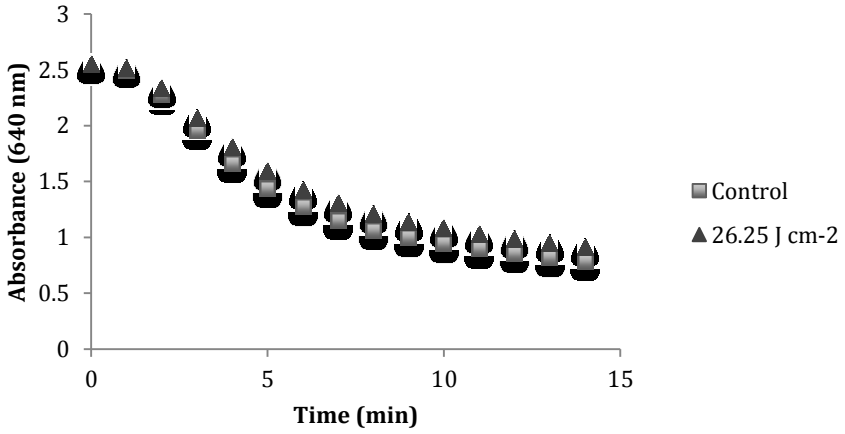


**Figure 6.1** Turbidity of untreated (Control) and PL treated (26.25 J $cm^{-2}$) 1% starch suspension as a function of measuring time.

The optical density at 640 nm was found to decrease as a function of time in both the untreated and the PL treated starch suspension with a similar trend. This decrease in turbidity can be associated to the sedimentation of starch particles on the bottom of the cuvette during the measurement time. Turbidity of starch suspension exposed to pulsed light was similar to that of the untreated starch at the beginning of the measurements (0-5 min). At longer observation time, a slight increase in turbidity was observed in starch suspension exposed to PL as compared to the untreated sample. It was inferred that the slightly slower sedimentation kinetic of PL treated starch might account for a modification in starch particle size. To verify this hypothesis starch samples were analysed for

particle size by light scattering analysis (Figure 6.2) as well as for microstructure by microscopy analysis (Figure 6.3).

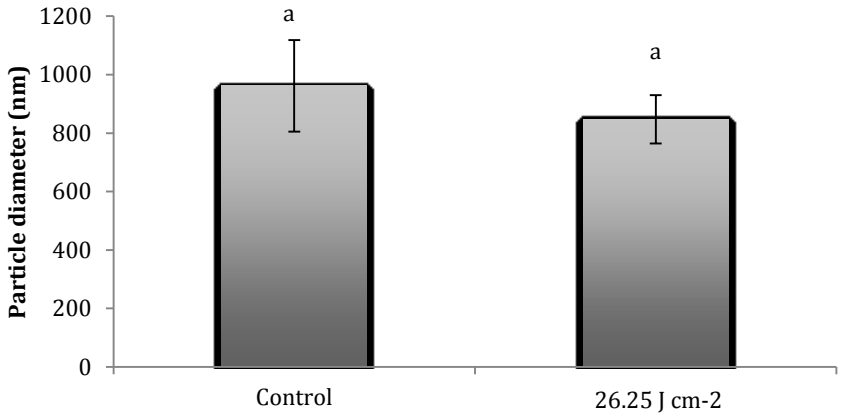


**Figure 6.2** Particle size of untreated (control) starch and 1% (w/v) starch suspension exposed to 26.25 J $cm^{-2}$ of pulsed light.

Light scattering analysis of untreated starch showed the presence of one class of particles with average diameter of 960 nm. Upon exposure to PL, a decrease in the average diameter of starch particles was detected. This slight difference, even if not significant, could reasonably explain the decrease in sedimentation observed by spectrophotometric analysis (Figure 6.1).
Light microscopy analysis of starch was also performed in order to confirm these results. The micrograph of PL treated starch suspension (26.25 J $cm^{-2}$) showed no significant difference in the size and shape of starch granules as compared to the untreated sample (Figure 6.3).

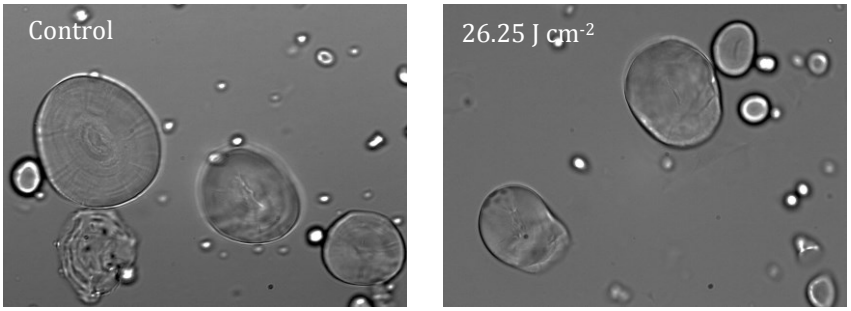


**Figure 6.3** Micrographs (200x) of untreated (control) starch and 1% (w/v) starch suspension exposed to 26.25 J $cm^{-2}$ of pulsed light.

Results obtained suggest that starch structure is not modified by PL exposure. The lack of chromophores in starch polymer chain and the absence or scarce presence of contaminants that can serve as photosensitizers, make starch photoresistant (Delville, Joly, Dole, & Bliard, 2003; Zhou, Ma, Zhang, & Tong, 2009; Zhou, Zhang, Ma, & Tong, 2008). As foods are rather complex matrices, the presence of contaminants that can behave as photosensitizers cannot be excluded.
To confirm this observation, gelatinisation of untreated and PL treated at 26.25 J $cm^{-2}$ starch suspension was performed. Samples were then analysed by light microscopy (Figure 6.4).

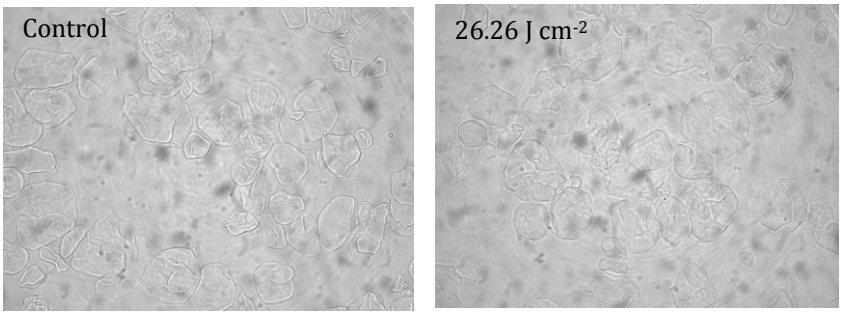


**Figure 6.4** Micrographs (100x) of untreated gelatinised (Control) starch and 1% (w/v) starch suspension exposed to 26.25 J $cm^{-2}$ of pulsed light and gelatinised.

No significant differences were observed in untreated gelatinised starch and PL treated gelatinised starch suspension.

**Conclusions**

Contrarily to what observed for proteins (Chapeters 3, 4.1, 4.2, and 5) no changes in starch structure could be observed upon exposure to PL. Consequently also starch performances were not affected by PL processing. The lack of absorption site capable to absorb light radiation within starch molecule, as well as the compact semi-crystalline structure organisation of starch granules makes starch photoresistant. Therefore, PL treatment could be potentially exploited as a sanitisation treatment, for instance against moulds, without impairing starch performances

## *Chapter 7 Effect of PL on wheat flour*

### Aim of the study

This chapter focuses on the effect of PL on wheat flour, taken as an example of a matrix composed of a mix of polysaccharides and proteins. Wheat flour is mainly composed of starch (ca. 70–75%), and gluten proteins (ca. 10–12%) (de Vuyst et al., 2005). As previously discussed, when starch was subjected to PL treatments, no changes in its structure and gelatinisation were observed (Chapter 6). On the other hand, conformational changes of gluten proteins resulting in a decrease in their immunoreactivity were detected upon exposure to PL (Chapter 5). The concomitant presence of both starch and gluten proteins in the food matrix could determine different effects of PL processing. For instance, gluten proteins could serve as photosensitizers favouring structural changes of starch. Likewise, starch granules, which are the major component of wheat flour, could conceal gluten proteins thus hindering the absorption of light radiation. Therefore, the aim of the present study was to investigate the effect of PL processing on the structure and function of a complex food matrix, such as wheat flour.

### Results and discussion

Similarly to gluten samples, wheat flour (powder) and wheat flour suspension 1% (w/v) were exposed to increasing PL fluence at room temperature (22.7±0.7 °C). The temperature of the samples was measured just after the treatment and did not exceed 40 °C (Figure 7.1).

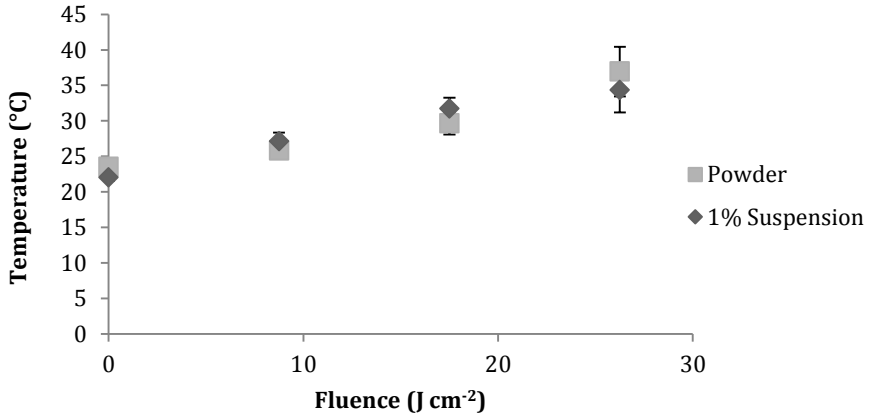


**Figure 7.1** Temperature of flour powder and 1% (w/v) flour suspension exposed to pulsed light with increasing fluence (0, 8.75, 17.50, 26.25 J $cm^{-2}$).

Being this temperature much lower than that associated to both conformational modifications of gluten proteins (Guerrieri et al., 1996), and gelatinisation of starch (Zobel, 1988), any modifications in the structure of flour constituents should be attributed to the sole effect of PL. The effect of PL on flour constituent structure was evaluated by spectrophotometric analyses of flour samples (Table 7.1).

**Table 7.1** Absorbance at 280 and 320 nm of untreated flour (Control), flour powder and 1% (w/v) flour suspension exposed to pulsed light with increasing fluence (0, 8.75, 17.50, 26.25 J $cm^{-2}$).

| | Powder | | 1% Suspension | |
|---|---|---|---|---|
| Fluence (J $cm^{-2}$) | Abs 280 nm | Abs 320 nm | Abs 280 nm | Abs 320 nm |
| 0 (Control) | 4.43±0.09 [b] | 4.34±0.07 [a] | 4.43±0.09 [b] | 4.34±0.07 [b] |
| 8.75 | 4.46±0.07 [b] | 4.14±0.01 [b] | 4.87±0.10 [a] | 4.69±0.03 [a] |
| 17.50 | 4.58±0.03 [a] | 3.74±0.02 [c] | 4.73±0.24 [a] | 4.74±0.31 [a] |
| 26.25 | 4.56±0.14 [a,b] | 3.82±0.16 [c] | 4.74±0.21 [a] | 4.38±0.03 [b] |

[a,b,c] Means on the same column indicated by the same letter are not statistically different (P>0.05).

Flour powder exposed to PL showed a slight increase in absorbance at 280 nm and a decrease in absorbance at 320 nm. On the other hand, flour suspension exposed to PL showed an increase in absorbance at both the wavelengths. In particular, a marked increase in absorbance at 280 nm was observed when flour suspension was subjected to 8.75 J $cm^{-2}$ PL fluence, and no additional increase was observed on further pulsing. Besides, a similar increase in absorbance at 320 nm was observed upon exposure to 8.75 and 17.50 J $cm^{-2}$, whilst absorbance values similar to the control samples were detected on further pulsing (26.25 J $cm^{-2}$). Similarly to the case of egg white and gluten proteins (Chapters 4.2.1 and 5, Tables 4.2.1 and 5.1), the increase in absorbance at these wavelengths can be attributed to the development of non-enzymatic browning reactions (Sheldon et al., 1988). In addition, as previously observed in gluten samples (Chapter 5, Table 5.1), the increase in absorbance was higher in flour suspension than in flour powder. Also in the case of flour, the higher hydration of the system would favour the condensation reactions typical of non-enzymatic browning due to the increase in reactants mobility (Roos, 2003). However, given the scarce presence of reducing groups in starch, PL light induced non-enzymatic browning was much lower in flour samples than what observed for both gluten and egg white samples.
The occurrence of structural modifications in wheat flour was further investigated by microscopy analysis (Figure 7.2).

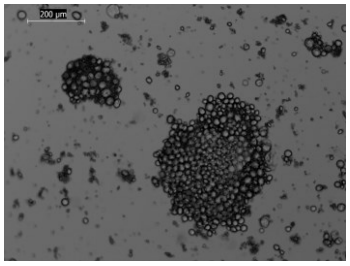

Control

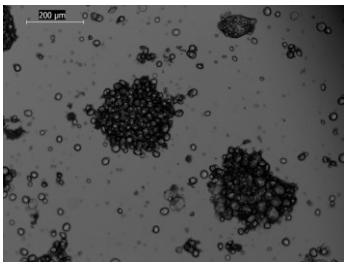

Powder 8.75 J $cm^{-2}$

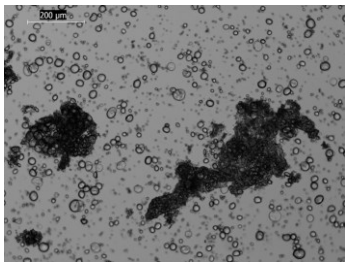

1% Suspension 8.75 J $cm^{-2}$

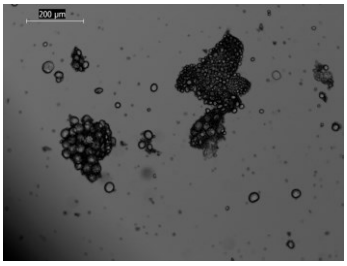

Powder 17.50 J $cm^{-2}$

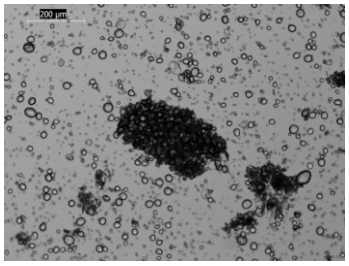

1% Suspension 17.50 J $cm^{-2}$

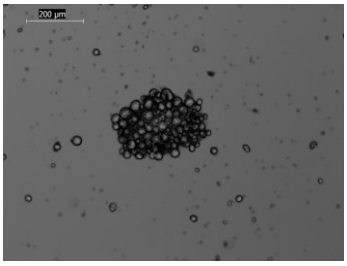

Powder 26.25 J $cm^{-2}$

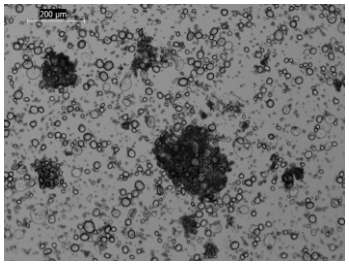

1% Suspension 26.25 J $cm^{-2}$

**Figure 7.2** Micrographs (40x) of untreated flour (Control), flour powder, and 1% (w/v) flour suspension exposed to PL with increasing fluence (0, 8.75, 17.50, 26.25 J $cm^{-2}$).

The micrograph of untreated flour showed the presence of large clusters. The latter are probably formed due to the interaction between gluten protein and starch granules. A slight decrease in the size of these clusters was observed when flour powder was treated with 8.75 J $cm^{-2}$ PL, and no additional changes in particle size were observed at higher PL fluences. By contrast, when flour suspension was exposed to PL, a progressive decrease in the size of the clusters was observed, accompanied by an increase in free starch granules, which were homogenously distributed in the sample. Observations made under light microscope were supported by light scattering analysis of flour samples (Figure 7.3).

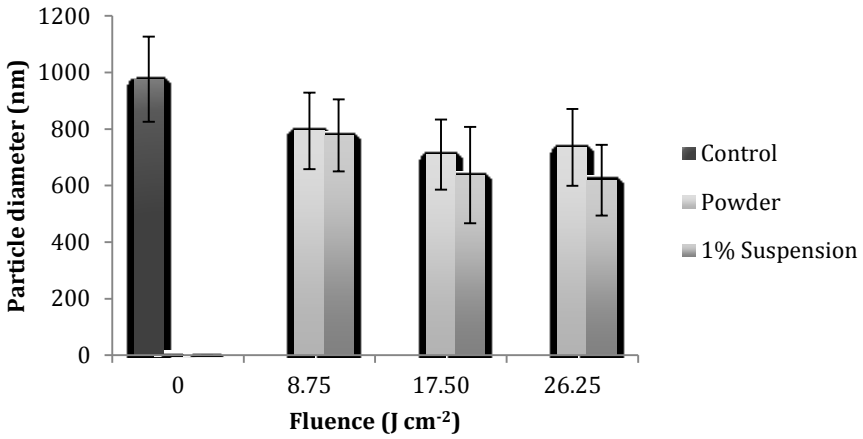


**Figure 7.3** Particle diameter of untreated flour (Control), flour powder, and 1% (w/v) flour suspension exposed to pulsed light with increasing fluence (0, 8.75, 17.50, 26.25 J $cm^{-2}$).

In the untreated control sample, one class of particles was observed with average diameter of 976±150 nm. Upon exposure to PL, flour powder showed an initial decrease in particle size upon 8.75 J $cm^{-2}$ PL fluence, and no additional modifications on further pulsing. These results and those obtained by microscopy analysis suggest that flour powder microstructure is not significantly affected by PL exposure. On the other hand, a progressive decrease in particle size was detected upon PL treatment of flour suspension. The decrease in particle size of the clusters as well as the increase in free starch, observed under light microscope (Figure 7.2), might account for PL-induced modifications of the interactions between starch and gluten proteins. Since no modifications of starch granules could be observed by light microscopy (Figure 7.2), the changes in particle size might be due to changes of gluten protein structure. As reported in the literature

(Wu et al., 2008), and accordingly to what observed for gluten proteins treated by PL (Chapter 5, Figure 5.3), light would affect the structure of proteins inducing the reduction of disulphide (S-S) bonds. As inter- and intramolecular S-S bonds are crucial for the state of aggregation of HMW glutenins with LMW glutenins, and gliadins, the S-S/SH exchange would directly disturb the structure of the protein matrix. To verify this hypothesis changes in free sulfhydryl (SH) groups were measured (Figure 7.4).

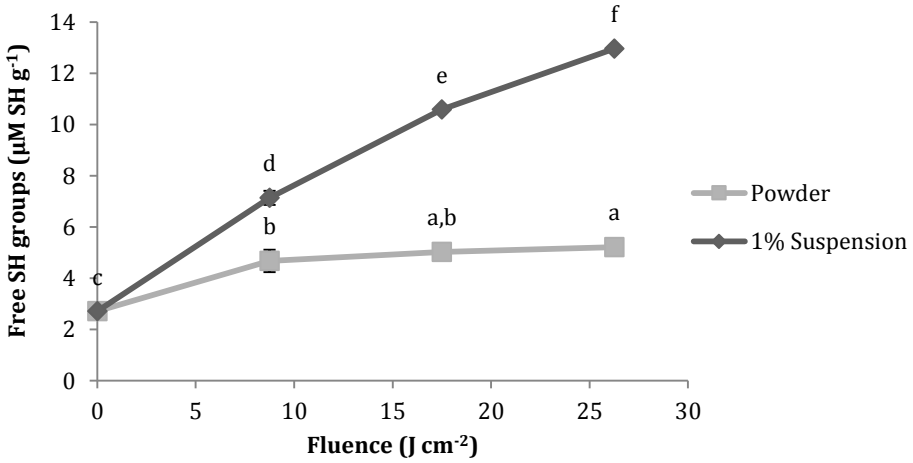


**Figure 7.4** Free sulfhydryl groups in flour powder and 1% (w/v) flour suspension exposed to pulsed light with increasing fluence (0, 8.75, 17.50, 26.25 J $cm^{-2}$). Means indicated by the same letter are not statistically different ($P$> 0.05).

Free SH groups of flour proteins were found to increase with PL fluence (Figure 7.4). In agreement with microscopy, as well as to particle size analysis, flour powder showed a slight initial increase in free SH groups upon exposure to 8.75 J $cm^{-2}$ PL fluence, and no significant changes in this parameter at higher fluences. These results are consistent whit the hypothesis that flour powder microstructure is not significantly altered by PL treatment. By contrast, a progressive increase in free SH groups was detected in flour suspension. To this regard, it is worth noting that a different trend in the increase in free SH groups as a function of PL fluence was observed for gluten proteins in flour, as compared to gluten samples (Chapter 5, Figure 5.3). In particular, a progressive increase in free SH groups was observed when gluten powder was exposed to PL. By contrast, gluten suspension showed a steep initial increased in free SH, and no changes in this parameter on further pulsing. The latter were attributed to the ability of intense PL fluences to induce oxidation of the newly formed SH groups, leading to rearrangements of

protein structure. This effect was not observed for gluten powder, which showed a similar trend to that of flour suspension. On the basis of these results, it was inferred that the effect of PL on gluten proteins could be reduced by the presence of starch in flour samples.

Further information about PL-induced protein structural modifications in flour samples were obtained by SDS-PAGE analysis (Figure 7.5).

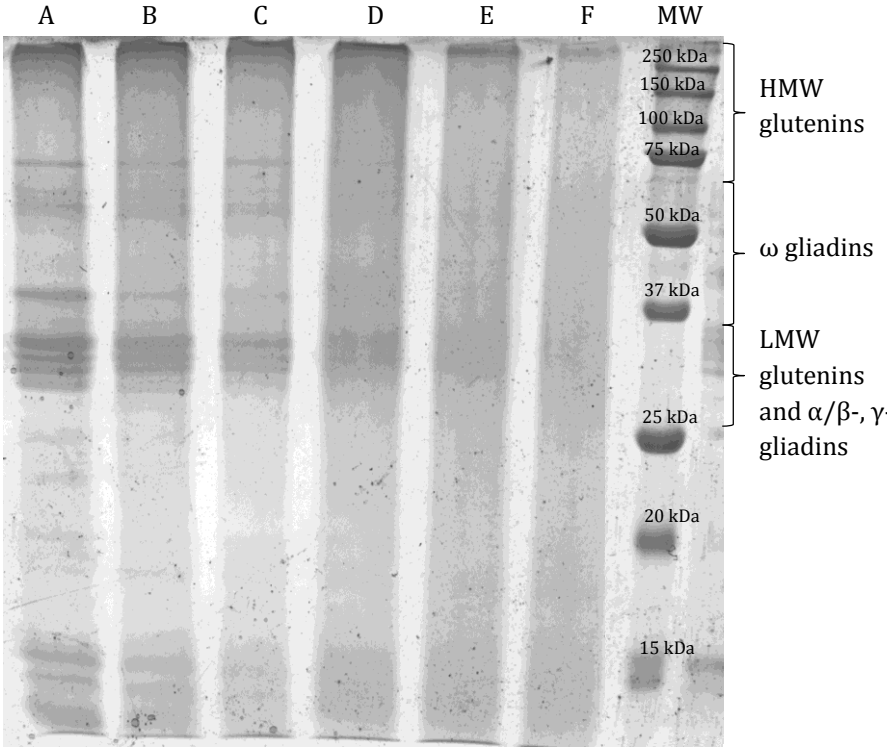


**Figure 7.5** SDS PAGE of untreated flour (A), flour powder exposed to 17.50 (B), and 26.25 J $cm^{-2}$ (C), and 1% (w/v) flour suspension exposed to 8.75 (D), 17.50 (E), and 26.25 J $cm^{-2}$ (F). (MW: standard molecular weights).

Gluten protein fractions in flour samples were identified by comparison of molecular weight and literature data (Belitz et al., 1986; Shewry & Tatham, 1997; Wieser, 2007; Zilić et al., 2011). In particular, untreated flour (A) showed few bands relevant to HMW-glutenins (66-150 kDa), ω-gliadins (46-65 kDa), as well as some intense bands associated to LMW-glutenins, α/β- and γ-gliadins (28-43 kDa). In addition, the high intensity and the smearing of the band at the top of the lane suggested the presence in the untreated gluten of high molecular weight protein fractions unable to enter the gel. As known, SDS is an anionic surfactant

able to disrupt non covalent bonds, such as hydrogen bonds, hydrophobic and electrostatic interactions among proteins. Therefore, the protein fractions unable to enter the gel probably account for protein clusters based on S-S bonds. Similar observations were made for gluten and confirmed by analysing gluten samples under reducing conditions (Chapter 5, Figure 5.5). When flour powder was exposed to PL, no significant changes in the electrophoretic pattern of flour proteins could be observed (Figure 7.5, B and C). By contrast, marked changes in the electrophoretic pattern proteins in flour suspensions exposed to PL were detected (Figure 7.5, D, E, and F). The electrophoretic patterns of PL treated flour proteins showed a progressive decrease in the intensity of the bands relevant to HMW-glutenins. These results confirm that PL can induce partial depolymerisation of HMW-glutenins by means of S-S/SH exchange, accordingly to what previously observed in the case of gluten (Chapter 5, Figure 5.5). Upon exposure to 8.75 J $cm^{-2}$ (Figure 7.5, D), an intense background coloration of the upper part of the lane was also observed. This coloration suggests that the depolymerisation of HMW-glutenins induced by PL treatment resulted in the formation of protein with a broad distribution of molecular weights. In addition, electrophoretic analysis of flour proteins supports the hypothesis that gluten proteins present different photosensitivity, being HMW-glutenins the most sensitive to PL exposure. Upon exposure to higher PL fluences, a progressive disappearance of the bands relevant to ω-gliadins, as well as to LMW-glutenins, α/β- and γ-gliadins was observed. These results are consistent with literature evidences, and confirm that PL can induce structure modification of proteins rich in aromatic and cysteine residues, such as the ω-gliadins, and LMW-glutenins, α/β- and γ-gliadins respectively (Lutz et al., 2012; Wieser et al., 1998; Wieser, 2007; Wu et al., 2008). Similar results were obtained also in the case of gluten proteins subjected to PL. However, when gluten was treated by PL, protein depolymerisation and degradation was accompanied by new protein-protein interaction, as suggested by the smearing and background coloration of the upper part of the lanes (Chapeter 5, Figure 5.5). By contrast, a diffuse background coloration of the whole lane relevant to PL treated flour suspension was observed, suggesting PL to induce changes in flour protein structure by means of depolymerisation and degradation phenomena solely (Figure 7.5, E and F). It can be inferred that the interactions which take place between gluten and starch granules in flour (Figure 7.2) could hinder gluten proteins to react upon light exposure. In fact results relevant to both free SH groups and SDS-PAGE (Figures 7.4 and 7.5), show that the lower the interaction between gluten and starch, the higher the photosensitivity of gluten proteins.

As previously observed for egg white and gluten proteins (Chapter 4.2 and 5, Figure 4.2.3 and 5.6), the modification of protein structure could affect protein allergenicity. In particular, on the one hand egg white immunoreactivity was found to increase, and on the other hand gluten immunoreactivity was found to decrease as a consequence of PL treatments. To evaluate whether the different protein structure modifications, could also result in different changes in protein functions, flour samples were analysed for immunoreactivity by an ELISA method (Figure 7.6).

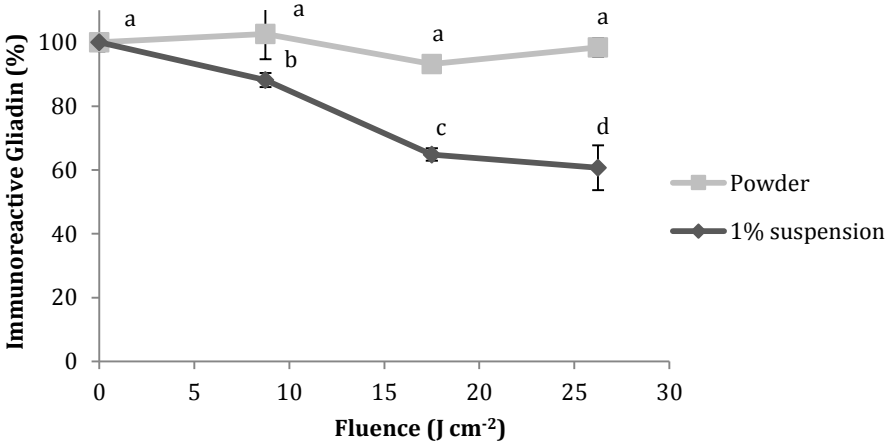


**Figure 7.6** Immunoreactive gliadin in flour powder and 1% (w/v) flour suspension exposed to pulsed light with increasing fluence (0, 8.75, 17.50, 26.25 J $cm^{-2}$). Means indicated by the same letter are not statistically different ($P$> 0.05).

No changes in protein immunoreactivity of flour powder could be observed upon PL exposure. This result was actually expected, since no significant changes in flour protein structure could be observed as a consequence of PL treatment (Figures 7.2, 7.3, 7.4, 7.5). By contrast, immunoreactive gliadin decreased by 40% when flour suspension was exposed to 26.25 J $cm^{-2}$ PL fluence. Therefore, as hypothesised in the case of gluten, it is likely that structural changes caused by pulsed light could lead to a lower exposure of gliadin epitopes or to their degradation, giving reason for the decrease in gluten immunoreactivity.

**Conclusions**

Results obtained suggest that PL could modify the structure and thus the immunoreactivity of gluten proteins in flour suspension. However, the extent of protein structural modifications was found to much lower when gluten was

included in a more complex matrix, such as flour, as compared to the gluten alone. The apparent interaction between starch granules and gluten proteins in flour samples seemed to hinder photoinduced modifications of gluten proteins. In fact, when the interaction between starch and gluten was not affected by PL (in flour powder), no changes in both protein structure and immunoreactivity could be observed. By contrast, in the case of flour suspension, the lower the interaction between gluten proteins and starch granules, the higher the photosensitivity of gluten proteins. Therefore, results achieved within this study, together with those relevant to the other investigated matrices (Chapters 3-6), show that besides processing conditions, hydration level, and protein nature, also the presence of other biomolecules are a key factor determining the effect of PL processing.

## *Conclusions Part I*

The first part of this PhD thesis dealt with the effect of UV-C and PL processing on food biomolecules. The potential of light processing to modify the structure of selected food biomolecules, and thus their functions was studied. Data obtained in this PhD thesis show that light processing, based on UV-C light or applied in a pulsed mode, can be exploited to modify biopolymer structure leading to functional changes. However, the overall effects of light on food biopolymers depend on several factors:

*1) Intrinsic photosensitivity of the target biomolecule*

Not all biopolymers are equally photosensitive. Biopolymers can be regarded as characterised by a different photosensitivity, which is strictly dependent on their chemical nature. In fact, the common feature of photoreactive biomolecules is the presence of light absorbing chemical sites, such as aromatic residues, conjugated double bonds, and chromophores. The latter should not only be present in the matrix but also be able to initiate photoreactions leading to structural modification of the polymer. In the light of these considerations and on the basis of the results acquired, proteins can be regarded as photosensitive biomolecules, as they are rich in aromatic residues, that can absorb radiation, leading to the occurrence of photoreactions. By contrast, starch, which does not include any absorption site in its molecule, can be considered as a photostable biomolecule. Therefore, when light processing is intended for food sanitization purposes, it can be efficiently exploited to decontaminate photostable biomolecules without impairing their functionalities. On the other hand, light processing can provide advantages well beyond decontamination when it is applied to photosensitive food biomolecules, such as proteins. In this case, it may allow interesting possibilities to steer biopolymer structure and functionality.

*2) Intensity of light radiation*

The nature and extent of structure/function modifications strictly depends on the prevalent wavelength of the radiation applied as well as on its intensity. By using UV-C light, which consists of short wavelength UV radiation (254 nm), biomolecule structure and functions are modified by means of photochemical effects. Whereas, by using PL, which includes also the visible and infrared radiations of the electromagnetic spectrum, localized heating phenomena can

occur leading to photothermal effects. Nevertheless, structure modifications observed in proteins seem to be due mainly to the UV component of PL, which is responsible for the activation the absorbing sites. For a same photosensitive matrix exposed to a given radiation, the higher the intensity of the light, the higher the extent of protein structure modifications. For instance, when the effect of either PL or UV-C light was investigated on different food proteins (PPO, egg white proteins and gluten proteins), in a wide range of fluence, similar mechanisms of structure modification were observed. For instance, upon UV-C and PL exposure structure modifications of egg white proteins, by means of aggregation/unfolding or backbone cleavage, could be observed and the higher the intensity of light processing, the larger the extent of the structure modifications. In this context, the processing variable which can be used to predict the extent of structural/function modifications can be the fluence, expressed as J $cm^{-2}$. To this regard, literature results showed PPO to undergo unfolding/ aggregation and cleavage phenomena upon UV-C light exposure. Similar structure modifications were also observed upon exposure to PL, however the delivery of additional fluence to PPO samples resulted in further changes of the protein.

*3) Structural arrangement of the target biomolecule*

The nature of the chemical changes promoted by light treatment are significantly affected by the interactions of the target biomolecule occurring at both intra- and inter molecular level. In the case of PPO and egg white, photoinduced structure modifications were found to occur by both conformational changes and backbone cleavage. Whereas, in the case of gluten proteins only conformational changes could be observed. The occurrence of different mechanisms of photoreactivity was attributed to the different structural arrangement of proteins. In fact, both PPO and egg white proteins are globular proteins, which are probably free enough to unfold, interact with other vicinal proteins, and even break upon intense light exposure. By contrast gluten proteins, which are structured in a network made of fibrous and globular proteins, are spatially hampered to react upon light exposure. In flour, gluten proteins closely interact with starch granules in a complex network. In this matrix, the photosensitivity of gluten proteins was found to be even lower than in the sole gluten. In general terms, the higher the possibility of the protein to undergo conformational changes, the higher its photosensitivity. Reversely, when the complexity of the interactions in the food system increases, conformational changes are structurally limited, controlling the overall photosensitivity of the system.

4) *Environmental conditions experienced by the target biomolecule during the treatment.*

The nature and extent of photo-induced structure/function changes is considerably affected by the environmental conditions experienced by the molecule during irradiation. In the case of proteins, the kinetics of conformational changes and aggregation phenomena are well known to depend on macromolecular crowding effects. Data relevant to PPO and gluten proteins show that the photostability increases with their concentration in the system. Similarly, the presence of starch significantly decreased the photosensitivity of gluten in flour. Environmental crowding can favour specific conformations, so that the higher the macromolecular concentration, the more compact and photostable the protein. Ideally, protein photosensitivity could be steered by changing its concentration in the system or adding macromolecules with high excluded volume.

These factors should be carefully considered when light processing is intended for modification of protein functionalities. Figure C schematically shows the combined effect of the different factors on the overall photosensitivity of some biomolecules considered in this study.

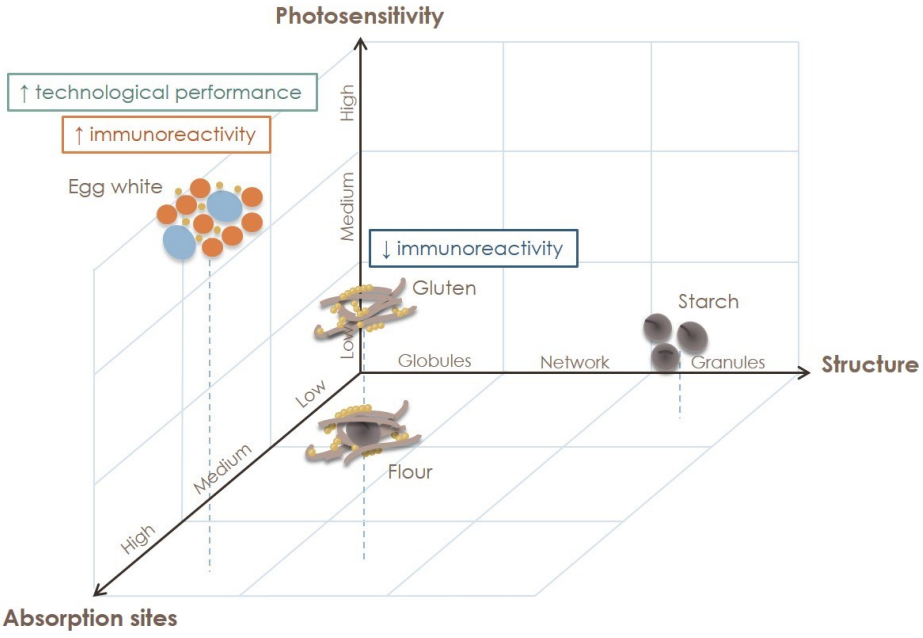


**Figure C** Combined effect of structural arrangement (structure) and chemical nature (presence absorption sites) on biomolecules photosensitivity.

The figure also shows that photoinduced structure modifications account for different modifications of biomolecule functions.

With regard to protein functionality, results obtained when egg white was exposed to PL showed that PL could efficiently improve the foaming properties of egg white proteins, but also increase their immunoreactivity. This suggests that light processing can concomitantly induce positive or negative effects on functionalities of the same protein matrix (egg white). Moreover, PL was found to increase the immunoreactivity in egg white proteins on the one hand, but on the other hand a decrease in gluten proteins immunoreactivity could be observed upon PL exposure. These results suggest that the effects of light processing on food proteins can be very different, since the overall effect of the process depends on a variety of factors that may interplay potentially leading to positive, negligible or negative function modifications.

# PART 2 Effect of HPH on food biomolecules

The second part of this PhD research aimed to investigate the effects of HPH processing on selected food biomolecules focusing on the process-structure-function relationship. Two different matrices were chosen, namely egg white and tomato puree, as an example of protein- and polysaccharide-containing matrix. The following chapters will discuss the effect of HPH on structure, technological performances (viscosity, gelling and foaming properties) and immunoreactivity of egg white proteins as well as the effect of HPH on structure, technological performances and carotenoid bioaccessibility of differently coloured tomato pulps.

## *Chapter 8 Effect of HPH on egg white*

### Aim of the study

Similarly to UV light processing, HPH processing represent a promising non-thermal alternative to conventional thermal processing for microbial inactivation of different food products (Diels, Callewaert, et al., 2005; Donsì et al., 2009; Maresca et al., 2011; Patrignani et al., 2013; Pedras & Pinho, 2012; Picart et al., 2006; Thiebaud et al., 2003). Beside microbial inactivation, the intense mechanical stresses induced by HPH have been shown to affect the structure of food proteins, resulting in changes in their functional properties. For instance, in liquid whole egg HPH induced unfolding of egg proteins, resulting in slight changes in product viscosity and improved foaming properties. In addition, HPH was shown to induce denaturation and/or aggregation of whey proteins, depending on the intensity of mechanical forces and/or the temperature of the sample (Bouaouina et al., 2006; Grácia-Juliá et al., 2008). Also, HPH-induced denaturation of soybean proteins resulted in better emulsifying and gelling properties (Wang et al., 2008). With regard to protein biologic activity, changes in enzymatic activity of several enzymes were observed as a consequence of HPH induced protein conformational changes (Calligaris et al., 2012b; Suárez-Jacobo et al., 2012; Vannini et al., 2004). On the basis of these evidences, HPH could be exploited to obtain protein-rich foods with specific functionalities. As mentioned

before, egg white is an interesting protein rich ingredient, which is extensively used in the food industry due to its multifunctional properties. The aim of this study was to investigate the effect of HPH on egg white protein structure and selected functional properties.

**Results and discussion**

Egg white was cooled at 4 °C and homogenised at 150 MPa for up to 17 passes. Untreated egg white and egg white homogenised at 0 MPa *via* a single pass were taken as controls. In order to minimise the increase in temperature during processing, the inlet and outlet of the homogeniser were connected to a cooling system set at 4 °C. Operating under these conditions, the temperature of homogenised egg white never exceeded 35 °C (Figure 8.1).

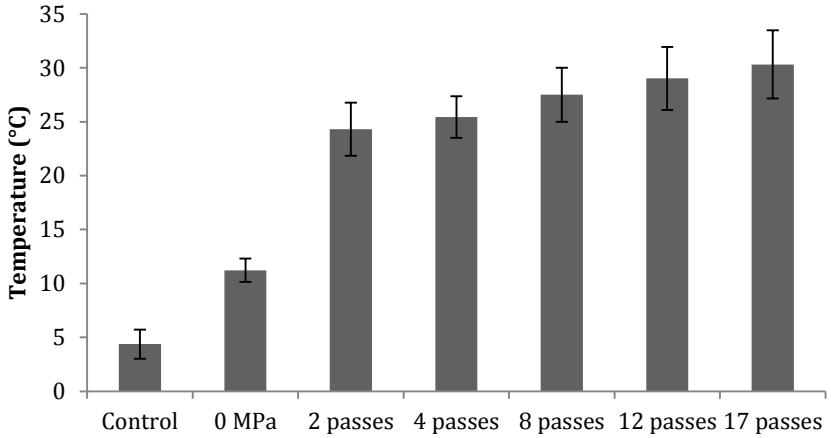


**Figure 8.1** Egg white temperature of untreated egg white (Control), egg white homogenised at 0 MPa (0 MPa), and egg white homogenised at 150 MPa *via* multiple passes (2, 4, 8, 12, 17 passes).

Being this temperature far lower than the denaturation temperature of ovotransferrin (61 °C), which is the most heat-sensitive egg white protein (Mine, 1995), any changes that have occurred in the samples can be attributed to the sole effect of the homogenisation process.

High pressure homogenisation induced changes in egg white optical density at 680 nm (Figure 8.2).

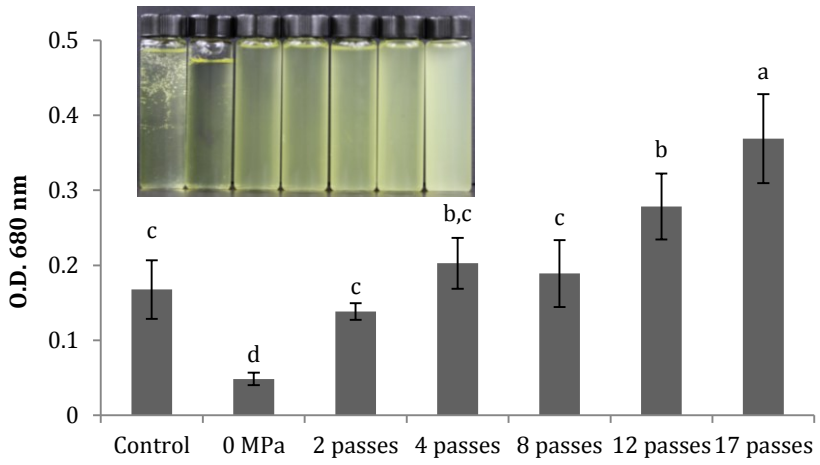


**Figure 8.2** Optical density (O.D.) at 680 nm, and visual appearance (inset) of untreated egg white (Control), egg white homogenised at 0 MPa (0 MPa), and egg white homogenised at 150 MPa *via* multiple passes (2, 4, 8, 12, 17 passes). Bars indicated by the same letter are not statistically different ($P$>0.05).

The initial decrease in optical density after a single homogenisation pass at 0 MPa was followed by a progressive increase upon multiple homogenisation passes at 150 MPa. These changes were accompanied by a progressive shift of egg white colour from yellow towards milky white (Figure 8.2, inset), suggesting the formation of protein aggregates/network able to scatter light. Dynamic light scattering analysis (Table 8.1) of untreated egg white showed the presence of two classes of particles with average diameter about 143 nm and larger than 8000 nm. The latter was the main class of particles in the sample and accounted for protein aggregates formed through non-covalent weak interactions. It is well known that in fresh egg white ovomucin, which is a highly glycosylated protein with a very high molecular weight, can aggregate with other egg white proteins by means of electrostatic interactions. In particular, the carboxylic groups of the ovomucin sialic acids can interact with the amino group of lysozyme lysine residues to form a lysozyme-ovomucin complex that would be responsible for the gel-like structure of egg white (Kato et al., 1975; Mine, 1995). These weak interactions would be easily broken by a single homogenisation pass at 0 MPa, leading to a significant increase in the presence of particles with average diameter equal to 143 nm as well as to the formation of smaller particles with average diameter about 35 nm. No significant differences in the size distribution of protein particles were observed upon further homogenisation at 150 MPa up to 8 passes. By contrast, egg white homogenised at 150 MPa for 12 and 17 passes showed the

occurrence of a novel class of particles with average diameter equal to 473 nm. The latter might account for HPH-induced protein unfolding or aggregation.

**Table 8.1** Percentage distribution of particles with average hydrodynamic radius (ø) equal to 13, 35, 143, 473, and larger than 8000 nm in untreated egg white (Control), egg white homogenised at 0 MPa (0 MPa), and egg white homogenised at 150 MPa *via* multiple passes (2, 4, 8, 12, 17 passes).

| | Particles (%) | | | | |
|---|---|---|---|---|---|
| | ø ≈ 13 nm | ø ≈ 35 nm | ø ≈ 143 nm | ø ≈ 473 nm | ø > 8000 nm |
| Control | n.d. | n.d. | 14.70 ± 2.19 | n.d. | 87.44 ± 9.59 |
| 0 MPa | n.d. | 5.37 ± 1.79 | 84.90 ± 13.19 | n.d. | n.d. |
| 2 passes | n.d. | 4.75 ± 1.64 | 92.02 ± 4.34 | n.d. | n.d. |
| 4 passes | 3.47 ± 1.25 | n.d. | 90.82 ± 6.19 | n.d. | n.d. |
| 8 passes | n.d. | 3.65 ± 0.64 | 85.30 ± 4.63 | n.d. | n.d. |
| 12 passes | 1.40 ± 0.66 | n.d. | 40.90 ± 4.16 | 58.43 ± 4.65 | n.d. |
| 17 passes | 0.80 ± 0.01 | n.d. | 49.67 ± 10.07 | 56.85 ± 6.01 | n.d. |

n.d.: not detected

To investigate the nature of HPH-induced protein structural modifications, samples were analysed for the concentration of free sulfhydryl groups (SH) (Figure 8.3). As previously mentioned, the decrease in free SH could indicate protein cross-linking, while their increase generally accounts for both protein unfolding and backbone fragmentation (Beveridge et al., 1974). In the case of egg white homogenised at 0 MPa *via* a single pass, an increase in free SH was observed. Such increase can be consistent with the exposure of free SH upon disruption of the large protein aggregates having hydrodynamic radius higher than 8000 nm (Table 8.1). With regard to the egg white homogenised at 150 MPa, after 2 homogenisation passes an intermediate content in free SH between the control and the egg white homogenised at 0 MPa was observed. On the other hand, further homogenisation passes led to a concentration of free SH similar to that of the egg white homogenised at 0 MPa.

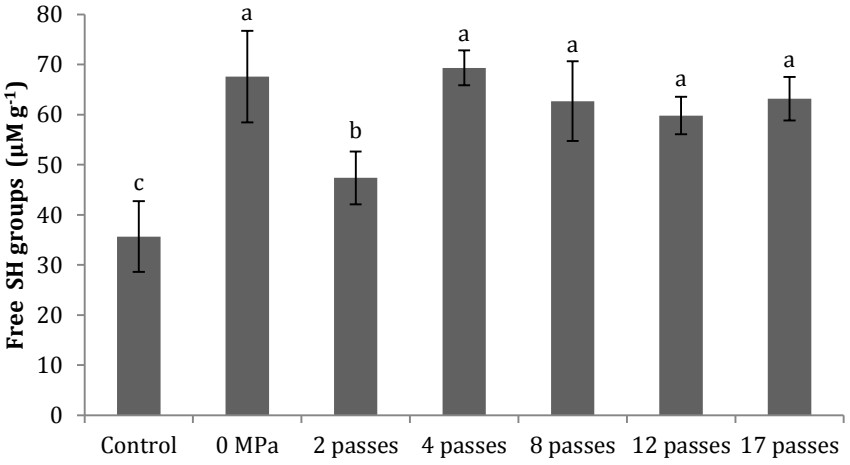


**Figure 8.3** Free SH groups in untreated egg white (Control), egg white homogenised at 0 MPa (0 MPa), and egg white homogenised at 150 MPa *via* multiple passes (2, 4, 8, 12, 17 passes). Bars indicated by the same letter are not statistically different (P> 0.05).

The initial decrease and subsequent increase in free SH upon multiple homogenisation passes at 150 MPa supports the hypothesis of protein structural modification by means of both unfolding and aggregation phenomena. The latter would be concomitantly induced by HPH, leading to counterbalancing effects on the changes in free SH. Two different mechanisms have been suggested for protein aggregation. First, the exposure of the hydrophobic regions as a consequence of protein unfolding can lead to hydrophobic interactions (Rao & Labuza, 2012). Second, sulfhydryl groups and disulphide bonds, which are buried in the native state of the protein, can become available in the unfolded proteins and react to form intermolecular cross-links (Ferry, 1948). In the present case, the changes in free SH groups are more likely attributable to the formation and breakage of hydrophobic interactions, rather than to protein crosslinking. In fact, weak interactions such as the hydrophobic ones can be easily formed and broken upon HPH. Instead, covalent bonds responsible for protein crosslinking are known to be hardly affected by HPH (Subirade et al., 1998).

To confirm this hypothesis egg white samples were analysed by SDS-PAGE (Figure 8.4).

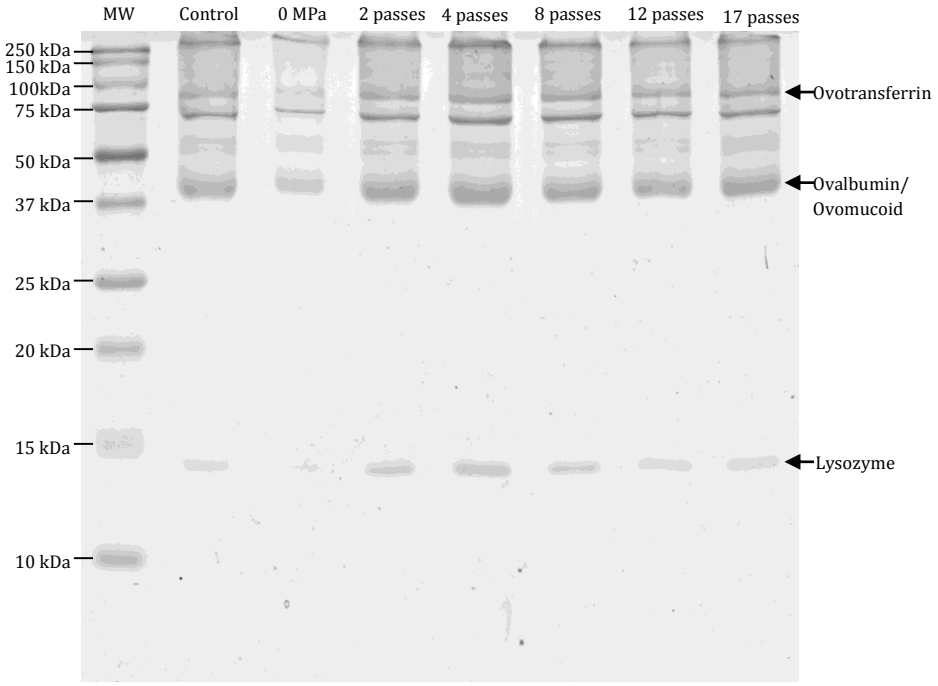


**Figure 8.4** Electrophoretic pattern of untreated egg white (Control), egg white homogenised at 0 MPa (0 MPa), and egg white homogenised at 150 MPa *via* multiple passes (2, 4, 8, 12, 17 passes). Molecular weight standards (MW) are in the far left lane.

As known, SDS is an anionic surfactant able to disrupt non covalent bonds, such as hydrophobic interactions among proteins, and impart a negative charge to proteins. The SDS-PAGE pattern of the untreated egg white exhibited three main bands that, by comparison with the standard molecular weights (MW) and literature information (Awadé & Efstathiou, 1999; Guérin-Dubiard et al., 2006; Mine, 1995), were attributed to ovotransferrin, ovalbumin/ovomucoid, and lysozyme. Whatever the pressure level, no difference between the SDS-PAGE patterns of the homogenised egg white samples and that of the untreated egg white was observed. Therefore, polyacrylamide gel electrophoresis under dissociating conditions confirmed that HPH-induced aggregation occurred mainly through hydrophobic interactions and not by the formation of covalent bonds. Similar results were also reported by Grácia-Juliá et al. (2008) for whey protein dispersions homogenised at pressures higher than 250 MPa, and by Marco-Molés & Hernando (2009) for liquid whole egg homogenised at 100 MPa for 3 cycles.

Results relevant to the distribution of the particle size (Table 8.1), free SH (Figure 8.3) and protein fractions (Figure 8.4) suggest HPH to promote structural

modifications of egg white proteins by means of unfolding and aggregation phenomena. In particular, homogenisation initially induced partial unfolding of egg white protein leading to exposure of protein hydrophobic regions. On further homogenisation partial aggregation of unfolded proteins also took place due to hydrophobic interactions.

To understand whether the HPH-induced unfolding and hydrophobic interaction among egg white proteins could be associated to modifications in their functional properties, samples were also analysed for apparent viscosity, gelling and foaming properties (Table 8.2).

**Table 8.2** Apparent viscosity, gel firmness, foam ability and stability of untreated egg white (Control), egg white homogenised at 0 MPa (0 MPa), and egg white homogenised at 150 MPa *via* multiple passes (2, 4, 8, 12, 17 passes).

| | Apparent viscosity (Pa s) | Gel firmness (N) | Foam ability (mL) | Foam stability (%) |
|---|---|---|---|---|
| Control | $0.057 \pm 0.005^{a}$ | $0.148 \pm 0.016^{b}$ | $18.7 \pm 0.6^{a}$ | $86.1 \pm 4.1^{a}$ |
| 0 MPa | $0.035 \pm 0.006^{b}$ | $0.181 \pm 0.022^{a}$ | $19.0 \pm 1.0^{a}$ | $89.1 \pm 7.1^{a}$ |
| 2 passes | $0.047 \pm 0.006^{a,b}$ | $0.067 \pm 0.003^{e}$ | $19.0 \pm 1.0^{a}$ | $84.0 \pm 7.1^{a}$ |
| 4 passes | $0.050 \pm 0.001^{a,b}$ | $0.080 \pm 0.005^{e}$ | $18.7 \pm 0.6^{a}$ | $86.0 \pm 3.8^{a}$ |
| 8 passes | $0.055 \pm 0.007^{a}$ | $0.095 \pm 0.007^{d,e}$ | $17.7 \pm 0.6^{a}$ | $88.7 \pm 4.4^{a}$ |
| 12 passes | $0.057 \pm 0.005^{a}$ | $0.110 \pm 0.002^{c,d}$ | $18.7 \pm 0.6^{a}$ | $85.2 \pm 3.3^{a}$ |
| 17 passes | $0.055 \pm 0.013^{a}$ | $0.118 \pm 0.002^{c}$ | $18.7 \pm 0.6^{a}$ | $84.3 \pm 6.3^{a}$ |

$^{a,b,c,d,e}$ Means on the same column indicated by the same letter are not statistically different ($P>0.05$).

Apparent viscosity, taken as an indicator of the rheological behaviour of egg white, was found to decrease after a single homogenisation pass at 0 MPa. This effect can be attributed to the disruption of the weak and unstable network characterising the large protein aggregates naturally occurring in the untreated egg white (Table 8.1). Upon further homogenisation passes at 150 MPa, viscosity values progressively approached that of the untreated egg white (Table 8.2), reasonably due to the formation of a novel protein network by weak hydrophobic interactions. Gel firmness, defined as the maximum load needed to puncture the gel, was also analysed as an indicator of the textural properties of egg white gels (Table 8.4). The firmest gel was obtained from the egg white homogenised at 0 MPa. By contrast, the least firm gel was obtained from the egg white homogenised at 150 MPa for 2 passes. Although on further homogenisation passes a progressive increase in gel firmness was observed, the egg white homogenised at 150 MPa always produced softer gels than those obtained from the untreated and 0 MPa homogenised egg white. As known, the thermal transformation of egg white proteins into a gel involves partial protein unfolding

with exposure of functional groups. Thereafter, ovalbumin, ovotransferrin and lysozyme form intermolecular β-sheet structures through hydrogen-bonding, electrostatic and hydrophobic interactions, resulting in a gel network (Mine, 1995). The strength of the protein gel network was reported to be dependent on the balance between protein hydrophobic interactions and electrostatic repulsive forces. In particular, the better the balance between electrostatic and hydrophobic interactions, the stronger the gel (Hatta et al., 1986). The decrease in particle dimensions (Table 8.3) in combination with the evidence of protein unfolding (Figure 8.3) after homogenisation at 0 MPa might favour the balance between the electrostatic and hydrophobic interactions and thus the formation of a firmer gel. Upon homogenisation at 150 MPa both protein unfolding and aggregation phenomena due to hydrophobic interactions were observed. It can be inferred that these concomitant phenomena unbalanced the attractive and repulsive forces between egg white proteins, favouring the formation of softer gels.

With regard to foaming properties (Table 8.3), no differences were observed in foam ability of HPH-treated egg white. Foams obtained from untreated and homogenised egg white samples were also held during 30 min at room temperature to evaluate foam stability. As expected, foam stability of all the samples was found to decrease after 30 min resting. The foam stability of the untreated egg white after 30 min was about 86% of the just prepared foam and no changes in egg white foam stability were observed upon homogenisation at both 0 and 150 MPa. These results were supported by microscopy analysis of just prepared and 30 min held egg white foams. As an example micrographs relevant to the foams obtained from the untreated egg white, egg white homogenised at 0 MPa, and egg white homogenised at 150 MPa for 17 passes are presented in figure 8.5. Microscopy images clearly show that no changes in bubble size could be observed among the samples for both just prepared foams and 30 min held foams.

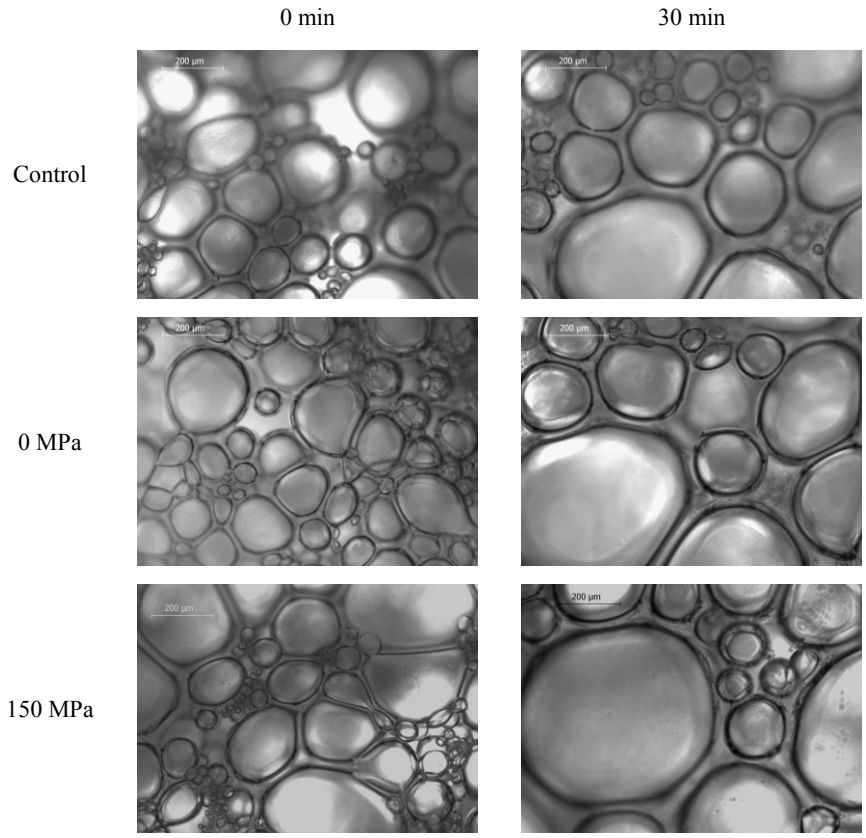


**Figure 8.5** Micrographs (100x) of just prepared (0 min) and 30 min held (30 min) foams obtained from untreated egg white (Control), egg white homogenised at 0 MPa (0 MPa), and egg white homogenised at 150 MPa *via* 17 passes.

Despite the great nutritional relevance of egg white, it also represents a critical issue for its allergenic potential. Ovalbumin, ovomucoid, lysozyme, and ovotranferrin are the major allergenic proteins of egg white (Mine & Yang, 2008). However, literature evidences as well as results obtained in the first part of this thesis (Chapters 4.1 and 4.2), show that thermal treatments and non-thermal processes can modify egg white allergenicity (Mine & Yang, 2008; Shriver & Yang, 2011). Based on these considerations, egg white samples processed by HPH were analysed for immunoreactivity by an ELISA method.

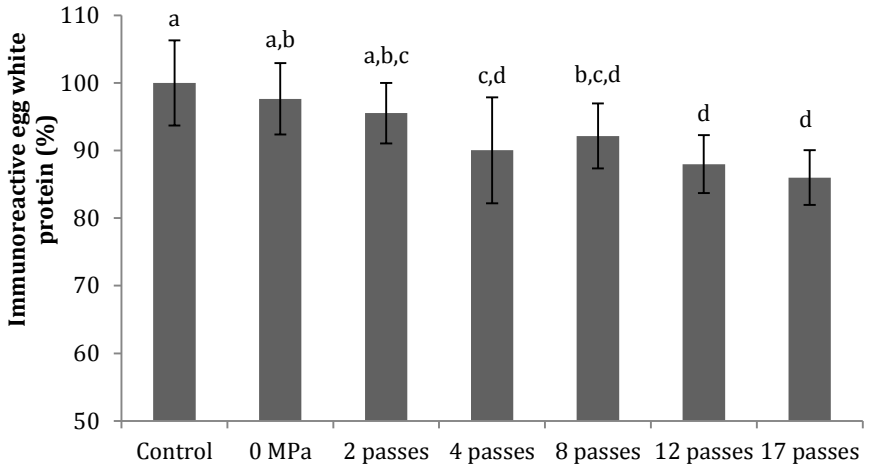


**Figure 8.6** Immunoreactive proteins in untreated egg white (Control), egg white homogenised at 0 MPa (0 MPa), and egg white homogenised at 150 MPa *via* multiple passes (2, 4, 8, 12, 17 passes). Bars indicated by the same letter are not statistically different ($P > 0.05$).

A slight, but significant decrease in immunoreactivity was observed upon HPH processing of egg white. Protein immunoreactivity was reduced by *circa* 10% when egg white was homogenised at 150 MPa for 4 or more passes. This suggests that HPH induced protein unfolding and aggregation might partially hide protein epitopes, leading to the decrease of immunoreactivity.

## Conclusions

Present results confirm the potential of HPH to modify protein structure and functions. In fact the intense shear the egg white samples underwent during multiple-pass HPH treatment resulted in the unfolding and formation of intramolecular interactions between proteins. Contrary to UV processing, HPH could induce only conformational changes in egg white proteins, even at very high shear intensity. Such conformational changes, which resulted in the formation of a weak and unstable protein network, did not affect the foaming properties of egg white. On the other hand, these structural modifications turned out to be sufficient to induce a decrease in egg white gel firmness and immunoreactivity. To this regard, by choosing proper processing conditions, some egg white functionalities, such as gel firmness and immunoreactivity, can be steered to obtain egg white with specific functional properties.

## *Chapter 9 Effect of HPH on tomato pulps*

**Aim of the study**

This chapter focuses on the effect of HPH on structure and carotenoid biaccessibility of differently coloured tomato pulps. The production of tomato derivatives, such as juices, pulps, or concentrates, involves the mechanical disruption of the plant material. The result is a dispersion that is a combination of a liquid phase containing pectic material, sugars and organic acids and a dispersed phase formed of all the plant insoluble solids such as cell wall material (Lopez-Sanchez, Nijsse, et al., 2011) The texture and rheological properties of tomato-based products are determined by the structure of the cell wall polysaccharide pectin (Sila et al., 2009). HPH has been shown to affect polysaccharides in fruit- and vegetable-based products, thus leading to modification of their textural and rheological properties. For instance, HPH has been shown to decrease the viscosity of carrot and broccoli puree (Christiaens et al., 2012; Lopez-Sanchez, Nijsse, et al., 2011). By contrast, the increase in viscosity of tomato puree and juice was attributed to the formation and strengthening of a fibre network due to HPH processing (Augusto, Ibarz, & Cristianini, 2013; Bayod et al., 2007; Beresovsky et al., 1995; Colle et al., 2010; Lopez-Sanchez, Svelander, et al., 2011; Lopez-Sanchez, Nijsse, et al., 2011). Such structural modifications have been suggested to affect the release and bioaccessibility of micronutrients, such as carotenoids, from the food matrix (Parada & Aguilera, 2007; van het Hof et al., 2000). Carotenoids are naturally occurring fat-soluble pigments responsible for tomato colour. They have received much attention because of their health related functions, such as preventing and protecting against cancer, heart disease, and macular degeneration (Rao & Rao, 2007). Health protective effects of carotenoids strongly depend on their bioavailability and bioaccessibility. The latter is defined as the fraction of the ingested carotenoids that is released from the food matrix, incorporated into mixed micelles and thus available for intestinal absorption (Parada & Aguilera, 2007). The structure of the food matrix, as well as the species of carotenoid, and their localisation within the plant tissue, seem to play a major role in determining carotenoid bioaccessibility (Castenmiller & West, 1998). The latter can be improved by the disruption of the matrix (van het Hof et al., 2000; Knockaert, Lemmens, Van Buggenhout, Hendrickx, & Van Loey, 2012; Svelander, Lopez-Sanchez, Pudney, Schumm, & Alminger, 2011). On the other hand, the formation of the network can trap carotenoids and impair their bioaccessibility (McClements, Decker, & Park, 2009). The aim of this study was

thus to investigate the effect of HPH on tomato pulp structure and carotenoid bioaccessibility.

**Results and discussion**

Pulps from tomatoes having different flesh colour (red, orange and yellow) were submitted to increasing homogenisation pressure and analysed for structural characteristics.

As HPH is known to induce mechanical disruption of the food matrix, tomato pulps were analysed for their particle size distributions (PSDs) (Figure 9.1).

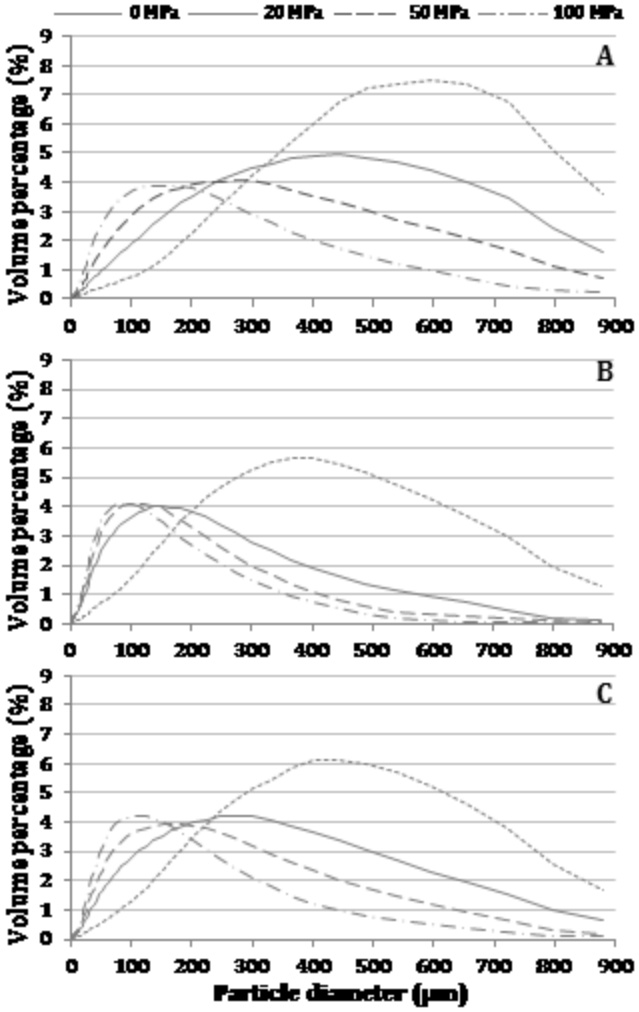


**Figure 9.1** Volumetric particle size distribution of red (A), orange (B), and yellow (C) tomato pulps homogenised at different pressure levels.

In the non homogenised red tomato pulp, particles with mean diameter around 600-700 μm were found. Nevertheless, the non homogenised orange and yellow samples presented particles with smaller mean diameter (300-500 μm). As expected, the increase of homogenisation pressure induced a progressive decrease in particle dimensions. After homogenisation at 100 MPa the mean particle diameter in red tomato pulps was about 100-200 μm. Moreover, the higher the homogenisation pressure the narrower the PSD and thus the more uniform the tomato particles. The same behaviour was observed in the orange and yellow tomatoes. However, in these cases the decrease in particle dimension with homogenisation pressure was less gradual than in red tomato.
PSD results are consistent with the observations made under light microscope (Figure 9.2).

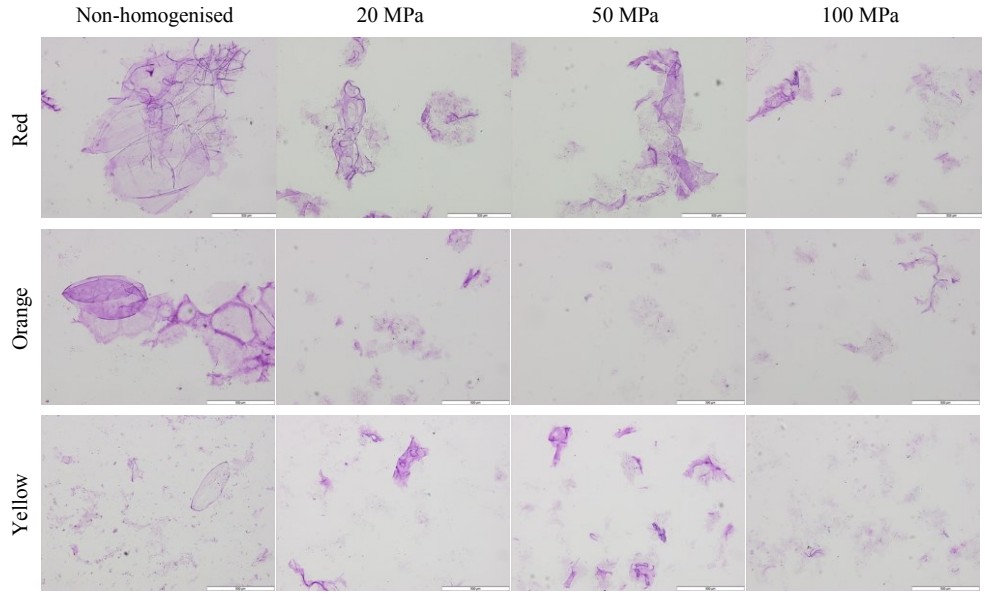


**Figure 9.2** Light micrographs of tomato pulps stained with toluidine blue (magnification: 10x). From top to bottom: red, orange and yellow tomato pulp. From left to right: non-homogenised and homogenised pulps at 20, 50 and 100 MPa.

In the non homogenised pulp of red tomato, cell clusters consisting of several cells were observed. Their presence accounts for the higher mean particle diameter (Figure 9.1). Upon homogenisation at 20 MPa, only single cells and broken cell material were observed in the sample. Homogenisation at 50 MPa led to further disruption of cell material and only cell fragments were observed in the samples. At 100 MPa the complete breakage of cells occurred and cell material

was uniformly distributed. In the non homogenised orange and yellow tomato pulps, only single cells and fragments of cell material were observed while no clear clusters were visible. The complete cell disruption and the release of the cellular content occurred by homogenisation at only 20 MPa and no clear additional structure modifications were observed on further increase in homogenisation pressure.

In order to evaluate the effect of HPH on the textural properties, the consistency index of tomato pulps was determined using a Bostwick consistometer (Figure 9.3).

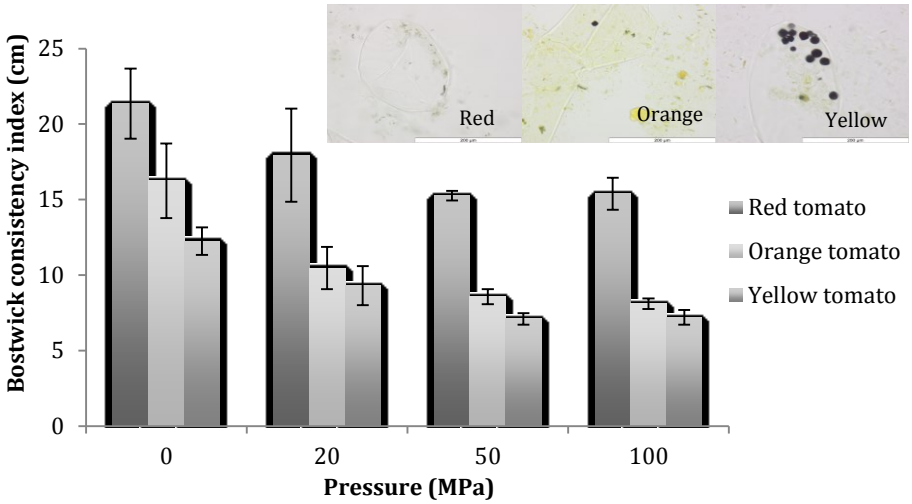


**Figure 9.3** Bostwick consistency indices of tomato pulp homogenised at different pressure levels. Inset: Light micrographs of non-homogenised tomato pulps stained with iodine, magnification 40x.

Non homogenised tomato pulps of different colours presented different consistency indices, with yellow tomato being the most consistent, followed by the orange and the red tomatoes. Such differences might be attributed to the amount of starch present in the different tomato pulps. The inset of Figure 9.3 shows micrographs of tomato pulps stained with iodine. The black spots represent the starch granules. Iodine staining of tomato pulps thus revealed a higher amount of starch for yellow tomatoes compared to orange and red tomatoes.

During HPH (Figure 9.3), increased pressure levels resulted in lower consistency indices and thus in higher consistency values for all the tomato pulps. As reported by other authors (Colle *et al*., 2010; Svelander *et al*., 2011), HPH would favour the interaction between cell wall polysaccharides (pectins, hemicellulose, and

cellulose) leading to the formation of a network, that determined the increase in consistency of tomato pulps. Similarly, Kjøniksen, Hiorth, & Nyström, (2005), observed thickening effects in aqueous pectin solution upon oscillatory and steady shear. The thickening effect was attributed to pectin association in a network by means of hydrogen bonds. Despite the differences observed in non homogenised samples, the trend of the consistency increase was similar for all the tomato varieties.

In order to determine the type and quantity of carotenoids present in red, orange and yellow tomatoes, HPLC analyses were performed on the corresponding non homogenised pulps. Results are shown in table 9.1.

**Table 9.1** Content of the main carotenoids in pulp ($C_0$) and digest ($C_d$) of non-homogenised red, orange and yellow tomatoes.

| | | $C_0$ (µg/g pulp) | $C_d$ (µg/g pulp) |
|---|---|---|---|
| Red tomato | Lycopene | 45.77 ± 2.41 [a] | 44.57 ± 3.02 [a] |
| | Lutein | n.d. | 1.48 ± 0.06 |
| Orange tomato | ζ-carotene | 6.62 ± 0.72 [a] | 7.43 ± 0.81 [a] |
| | Lutein | n.d. | 0.80 ± 0.10 |
| Yellow tomato | Lutein | 0.68 ± 0.13 [a] | 1.70 ± 0.13 [b] |

n.d. not detected

[a,b] means with the same letter in the same row are not significantly different ($P$<0.05)

As expected, chromatograms showed the presence of lycopene ($\lambda_{max}$: 444; 471; 502 nm; retention time: 36 min) and lutein ($\lambda_{max}$: 421; 444; 472 nm; retention time: 10 min) in red and yellow tomato respectively. The chromatograms relevant to orange tomato showed the presence of one peak with retention time similar to that of *β*-carotene (retention time: 23 min) but a completely different spectrum ($\lambda_{max}$: 379; 400; 425 nm). By comparison with literature information (Mackinney & Jenkins, 1949; Tomes, Quackenbush, & North, 1953) and spectral characteristics (comparison with standards, data not shown), this peak was tentatively attributed to the elution of ζ-carotene. Since the spectral characteristics revealed the presence of a second component, it is likely that, together with ζ-carotene, other carotenoid compounds (such as prolycopene) are eluted with the same retention time (Tomes *et al*., 1953).

Since digestive enzymes could promote the release of carotenoids from the matrix, analyses of the carotenoid content were also performed after digestion of the different tomato pulps (Table 9.1). No differences for lycopene and ζ-carotene content in the pulp and in the digest were observed. Lycopene and ζ-carotene, being carotenes, do not contain hydroxyl groups which can form esters. The latter could hinder carotenoid extraction from the food matrix, giving reason for the difference in carotenoid amount between the digest and the pulp. As regards

lutein in yellow tomatoes, the content in the digest was found to be two times higher than in the pulp. In red and orange tomato, lutein was detected only in the digest. It was speculated that lutein might be embedded in the matrix (xanthophylls can form esters more easily due to the presence of oxygen groups) and is thus hardly extractable by hexane solely. Comparing the different tomato varieties, lutein content in red and yellow tomatoes was similar and twice as much as the amount that was observed in the orange tomato digest.
Light microscopy was also performed to visualise the carotenoid containing chromoplasts in the different tomato varieties (Figure 9.4).

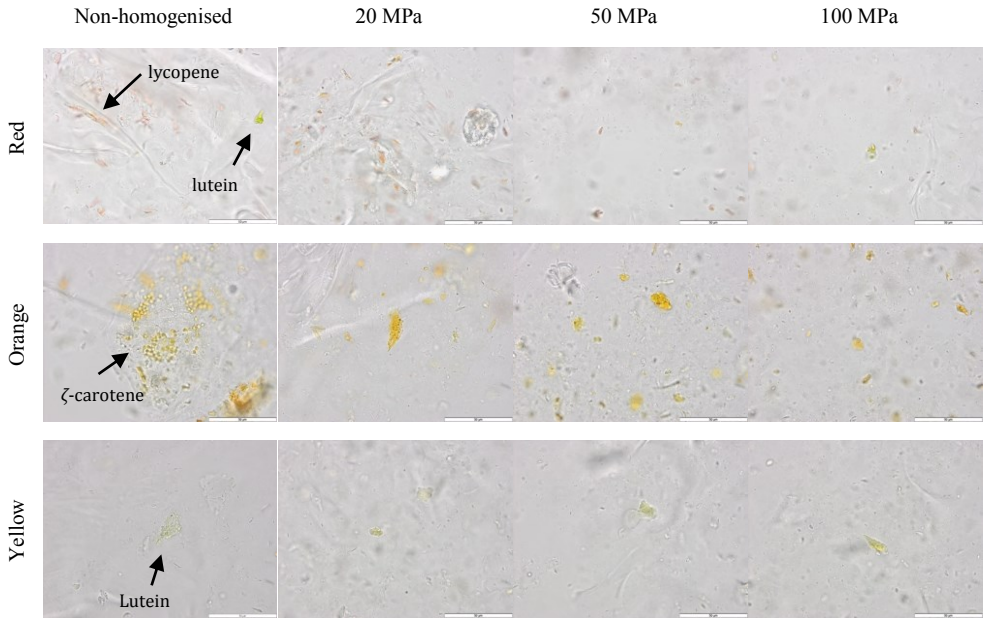


**Figure 9.4** Light micrographs of chromoplasts of tomato pulps (magnification: 100x). From top to bottom: red, orange and yellow tomato pulp. From left to right: non homogenised and homogenised pulps at 20, 50 and 100 MPa.

Two types of chromoplast structures were observed in the red tomato pulp: red, large and needle-shaped chromoplasts and yellowish round-shaped chromoplasts. The former type was largely the most abundant. Based on the colour and shape as well as by comparison with literature evidences (Jeffery, Holzenburg, & King, 2012; Schweiggert, Steingass, Heller, Esquivel, & Carle, 2011; Schweiggert, Steingass, Mora, Esquivel, & Carle, 2011), it was speculated that the needle-shaped structures contain crystalline lycopene, and the yellowish round-shaped structures contain lipid dissolved lutein. However, further analysis could be

performed to confirm this hypothesis. Upon homogenisation, chromoplasts containing crystalline lycopene were reduced in size, while no differences were observed for the globular lutein containing ones. It can be hypothesised that crystalloid chromoplasts are more fragile than the globular ones and thus more prone to mechanical rupture. In orange and yellow tomato, only round-shaped chromoplasts probably containing lipid dissolved ζ-carotene and lutein respectively were present. In the homogenised samples of both varieties, chromoplasts were found to be distributed all over the medium as a consequence of matrix disruption, but no changes in their dimension were observed.
The effect of HPH on the bioaccessibility of the carotenoids occurring in the different tomato varieties was studied (Table 9.2).

**Table 9.2** Relative amount of carotenoid incorporated in micelles (% $C_m/C_d$) of red, orange and yellow tomato pulp submitted to different homogenization pressure levels.

| Tomato variety | Carotenoid | Homogenization pressure (MPa) | | | |
|---|---|---|---|---|---|
| | | 0 | 20 | 50 | 100 |
| Red | Lycopene | 13.1 ± 0.9 [a] | 9.4 ± 0.7 [b] | 6.7 ± 1.1 [c] | 7.1 ± 0.8 [c] |
| | Lutein | 93.0 ± 4.0 [a] | 92.4 ± 5.7 [a] | 78.3 ± 3.9 [b] | 72.1 ± 6.7 [b] |
| Orange | ζ-carotene | 29.4 ± 3.2 [a] | 17.7 ± 1.9 [b] | 14.7 ± 1.7 [c] | 13.7 ± 1.6 [c] |
| | Lutein | 74.2 ± 22.3 [a] | 64.5 ± 9.0 [a] | 68.5 ± 11.3 [a] | 63.0 ± 13.2 [a] |
| Yellow | Lutein | 96.2 ± 9.8 [a] | 81.1 ± 8.5 [b] | 69.2 ± 6.6 [b] | 73.3 ± 6.0 [b] |

[a,b,c] means with the same letter in the same row are not significantly different ($P$<0.05)

Interestingly, as regards the non homogenised tomato pulps, the relative amount of lycopene and ζ-carotene incorporated into micelles was about 13 and 30% respectively. By contrast, the average content of lutein in micelles was *circa* 88% for the different tomatoes. These differences might be explained by considering the nature of the carotenoid compounds and the structure of the chromoplasts in which they are embedded in the different tomato varieties (Figure 9.4). Among the carotenoids under consideration, lycopene is, indeed, the most hydrophobic followed by ζ-carotene and lutein. The higher incorporation of lutein into mixed micelles compared to ζ-carotene and lycopene is in agreement with previous studies demonstrating that the extent of incorporation of lipophilic compounds into mixed micelles was inversely related to their hydrophobicity (Borel, 2003; Schweiggert, Mezger, Schimpf, Steingass, & Carle, 2012). Therefore, despite its larger total amount (Table 9.1), lycopene turned out to be the carotenoid, which is the least bioaccessible. The molecular structure of ζ-carotene is similar to that of lycopene. Nevertheless, microscopy analysis highlighted a marked structural difference between lycopene and ζ-carotene bearing chromoplasts, the former being crystalloid and the latter being globular. Literature data indicate that the higher incorporation into mixed micelles of ζ-carotene can be explained by the

better release of carotenoids from non-crystalline chromoplasts (Schweiggert et al., 2011; Vasquez-Caicedo, Heller, Neidhart, & Carle, 2006). The present results show that HPH resulted in an overall decrease of carotenoid *in vitro* bioaccessibility for all carotenoids and for all matrices. Lycopene and ζ-carotene bioaccessibility in red and orange tomatoes respectively decreased as homogenisation pressure increased up to 50 MPa. No significant differences were observed on further increasing homogenisation pressure. Similarly, lutein bioaccessibility was found to decrease in red and yellow tomatoes upon HPH at increasing pressure levels. A slight decrease could also be observed in orange tomato, however the differences between the non- and the homogenised samples were not significant. The low amount of lutein measured in orange tomato (Table 9.1) could impair bioaccessibility data accuracy, giving reason for the apparent limited effect of HPH.

Based on the present HPLC data and in agreement with literature results (Colle *et al*., 2010; Svelander *et al*., 2011), the decrease in carotenoid bioaccessibility upon HPH (Table 9.2) can not be attributed to their loss or isomerisation. By contrast, it is more reasonable to hypothesise a relation between structural modifications and carotenoid *in vitro* bioaccessibility (Parada & Aguilera, 2007).

The data obtained demonstrate that HPH affects the tomato matrix by means of two counterbalancing effects: (i) the disruption of the matrix (Figures 9.1 and 9.2) which facilitates carotenoid release; (ii) the increase in consistency (Figure 9.3) due to the formation and strengthening of a fibre network entrapping carotenoids (Colle *et al*., 2010; McClements *et al*., 2009). The observed decrease in carotenoid *in vitro* bioaccessibility with increasing homogenisation pressure suggests the structure enabling effect of HPH to dominate on the disruption one. In order to clearly observe this relationship, The relative *in vitro* bioaccessibility of lycopene, ζ-carotene, and lutein was thus plotted against the average Bostwick consistency of tomato pulps (Figure 9.5). Regression lines, equations and determination coefficients values ($R^2$) are also shown.

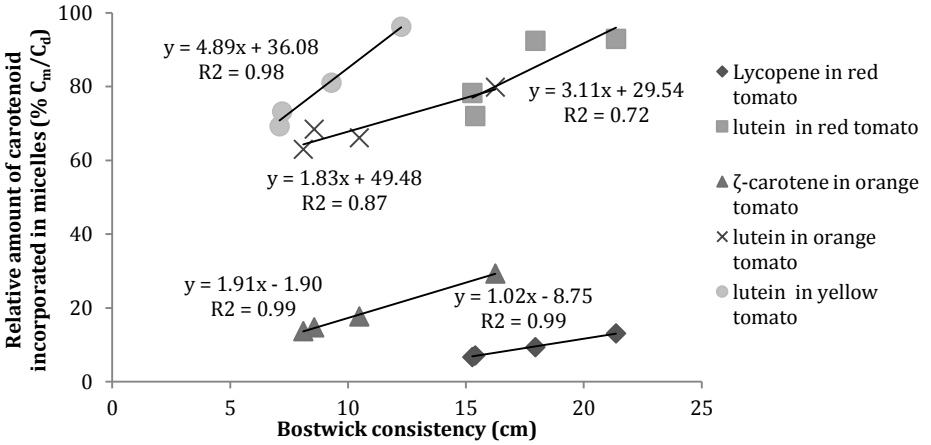


**Figure 9.5** Relative amount of carotenoids incorporated into micelles as a function of the Bostwick consistency index of homogenised tomato pulps. Results of the regression analysis are also shown.

The high values of the determination coefficients ($R^2$) confirm the relation between the amount of carotenoids incorporated into micelles and the Bostwick consistency index. Figure 9.5 clearly shows that the values of the slope ($\beta$) of all the regression lines are positive, indicating this relation to be positive. Basically, the higher the consistency of the matrix the lower the bioaccessibility of carotenoids. Analogous results were also reported by Colle *et al*. (2010) and Anese, Mirolo, Beraldo, & Lippe (2013). These authors observed a decrease in lycopene *in vitro* bioaccessibility upon process-induced structurisation of tomato pulps.

The dependence of bioaccessibility on Bostwick consistency (Figure 9.5) was also affected by both the tomato nature and the carotenoid species. As regards red tomato, the increase in consistency upon HPH had minor effects on lycopene bioaccessibility ($\beta$=1.02) while it considerably affected that of lutein ($\beta$=3.11). Although HPH seemed not to modify the structure of lutein bearing chromoplasts (Fig 9.4), the possible formation of a fibre network could impair lutein release from the matrix. By contrast, HPH would lead to the breakage of crystalloid lycopene chromoplasts (Fig 9.4), possibly lowering the effect of the network formation on its bioaccessibility. In orange tomato, a similar dependence of ζ-carotene and lutein bioaccessibility on the Bostwick consistency was observed ($\beta$=1.91 and 1.83 respectively), probably due to the similar structure of the chromoplasts they are embedded in. The highest dependence of bioaccessibility on the Bostwick consistency was found for the lutein in the yellow tomato. In this

case, the fibre network formed upon HPH seemed to markedly hinder the release of lutein from the matrix. Nevertheless lutein *in vitro* bioaccessibility was found to be always higher than *circa* 70%.
A remarkable observation in this study is that in one matrix, i.e. red (homogenised) tomato, both carotenoids with a very high bioaccessibility (lutein) and carotenoids with a very low bioaccessibility (lycopene) are present. This suggests the carotenoid bioaccessibility to be not dependent on the matrix solely. The importance of the carotenoid species for the bioaccessibility can clearly be seen in Fig. 4, since it shows that different types of carotenoids were clearly separated into two groups: lycopene and ζ-carotene in the lower part (low bioaccessibility), and lutein in the upper part of the graph (high bioaccessibility). In general it can thus be concluded that the matrix effects, as well as carotenoid characteristics are important factors for carotenoid bioaccessibility.

**Conclusions**

Accordingly to literature evidences, present results show that HPH can be used to improve the texture and stability of tomato pulps. In fact, HPH resulted in the formation and strengthening of a polysaccharide (pectin) network, and in the decrease of particle size due to matrix disruption. Unfortunately, HPH results also in a decrease in the relative bioaccessibility of all the carotenoids. Such decrease was attributed to the presence of the fibre network, which can trap carotenoids thus hindering their release from the food matrix and incorporation into micelles. Nevertheless, the differences among the carotenoid species and tomato varieties suggest that considering the structure enabling effect of HPH solely is not sufficient to predict the consequences of the process on carotenoid bioaccessibility. A particular matrix can contain different carotenoid species, which can have considerably different bioaccessibility. This was e.g. the case for the red tomatoes. On the other hand, different tomato varieties can have very different structural characteristics. Therefore the characterisation of other factors, such as the activity of endogenous enzymes, as well as the composition of the cell wall and membranes, would deliver useful additional insights into the effects of HPH on carotenoid bioaccessibility. The design of a process aimed to improve both the structural and nutritional properties of plant-based foods should therefore take into account the complex interplay of these factors.

## *Conclusions part II*

Results obtained in the second part of this PhD thesis show that HPH processing can be regarded as a promising technological strategy for improving the functional properties of both proteins and polysaccharides. In the case of globular proteins (egg white), HPH-induced modifications included the destruction of the original protein-protein interactions, protein unfolding, and formation of novel intramolecular interactions between unfolded proteins that resulted in the formation of a weak and unstable network. With regard to fibrous polysaccharides (cell wall polysaccharides in tomato), HPH promoted the interactions between fibres resulting in the formation of a network.

Despite different mechanisms are involved in the formation of protein and polysaccharides network, it is noteworthy that HPH induced structure modification of both proteins and polysaccharides by favouring the interactions between biomolecules functional groups. In particular, the disarrangement and rearrangement of proteins in a novel architecture is driven by the occurrence of hydrophobic interaction between proteins. By contrast, the formation of the pectin network upon shear stresses was suggested to be due to the formation of hydrogen bonds.

The observed protein and polysaccharide structure modifications accounted for different function modifications. With regard to egg white proteins, structure modification did not impair the technological functionalities, but turned out to be sufficient to hide protein epitopes, leading to a slight decrease in egg white immunoreactivity. In the case of tomato pulps, if on the one hand the formation of structure in the food matrix could improve texture, stability and sensory attributes, on the other hand this structure could impair the bioavailability of micronutrients, such as carotenoids.

Based on the results acquired HPH could be exploited to steer the rheological properties of foods, by modulating the strength of protein and polysaccharide networks. In addition, the exploitation of HPH to engineer the natural structuring effect of food components, such as globular proteins and plant fibres, offers the interesting possibility to obtain food products with improved textural quality without the addition of texturizing agents, thus meeting consumers' demand for fresh-like, healthier, and natural food products.

## Final remarks

Driven by new consumers' needs, over the last years, food processing shifted from the prior emphasis in process and unit operations to the design of products meeting specific requirements in terms of nutritional, biological and functional properties (tailor made foods). As food structure and functions are closely interlinked, structural changes of food constituents can lead to new product characteristics or improved functionalities. The development of unconventional technologies addresses these new consumer needs and represent an interesting tool to modify the structure of food biomolecules and thus their functions.

Results obtained during this PhD research project show that unconventional technologies, such as light and HPH processing represent promising technological strategies to fulfil the new consumers' needs towards safe, fresh-like, healthier food products. UV-C and PL or HPH processes can be exploited as driving forces to modify the structure of food biomolecules and their technological and nutritional functions. In this context, UV processing can be regarded as an interesting tool to modify protein structure and functionalities. Similarly, HPH resulted to be effective in modifying both protein- and polysaccharide-containing food matrices.

The choice of the type of processing is driven by the nature of the biomolecule and the expected effect on its structure and functions. For instance, intense protein structure modifications, up to the cleavage of protein backbone, can be only achieved by exploiting high energetic levels of electromagnetic radiation. In this case, the electromagnetic energy captured by the absorbing site is converted to a chemical signal due to photoisomerisation. The latter allows the chemical signal to be easily transferred to the functional part of the protein that controls its overall properties. By contrast, turbulence, cavitation and impacts induced by HPH generally increase hydrophobicity at the protein surface. The latter are hardly associated to significant changes of proteins secondary structure, but modify the interactions among particles, leading to a novel structural arrangement of the protein network. As a consequence, only the functions, which directly depend on the modification of protein network and availability of functional groups, will be affected by HPH.

By contrast, HPH can be efficiently exploited to modify biomolecules that do not include absorbing sites, such as polysaccharides. The latter can not react upon light exposure, unless they might be activated by a photosensitizer which serves as a trigger of photoreactivity.

Results acquired show that the functions of proteins and polysaccharides can be steered by choosing the proper process with adequate processing conditions. To this regard, the results of this thesis suggest that the designing of the process should be carefully evaluated on a case by case basis, since undesired effects (i.e. increase in immunoreactivity of proteins or decrease in micronutrients bioaccessibility) may also occur under specific technological conditions. For this reason, understanding the mechanism that control the effect of the process on food structure and functions is crucial for engineering food biomolecule and obtaining foods with the desired characteristics.

# References


Aguilera, J. M. (2005). Why food microstructure? *Journal of Food Engineering*, *67*, 3–11.

Aguilera, J. M. (2006). Seligman lecture 2005 food product engineering: building the right structures. *Journal of the Science of Food and Agriculture*, *86*, 1147–1155.

Aguilera, J. M., & Lillford, P. J. (2008). Structure-Property Relationships in Foods. In J. M. Aguilera & P. J. Lillford (Eds.), *Food Material Science Principles and Practice* (pp. 229–253). New York, NY: Springer New York.

Almeida, M., & Nogueira, J. (1995). The control of polyphenol oxidase activity in fruits and vegetables. *Plant Foods for Human Nutrition*, *47*, 245–256.

Anese, M., Mirolo, G., Beraldo, P., & Lippe, G. (2013). Effect of ultrasound treatments of tomato pulp on microstructure and lycopene in vitro bioaccessibility. *Food chemistry*, *136*, 458–63.

Anugu, A. K., Yang, W., Shriver, S., Chung, S.-Y., & Percival, S. S. (2010). Efficacy of pulsed ultraviolet light in reducing the allergenicity of isolated egg proteins. In *IFT, Chicago, IL, July 2010*. Chicago (IL).

Augusto, P. E. D., Ibarz, A., & Cristianini, M. (2013). Effect of high pressure homogenization (HPH) on the rheological properties of tomato juice: Viscoelastic properties and the Cox–Merz rule. *Journal of Food Engineering*, *114*, 57–63.

Awadé, A. C., & Efstathiou, T. (1999). Comparison of three liquid chromatographic methods for egg-white protein analysis. *Journal of Chromatography B: Biomedical Sciences and Applications*, *723*, 69–74.

Bayod, E., Månsson, P., Innings, F., Bergenståhl, B., & Tornberg, E. (2007). Low Shear Rheology of Concentrated Tomato Products. Effect of Particle Size and Time. *Food Biophysics*, *2*, 146–157.

Belitz, H., Kieffer, R., Seilmeier, W., & Wieser, H. (1986). Structure and function of gluten proteins. *Cereal Chemistry*, *63*, 336–341.

Beresovsky, N., Kopelman, I. J., & Mizrahi, S. (1995). The role of pulp interparticle interaction in determining tomato juice viscosity. *Journal of Food Processing and Preservation*, *19*, 133–146.

Beveridge, T., Toma, S. J., & Nakai, S. (1974). Determination of SH- and SS-groups in some food protein using Ellman's reagent. *Journal of Food Science*, *39*, 49–51.

Bhat, R., & Karim, A. A. (2009). Ultraviolet irradiation improves gel strength of fish gelatin. *Food Chemistry*, *113*, 1160–1164.

Bintsis, T., Litopoulou-Tzanetaki, E., & Robinson, R. K. (2000). Existing and potential applications of ultraviolet light in the food industry – A critical review. *Journal of the Science of Food and Agriculture*, *80*, 637–645.

Bolton, J. R., & Linden, K. G. (2003). Standardization of Methods for Fluence (UV Dose) Determination in Bench-Scale UV Experiments. *Journal of Environmental Engineering*, *129*, 209–215.

Borel, P. (2003). Factors affecting intestinal absorption of highly lipophilic food microconstituents (fat-soluble vitamins, carotenoids and phytosterols). *Clinical chemistry and laboratory medicine : CCLM / FESCC*, *41*, 979–94.

Bouaouina, H., Desrumaux, A., Loisel, C., & Legrand, J. (2006). Functional properties of whey proteins as affected by dynamic high-pressure treatment. *International Dairy Journal*, *16*, 275–284.

Calligaris, S., Foschia, M., Bartolomeoli, I., Maifreni, M., & Manzocco, L. (2012a). LWT - Food Science and Technology Study on the applicability of high-pressure homogenization for the production of banana juices. *LWT - Food Science and Technology*, *45*, 117–121.

Calligaris, S., Foschia, M., Bartolomeoli, I., Maifreni, M., & Manzocco, L. (2012b). Study on the applicability of high-pressure homogenization for the production of banana juices. *LWT - Food Science and Technology*, *45*, 117–121.

Caminiti, I. M., Noci, F., Muñoz, A., Whyte, P., Morgan, D. J., Cronin, D. a., & Lyng, J. G. (2011). Impact of selected combinations of non-thermal processing technologies on the quality of an apple and cranberry juice blend. *Food Chemistry*, *124*, 1387–1392.

Castenmiller, J. J., & West, C. E. (1998). Bioavailability and bioconversion of carotenoids. *Annual review of nutrition*, *18*, 19–38.

Chanvrier, H., Uthayakumaran, S., & Lillford, P. (2007). Rheological properties of wheat flour processed at low levels of hydration: Influence of starch and gluten. *Journal of Cereal Science*, *45*, 263–274.

Charles, F., Vidal, V., Olive, F., Filgueiras, H., & Sallanon, H. (2013). Pulsed light treatment as new method to maintain physical and nutritional quality of fresh-cut mangoes. *Innovative Food Science & Emerging Technologies*, *18*, 190–195.

Chen, L., & Phillips, R. (2005). Effects of twin-screw extrusion of peanut flour on in vitro digestion of potentially allergenic peanut proteins. *International Journal of Food Protection*, *68*, 1712–1719.

Choi, M.-S., Cheigh, C.-I., Jeong, E.-A., Shin, J.-K., & Chung, M.-S. (2010a). Nonthermal sterilization of Listeria monocytogenes in infant foods by intense pulsed-light treatment. *Journal of Food Engineering*, *97*, 504–509.

Choi, M.-S., Cheigh, C.-I., Jeong, E.-A., Shin, J.-K., & Chung, M.-S. (2010b). Nonthermal sterilization of Listeria monocytogenes in infant foods by intense pulsed-light treatment. *Journal of Food Engineering*, *97*, 504–509.

Christiaens, S., Mbong, V. B., Van Buggenhout, S., David, C. C., Hofkens, J., Van Loey, A. M., & Hendrickx, M. E. (2012). Influence of processing on the pectin structure–function relationship in broccoli purée. *Innovative Food Science & Emerging Technologies*, *15*, 57–65.

Chung, S.-Y., Yang, W., & Krishnamurthy, K. (2008). Effects of pulsed UV-light on peanut allergens in extracts and liquid peanut butter. *Journal of Food Science*, *73*, C400–4.

Colle, I., Van Buggenhout, S., Van Loey, A., & Hendrickx, M. (2010). High pressure homogenization followed by thermal processing of tomato pulp: Influence on microstructure and lycopene in vitro bioaccessibility. *Food Research International*, *43*, 2193–2200.

Cortés-Muñoz, M., Chevalier-Lucia, D., & Dumay, E. (2009). Characteristics of submicron emulsions prepared by ultra-high pressure homogenisation: Effect of chilled or frozen storage. *Food Hydrocolloids*, *23*, 640–654.

Cruz, N., Capellas, M., Hernández, M., Trujillo, A. J., Guamis, B., & Ferragut, V. (2007). Ultra high pressure homogenization of soymilk: Microbiological, physicochemical and microstructural characteristics. *Food Research International*, *40*, 725–732.

Davies, M. J. (2003). Singlet oxygen-mediated damage to proteins and its consequences. *Biochemical and Biophysical Research Communications*, *305*, 761–770.

Davies, M. J., & Truscott, R. J. (2001). Photo-oxidation of proteins and its role in cataractogenesis. *Journal of photochemistry and photobiology. B, Biology*, *63*, 114–25.

Day, L., Augustin, M. A., Batey, I. L., & Wrigley, C. W. (2006). Wheat-gluten uses and industry needs. *Trends in Food Science & Technology*, *17*, 82–90.

De Souza, P. M., & Fernández, A. (2011). Effects of UV-C on physicochemical quality attributes and Salmonella enteritidis inactivation in liquid egg products. *Food Control*, *22*, 1385–1392.

De Vuyst, L., Gaenzle, M., Goesaert, H., Brijs, K., Veraverbeke, W. S., Courtin, C. M., … Delcour, J. A. (2005). Wheat flour constituents: how they impact bread quality, and how to impact their functionality. *Trends in Food Science & Technology*, *16*, 12–30.

Delincée, H. R. (1983). Recent advances in radiation chemistry of proteins. In P. S. Elias & A. J. Cohen (Eds.), *Recent advances in food irradiation* (pp. 129–147). Amsterdam: The Netherlands: Elsevier Biomedical.

Delville, J., Joly, C., Dole, P., & Bliard, C. (2003). Influence of photocrosslinking on the retrogradation of wheat starch based films. *Carbohydrate Polymers*, *53*, 373–381.

Diels, A. M. J., Callewaert, L., Wuytack, E. Y., Masschalck, B., & Michiels, C. W. (2005). Inactivation of Escherichia coli by high-pressure homogenisation is influenced by fluid viscosity but not by water activity and product composition. *International Journal of Food Microbiology*, *101*, 281–291.

Diels, A. M. J., De Taeye, J., & Michiels, C. W. (2005). Sensitisation of Escherichia coli to antibacterial peptides and enzymes by high-pressure homogenisation. *International Journal of Food Microbiology*, *105*, 165–175.

Diels, A. M. J., & Michiels, C. W. (2006). High-pressure homogenization as a non-thermal technique for the inactivation of microorganisms. *Critical Reviews in Microbiology*, *32*, 201–16.

Dogan, N., McCarthy, M., & Powell, R. (2005). Application of an in-line rheological characterization method to chemically modified and native corn starch. *Journal of Texture Studies*, *36*, 237–254.

Donsì, F., Annunziata, M., & Ferrari, G. (2013). Microbial inactivation by high pressure homogenization: Effect of the disruption valve geometry. *Journal of Food Engineering*, *115*, 362–370.

Donsì, F., Ferrari, G., Lenza, E., & Maresca, P. (2009). Main factors regulating microbial inactivation by high-pressure homogenization: Operating parameters and scale of operation. *Chemical Engineering Science*, *64*, 520–532.

Dumay, E., Chevalier-Lucia, D., Picart-Palmade, L., Benzaria, A., Gràcia-Julià, A., & Blayo, C. (2013). Technological aspects and potential applications of (ultra) high-pressure homogenisation. *Trends in Food Science & Technology*, *31*, 13–26.

Dunn, J. E., Clark, R. W., & Asmus, J. F. (1989). Methods for preservation of foodstuffs. *US Patent 4871559*.

Ellis, R. J., & Minton, A. P. (2006). Protein aggregation in crowded environments. *Biological Chemistry*, *387*, 485–97.

Ellman, G. L. (1959). Tissue sulfhydryl groups. *Archives of Biochemistry and Biophysics*, *82*, 70–77.

Elmnasser, N, Guillou, S., Leroi, F., Orange, N., Bakhrouf, A., & Federighi, M. (2007). Pulsed-light system as a novel food decontamination technology: a review. *Canadian Journal of Microbiology*, *53*, 813–21.

Elmnasser, N., Dalgalarrondo, M., Orange, N., Bakhrouf, A., Haertlé, T., Federighi, M., & Chobert, J-M. (2008). Effect of pulsed-light treatment on milk proteins and lipids. *Journal of agricultural and food chemistry*, *56*, 1984–91.

Falguera, V., Pagán, J., Garza, S., Garvín, A., & Ibarz, A. (2011). Ultraviolet processing of liquid food: A review. Part 1: Fundamental engineering aspects. *Food Research International*, *44*, 1571–1579.

Fernández, E., Artiguez, M. L., Martínez de Marañón, I., Villate, M., Blanco, F. J., & Arboleya, J.-C. (2012). Effect of pulsed-light processing on the surface and foaming properties of β-lactoglobulin. *Food Hydrocolloids*, *27*, 154–160.

Ferry, J. D. (1948). Protein Gels. *Advances in Protein Chemistry*, *4*, 1–78.

Fine, F., & Gervais, P. (2004). Efficiency of pulsed UV light for microbial decontamination of food powders. *Journal of food protection*, *67*, 787–92.

Fischer, P., & Windhab, E. J. (2011). Rheology of food materials. *Current Opinion in Colloid & Interface Science*, *16*, 36–40.

Floury, J., Desrumaux, A., & Legrand, D. (2002). Effect of Ultra-high-pressure Homogenization on Structure and on Rheological Properties of Soy Protein-stabilized Emulsions. *Journal of food science*, *67*, 3388–3395.

Floury, J., Bellettre, J., Legrand, J., & Desrumaux, A. (2004). Analysis of a new type of high pressure homogeniser. A study of the flow pattern. *Chemical Engineering Science*, *59*, 843–853.

Floury, J., Legrand, J., & Desrumaux, A. (2004). Analysis of a new type of high pressure homogeniser. Part B. study of droplet break-up and recoalescence phenomena. *Chemical Engineering Science*, *59*, 1285–1294.

Geveke, D. J. (2008). UV Inactivation of E. coli in Liquid Egg White. *Food and Bioprocess Technology*, *1*, 201–206.

Geveke, D. J., & Torres, D. (2013). Liquid egg white pasteurization using a centrifugal UV irradiator. *International Journal of Food Microbiology*, *162*, 43–47.

Gianibelli, M. C., Larroque, O. R., MacRitchie, F., & Wrigley, C. W. (2001). Biochemical, Genetic, and Molecular Characterization of Wheat Glutenin and Its Component Subunits. *Cereal Chemistry*, *78*, 635–646.

Gogate, P. R., & Pandit, A. B. (2008). Application of Cavitational reactors for cell disruption for recovery of intracellular enzymes. *Journal of Chemical Technology and Biotechnology*, *83*, 1083–1093.

Grácia-Juliá, A., René, M., & Cortés-Muñoz, M. (2008). Effect of dynamic high pressure on whey protein aggregation : A comparison with the effect of continuous short-time thermal treatments. *Food hydrocolloids*, *22*, 1014–1032.

Gruber, P., Vieths, S., Wangorsch, A., Nerkamp, J., & Hofmann, T. (2004). Maillard reaction and enzymatic browning affect the allergenicity of Pru av 1, the major

allergen from cherry (Prunus avium). *Journal of Agricultural and Food Chemistry*, *52*, 4002–4007.

Guérin-Dubiard, C., Pasco, M., Mollé, D., Désert, C., Croguennec, T., & Nau, F. (2006). Proteomic analysis of hen egg white. *Journal of Agricultural and Food Chemistry*, *54*, 3901–10.

Guerrero-Beltrán, J. A., & Barbosa-Cánovas, G. V. (2006). Inactivation of Saccharomyces cerevisiae and Polyphenoloxidase in Mango Nectar Treated with UV Light. *Journal of Food Protection*, *69*, 362–368.

Guerrieri, N., Alberti, E., Lavelli, V., & Cerletti, P. (1996). Use of spectroscopic and fluorescence techniques to assess heat-induced molecular modifications of gluten. *Cereal chemistry*, *73*, 368–374.

Gupta, R. B., Khan, K., & Macritchie, F. (1993). Biochemical Basis of Flour Properties in Bread Wheats. I. Effects of Variation in the Quantity and Size Distribution of Polymeric Protein. *Journal of Cereal Science*, *18*, 23–41.

Hedrén, E., Diaz, V., & Svanberg, U. (2002). Estimation of carotenoid accessibility from carrots determined by an in vitro digestion method. *European Journal of Clinical Nutrition*, *56*, 425–30.

Heldman, D. R., Lund, D. B., & Husain, a. (2008). Cross-process Issues Impacting Innovative Food Processing Technologies. *Food Science and Technology International*, *14*, 411–412.

Hermansson, A. (2002). Structure engineering in Foods. *Annual Transactions of the Nordic Rheology Society, 10,* 19-24.

Hierro, E., Barroso, E., la Hoz, L. de, Ordóñez, J. A., Manzano, S., & Fernández, M. (2011). Efficacy of pulsed light for shelf-life extension and inactivation of Listeria monocytogenes on ready-to-eat cooked meat products. *Innovative Food Science & Emerging Technologies*, *12*, 275–281.

Hierro, E., Manzano, S., Ordóñez, J. A., de la Hoz, L., & Fernández, M. (2009). Inactivation of Salmonella enterica serovar Enteritidis on shell eggs by pulsed light technology. *International Journal of Food Microbiology*, *135*, 125–130.

Hoffman, D. (1983). Immunochemical identification of the allergens in egg white. *Journal of Allergy and Clinical Immunology*, *71*, 481–486.

Jeffery, J., Holzenburg, A., & King, S. (2012). Physical barriers to carotenoid bioaccessibility. Ultrastructure survey of chromoplast and cell wall morphology in nine carotenoid-containing fruits and vegetables. *Journal of the Science of Food and Agriculture*, *92*, 2594–602.

Jolley, R. L., Nelson, R. M., & Robb, D. A. (1969). The Multiple Forms of Mushroom Tyrosinase. *Journal of Biological Chemistry*, *244*, 3251–3257.

Kahn, V. (1985). Effect of Proteins, Protein Hydrolyzates and Amino Acids on o-Dihydroxyphenolase Activity of Polyphenol Oxidase of Mushroom, Avocado, and Banana. *Journal of Food Science*, *50*, 111–115.

Kjøniksen, A.-L., Hiorth, M., & Nyström, B. (2005). Association under shear flow in aqueous solutions of pectin. *European Polymer Journal*, *41*, 761–770.

Kleinig, A. R., & Middelberg, A. P. J. (1998). On the mechanism of microbial cell disruption in high-pressure homogenisation. *Chemical Engineering Science*, *53*, 891–898.

Knockaert, G., Lemmens, L., Van Buggenhout, S., Hendrickx, M., & Van Loey, A. (2012). Changes in β-carotene bioaccessibility and concentration during processing of carrot puree. *Food Chemistry*, *133*, 60–67.

Knorr, D., Froehling, a, Jaeger, H., Reineke, K., Schlueter, O., & Schoessler, K. (2011). Emerging technologies in food processing. *Annual Review of Food Science and Technology*, *2*, 203–35.

Koutchma, T. (2009). Advances in Ultraviolet Light Technology for Non-thermal Processing of Liquid Foods. *Food and Bioprocess Technology*, *2*, 138–155.

Koutchma, T., Keller, S., Chirtel, S., & Parisi, B. (2004). Ultraviolet disinfection of juice products in laminar and turbulent flow reactors. *Innovative Food Science & Emerging Technologies*, *5*, 179–189.

Krishnamurthy, K., Demirci, A., & Irudayaraj, J. (2004). Inactivation of Staphylococcus aureus by pulsed UV-light sterilization. *Journal of Food Protection*, *67*, 1027–1030.

Krishnamurthy, K., Tewari, J. C., Irudayaraj, J., & Demirci, A. (2008). Microscopic and Spectroscopic Evaluation of Inactivation of Staphylococcus aureus by Pulsed UV Light and Infrared Heating. *Food and Bioprocess Technology*, *3*, 93–104.

Kuan, Y.-H., Bhat, R., & Karim, A. a. (2011). Emulsifying and foaming properties of ultraviolet-irradiated egg white protein and sodium caseinate. *Journal of Agricultural and Food Chemistry*, *59*, 4111–8.

Laemmli, U. K. (1970). Cleavage of Structural Proteins during the Assembly of the Head of Bacteriophage T4. *Nature*, *227*, 680–685.

Langeland, T. (1982). A Clinical and Immunological Study of Allergy to Hen's Egg White. *Allergy*, *37*, 323–333.

Lapasin, R., & Pricl, S. (1995). *Rheology of Industrial Polysaccharides: Theory and Applications* (Vol. 4, p. 620). Glasgow: Blakie Academic & Professional.

Li, J.-Y., & Yeh, A.-I. (2001). Relationships between thermal, rheological characteristics and swelling power for various starches. *Journal of Food Engineering*, *50*, 141–148.

Lopez-Sanchez, P., Nijsse, J., Blonk, H. C. G., Bialek, L., Schumm, S., & Langton, M. (2011). Effect of mechanical and thermal treatments on the microstructure and rheological properties of carrot, broccoli and tomato dispersions. *Journal of the Science of Food and Agriculture*, *91*, 207–17.

Lopez-Sanchez, P., Svelander, C., Bialek, L., Schumm, S., & Langton, M. (2011). Rheology and microstructure of carrot and tomato emulsions as a result of high-pressure homogenization conditions. *Journal of Food Science*, *76*, E130–40.

Lutz, E., Wieser, H., & Koehler, P. (2012). Identification of disulfide bonds in wheat gluten proteins by means of mass spectrometry/electron transfer dissociation. *Journal of Agricultural and Food Chemistry*, *60*, 3708–16.

Mackinney, G., & Jenkins, J. (1949). Inheritance of carotenoid differences in *Lycopersicon esculentum* strains. *Genetics*, *35*, 284-291.

Manzocco, L., Dri, A., & Quarta, B. (2009). Inactivation of pectic lyases by light exposure in model systems and fresh-cut apple. *Innovative Food Science & Emerging Technologies*, *10*, 500–505.

Manzocco, L., & Nicoli, M. C. (2012). Macromolecular crowding affects protein photosensitivity: The case of egg white immunoreactivity. *Food Chemistry*, *132*, 982–988.

Manzocco, L., Quarta, B., & Dri, A. (2009). Polyphenoloxidase inactivation by light exposure in model systems and apple derivatives. *Innovative Food Science & Emerging Technologies*, *10*, 506–511.

Marco-Molés, R., & Hernando, I. (2009). Main Chemical Changes in Proteins and Structure of Egg treated with High Pressure Homogenisation. *Czech Journal of Food Science*, *27*, 271–273.

Maresca, P., Donsì, F., & Ferrari, G. (2011). Application of a multi-pass high-pressure homogenization treatment for the pasteurization of fruit juices. *Journal of Food Engineering*, *104*, 364–372.

Marquenie, D., Michiels, C. W., Van Impe, J. F., Schrevens, E., & Nicolaï, B. N. (2003). Pulsed white light in combination with UV-C and heat to reduce storage rot of strawberry. *Postharvest Biology and Technology*, *28*, 455–461.

Martinez, M., & Whitaker, J. (1995). The biochemistry and control of enzymatic browning. *Trends in Food Science & Technology*, *6*, 195–200.

McClements, D. J., Decker, E. A., & Park, Y. (2009). Controlling lipid bioavailability through physicochemical and structural approaches. *Critical Reviews in Food Science and Nutrition*, *49*, 48–67.

Middelberg, A. P. J. (1995). Process-scale disruption of microorganisms. *Biotechnology Advances*, *13*, 491–551.

Mine, Y. (1995). Recent advances in the understanding of egg white protein functionality. *Trends in Food Science & Technology*, *6*, 225–232.

Mine, Y., & Yang, M. (2008). Recent advances in the understanding of egg allergens: basic, industrial, and clinical perspectives. *Journal of Agricultural and Food Chemistry*, *56*, 4874–900.

Minton, K. W., Karmin, P., Hahn, G. M., & Minton, A. P. (1982). Nonspecific stabilization of stress-susceptible proteins by stress-resistant proteins: a model for the biological role of heat shock proteins. *Proceedings of the National Academy of Sciences*, *79*, 7107–7111.

Moelants, K. R. N., Lemmens, L., Vandebroeck, M., Van Buggenhout, S., Van Loey, A. M., & Hendrickx, M. E. (2012). Relation between particle size and carotenoid

bioaccessibility in carrot- and tomato-derived suspensions. *Journal of Agricultural and Food Chemistry*, *60*, 11995–2003.

Murray, B. S., Durga, K., Yusoff, A., & Stoyanov, S. D. (2011). Stabilization of foams and emulsions by mixtures of surface active food-grade particles and proteins. *Food Hydrocolloids*, *25*, 627–638.

Norton, I., Moore, S., & Fryer, P. (2007). Understanding food structuring and breakdown: engineering approaches to obesity. *Obesity reviews : an official journal of the International Association for the Study of Obesity*, *8 Suppl 1*, 83–8.

Oms-Oliu, G., Martín-Belloso, O., & Soliva-Fortuny, R. (2010). Pulsed Light Treatments for Food Preservation. A Review. *Food and Bioprocess Technology*, *3*, 13–23.

Palgan, I., Caminiti, I. M., Muñoz, A., Noci, F., Whyte, P., Morgan, D. J., … Lyng, J. G. (2011). Effectiveness of High Intensity Light Pulses (HILP) treatments for the control of Escherichia coli and Listeria innocua in apple juice, orange juice and milk. *Food Microbiology*, *28*, 14–20.

Paquin, P. (1999). Technological properties of high pressure homogenizers: the effect of fat globules, milk proteins, and polysaccharides. *International Dairy Journal*, *9*, 329–335.

Parada, J., & Aguilera, J. M. (2007). Food microstructure affects the bioavailability of several nutrients. *Journal of Food Science*, *72*, R21–32.

Pataro, G., Muñoz, A., Palgan, I., Noci, F., Ferrari, G., & Lyng, J. G. (2011). Bacterial inactivation in fruit juices using a continuous flow Pulsed Light (PL) system. *Food Research International*, *44*, 1642–1648.

Patrignani, F., Vannini, L., Sado Kamdem, S. L., Hernando, I., Marco-Molés, R., Guerzoni, M. E., & Lanciotti, R. (2013). High pressure homogenization vs heat treatment: safety and functional properties of liquid whole egg. *Food Microbiology*, *36*, 63–9.

Pattison, D. I., Rahmanto, A. S., & Davies, M. J. (2012). Photo-oxidation of proteins. *Photochemical & Photobiological Sciences*, *11*, 38–53.

Pedras, M., & Pinho, C. (2012). The effect of high pressure homogenization on microorganisms in milk. *International Food Research Journal*, *19*, 1–5.

Pereda, J., Ferragut, V., Quevedo, J. M., Guamis, B., & Trujillo, A. J. (2007). Effects of Ultra-High Pressure Homogenization on Microbial and Physicochemical Shelf Life of Milk. *Journal of Dairy Science*, *90*, 1081–1093.

Picart, L., Thiebaud, M., René, M., Pierre Guiraud, J., Cheftel, J. C., & Dumay, E. (2006). Effects of high pressure homogenisation of raw bovine milk on alkaline phosphatase and microbial inactivation. A comparison with continuous short-time thermal treatments. *The Journal of Dairy Research*, *73*, 454–463.

Pickering, S. U. (1907). Emulsions. *Journal of the Chemical Society*, *91*, 2001–2021.

Poliseli-Scopel, F. H., Hernández-Herrero, M., Guamis, B., & Ferragut, V. (2012). Comparison of ultra high pressure homogenization and conventional thermal treatments on the microbiological, physical and chemical quality of soymilk. *LWT - Food Science and Technology*, *46*, 42–48.

Raikos, V., Campbell, L., Stephen, R., & Euston, S. R. (2007). Rheology and texture of hen's egg protein heat-set gels as affected by pH and the addition of sugar and/or salt. *Food Hydrocolloids*, *21*, 237–244.

Ramos-Villarroel, A. Y., Martín-Belloso, O., & Soliva-Fortuny, R. (2011). Bacterial inactivation and quality changes in fresh-cut avocado treated with intense light pulses. *European Food Research and Technology*, *233*, 395–402.

Ramos-Villarroel, Ana Y., Aron-Maftei, N., Martín-Belloso, O., & Soliva-Fortuny, R. (2012). The role of pulsed light spectral distribution in the inactivation of Escherichia coli and Listeria innocua on fresh-cut mushrooms. *Food Control*, *24*, 206–213.

Rao, Q., & Labuza, T. P. (2012). Effect of moisture content on selected physicochemical properties of two commercial hen egg white powders. *Food Chemistry*, *132*, 373–384.

Rao, A. V, & Rao, L. G. (2007). Carotenoids and human health. *Pharmacological research*, *55*, 207–216.

Rhim, J. W., Gennadios, A., Fu, D., Weller, C. L., & Hanna, M. a. (1999). Properties of Ultraviolet Irradiated Protein Films. *LWT - Food Science and Technology*, *32*, 129–133.

Rizzi, G. (1994). The Maillard reaction in food. In T. Labuza, G. Reineccius, V. Morrier, J. O'Brien, & W. Bynes (Eds.), *Maillard Reaction in Chemistry Food and Health* (pp. 11–19). Cambridge: The Royal Sciety of Chemistry.

Roos, Y. R. (2003). Thermal analysis, state transitions and food quality. *Journal of Thermal Analysis and Calorimetry*, *71*, 197–203.

Sadler, G., Davis, J., & Dezman, D. (1990). Rapid Extraction of Lycopene and β-Carotene from Reconstituted Tomato Paste and Pink Grapefruit Homogenates. *Journal of Food Science*, *55*, 1460–1461.

Schweiggert, Ralf M, Steingass, C. B., Heller, A., Esquivel, P., & Carle, R. (2011). Characterization of chromoplasts and carotenoids of red- and yellow-fleshed papaya (Carica papaya L.). *Planta*, *234*, 1031–44.

Schweiggert, Ralph M, Mezger, D., Schimpf, F., Steingass, C. B., & Carle, R. (2012). Influence of chromoplast morphology on carotenoid bioaccessibility of carrot, mango, papaya, and tomato. *Food Chemistry*, *135*, 2736–2742.

Schweiggert, Ralph M, Steingass, C. B., Mora, E., Esquivel, P., & Carle, R. (2011). Carotenogenesis and physico-chemical characteristics during maturation of red fleshed papaya fruit (Carica papaya L.). *Food Research International*, *44*, 1373–1380.

Sheldon, S. A., Jones, A. D., & Shibamoto, T. (1988). Photochemical products of a cysteine/D-glucose browning model system. *Journal of Agricultural and Food Chemistry*, *36*, 604–606.

Shen, H.-R., Spikes, J. D., Smith, C. J., & Kopeček, J. (2000). Photodynamic cross-linking of proteins. *Journal of Photochemistry and Photobiology A: Chemistry*, *130*, 1–6.

Shewry, P.R., & Tatham, A. S. (1997). Disulphide Bonds in Wheat Gluten Proteins. *Journal of Cereal Science*, *25*, 207–227.

Shewry, P. R., Halford, N. G., Belton, P. S., & Tatham, A. S. (2002). The structure and properties of gluten: an elastic protein from wheat grain. *Philosophical transactions of the Royal Society of London. Series B, Biological sciences*, *357*, 133–42.

Shriver, S. K., & Yang, W. W. (2011). Thermal and Nonthermal Methods for Food Allergen Control. *Food Engineering Reviews*, *3*, 26–43.

Sila, D. N., Van Buggenhout, S., Duvetter, T., Fraeye, I., De Roeck, a., Van Loey, a., & Hendrickx, M. (2009). Pectins in Processed Fruits and Vegetables: Part II-Structure-Function Relationships. *Comprehensive Reviews in Food Science and Food Safety*, *8*, 86–104.

Sommers, C. H., Sites, J. E., & Musgrove, M. (2010). Ultraviolet (254 nm) inactivation of pathogens on foods and stainless steel surfaces. *Journal of Food Safety*, *30*, 470–479.

Stathopoulos, C. E., Tsiami, A. a., David Schofield, J., & Dobraszczyk, B. J. (2008). Effect of heat on rheology, surface hydrophobicity and molecular weight distribution of glutens extracted from flours with different bread-making quality. *Journal of Cereal Science*, *47*, 134–143.

Stewart, E. M. (2001). Food irradiation chemistry. In R. A. Molins (Ed.), *Food irradiation: Principles and applications* (pp. 37&76). New York, USA: John Wiley & Sons, Inc.

Suárez-Jacobo, Á., Saldo, J., Rüfer, C. E., Guamis, B., Roig-Sagués, A. X., & Gervilla, R. (2012). Aseptically packaged UHPH-treated apple juice: Safety and quality parameters during storage. *Journal of Food Engineering*, *109*, 291–300.

Subirade, M., Loupil, F., Allain, A.-F., & Paquin, P. (1998). Effect of Dynamic High Pressure on the Secondary Structure of β-Lactoglobulin and on its Conformational Properties as Determined by Fourier Transform Infrared Spectroscopy. *International Dairy Journal*, *8*, 135–140.

Svelander, C. a., Lopez-Sanchez, P., Pudney, P. D. a., Schumm, S., & Alminger, M. a. G. (2011). High Pressure Homogenization Increases the In Vitro Bioaccessibility of α- and β-Carotene in Carrot Emulsions But Not of Lycopene in Tomato Emulsions. *Journal of Food Science*, *76*, H215–H225.

Taheri-Kafrani, A., Gaudin, J.-C., Rabesona, H., Nioi, C., Agarwal, D., Drouet, M., … Haertle, T. (2009). Effects of heating and glycation of beta-lactoglobulin on its recognition by IgE of sera from cow milk allergy patients. *Journal of agricultural and food chemistry*, *57*, 4974–82.

Takeshita, K., Shibato, J., Sameshima, T., Fukunaga, S., Isobe, S., Arihara, K., & Itoh, M. (2003). Damage of yeast cells induced by pulsed light irradiation. *International Journal of Food Microbiology*, *85*, 151–158.

Tester, R., & Morrison, W. (1990). Swelling and gelatinization of cereal starches. I. Effects of amylopectin, amylose, and lipids. *Cereal Chemistry*, *67*, 551–557.

Thiebaud, M., Dumay, E., Picart, L., Guiraud, J. P., & Cheftel, J. C. (2003). High-pressure homogenisation of raw bovine milk. Effects on fat globule size distribution and microbial inactivation. *International Dairy Journal*, *13*, 427–439.

Toepfl, S., Mathys, A., Heinz, V., & Knorr, D. (2006). Review: Potential of High Hydrostatic Pressure and Pulsed Electric Fields for Energy Efficient and Environmentally Friendly Food Processing. *Food Reviews International*, *22*, 405–423.

Tomes, M., Quackenbush, F., Jr, O. N., & North, B. (1953). The inheritance of carotenoid pigment systems in the tomato. *Genetics*, 117–127.

Unluturk, S., Atilgan, M. R., Baysal, a H., & Unluturk, M. S. (2010). Modeling inactivation kinetics of liquid egg white exposed to UV-C irradiation. *International Journal of Food Microbiology*, *142*, 341–7.

Unluturk, S., Atilgan, M. R., Handan Baysal, a., & Tari, C. (2008). Use of UV-C radiation as a non-thermal process for liquid egg products (LEP). *Journal of Food Engineering*, *85*, 561–568.

Van den Berg, B., Ellis, R. J., & Dobson, C. M. (1999). Effects of macromolecular crowding on protein folding and aggregation. *The EMBO Journal*, *18*, 6927–33.

Van den Berg, B., Wain, R., Dobson, C. M., & Ellis, R. J. (2000). Macromolecular crowding perturbs protein refolding kinetics: implications for folding inside the cell. *The EMBO Journal*, *19*, 3870–5.

Van der Zalm, E. E. J., van der Goot, A. J., & Boom, R. M. (2011). Quality of shear fractionated wheat gluten – Comparison to commercial vital wheat gluten. *Journal of Cereal Science*, *53*, 154–159.

Van Eckert, R., Bond, J., Rawson, P., Klein, C. L., Stern, M., & Jordan, T. W. (2010). Reactivity of gluten detecting monoclonal antibodies to a gliadin reference material. *Journal of Cereal Science*, *51*, 198–204.

Van het Hof, K. H., de Boer, B. C. J., Tijburg, L. B. M., Lucius, B. R. H. M., Zijp, I., West, C. E., … Weststrate, J. A. (2000). Carotenoid Bioavailability in Humans from Tomatoes Processed in Different Ways Determined from the Carotenoid Response

in the Triglyceride-Rich Lipoprotein Fraction of Plasma after a Single Consumption and in Plasma after Four Days of Consumption. *The Journal of Nutrition*, *130*, 1189–1196.

Vannini, L., Lanciotti, R., Baldi, D., & Guerzoni, M. E. (2004). Interactions between high pressure homogenization and antimicrobial activity of lysozyme and lactoperoxidase. *International Journal of Food Microbiology*, *94*, 123–35.

Vasquez-Caicedo, A. L., Heller, A., Neidhart, S., & Carle, R. (2006). Chromoplast morphology and beta-carotene accumulation during postharvest ripening of Mango Cv. "Tommy Atkins". *Journal of Agricultural and Food Chemistry*, *54*, 5769–76.

Wang, T., Macgregor, S. J., Anderson, J. G., & Woolsey, G. A. (2005). Pulsed ultra-violet inactivation spectrum of Escherichia coli. *Water research*, *39*, 2921–5.

Wang, X.-S., Tang, C.-H., Li, B.-S., Yang, X.-Q., Li, L., & Ma, C.-Y. (2008). Effects of high-pressure treatment on some physicochemical and functional properties of soy protein isolates. *Food Hydrocolloids*, *22*, 560–567.

Wekhof, A. (2000). Disinfection with flash lamps. *PDA journal of pharmaceutical science and technology / PDA*, *54*, 264–76.

Wieser, H. (2007). Chemistry of gluten proteins. *Food microbiology*, *24*, 115–9.

Wieser, H., Antes, S., & Seilmeier, W. (1998). Quantitative Determination of Gluten Protein Types in Wheat Flour by Reversed-Phase High-Performance Liquid Chromatography. *Cereal Chemistry*, *75*, 644–650.

Wieser, H., & Koehler, P. (2008). The Biochemical Basis of Celiac Disease. *Cereal Chemistry*, *85*, 1–13.

Wondraczek, H., Kotiaho, A., Fardim, P., & Heinze, T. (2011). Photoactive polysaccharides. *Carbohydrate Polymers*, *83*, 1048–1061.

Wright, J. R., Sumner, S. S., Hackney, C. R., Pierson, M. D., & Zoecklein, B. W. (2000). Efficacy of ultraviolet light for reducing Escherichia coli O157:H7 in unpasteurized apple cider. *Journal of Food Protection*, *63*, 563–7.

Wrigley, C. W. (1996). Giant proteins with flour power. *Nature*, *381*, 738–9.

Wu, L.-Z., Sheng, Y.-B., Xie, J.-B., & Wang, W. (2008). Photoexcitation of tryptophan groups induced reduction of disulfide bonds in hen egg white lysozyme. *Journal of Molecular Structure*, *882*, 101–106.

Wuytack, E. Y., Phuong, L. D. T., Aertsen, A., Reyns, K. M. F., Marquenie, D., De Ketelaere, B., … Michiels, C. W. (2003). Comparison of sublethal injury induced in Salmonella enterica serovar Typhimurium by heat and by different nonthermal treatments. *Journal of Food Protection*, *66*, 31–37.

Yang, W. W., Chung, S.-Y., Ajayi, O., Krishnamurthy, K., Konan, K., & Goodrich-Schneider, R. (2010). Use of Pulsed Ultraviolet Light to Reduce the Allergenic Potency of Soybean Extracts. *International Journal of Food Engineering*, *6*, 1-12.

Zhou, J., Ma, Y., Zhang, J., & Tong, J. (2009). Influence of surface photocrosslinking on properties of thermoplastic starch sheets. *Journal of Applied Polymer Science*, *112*, 99–106.

Zhou, J., Zhang, J., Ma, Y., & Tong, J. (2008). Surface photo-crosslinking of corn starch sheets. *Carbohydrate Polymers*, *74*, 405–410.

Ziegler, G. R., Thompson, D. B., & Casasnovas, J. (1993). Dynamic measurements of starch granules swelling during gelatinization. *Cereal Chemistry*, *70*, 247–251.

Zilić, S., Barać, M., Pešić, M., Dodig, D., & Ignjatović-Micić, D. (2011). Characterization of proteins from grain of different bread and durum wheat genotypes. *International Journal of Molecular Sciences*, *12*, 5878–94.

Zobel, H. F. (1988). Starch Crystal Transformations and Their Industrial Importance. *Starch - Stärke*, *40*, 1–7.

**About the Author**

Agnese Panozzo was born on April 23 1983 in Moraro (Italy). After the high school diploma (Maturità Scientifica) in 2002, she started studying Food Science and technology at the University of Udine. She took the Bachelor's and Master's studies, and she graduated from Food Science and Technology at the University of Udine in 2010 with a thesis dealing with the oxidative stability of cod liver oil as affected by its physical state. Thereafter, she worked as a research fellow at the University of Udine in the Department of Food Science. In January 2011, she started her PhD, which ended in the present PhD thesis. Currently she is working as a Marie Curie Fellow at the Katholieke Univeristeit Leuven.

**List of publications relevant to this PhD research activity**

Manzocco, L., Panozzo, A., & Nicoli, M. C. (2012). Effect of ultraviolet processing on selected properties of egg white. *Food chemistry*, *135*, 522–7.

Manzocco, L., Panozzo, A., & Nicoli, M. C. (2013). Effect of pulsed light on selected properties of egg white. *Innovative Food Science & Emerging Technologies*, *18*, 183–189.

Manzocco, L., Panozzo, A., & Nicoli, M. C. (2013b). Inactivation of polyphenoloxidase by pulsed light. *Journal of food science*, *78*, E1183–7.

Panozzo, A., Lemmens, L., Van Loey, A., Manzocco, L., Nicoli, M. C., & Hendrickx, M. (2013). Microstructure and bioaccessibility of different carotenoid species as affected by high pressure homogenisation: A case study on differently coloured tomatoes. *Food chemistry*, *141*, 4094–100.

**Additional publication**

Da Pieve S., Calligaris S., Panozzo A., Arrighetti M., Nicoli M.C. 2011. Effect of monoglyceride organogel structure on cod liver oil stability. *Food Research International*, 44, 2978-2983.

Manzocco L., Panozzo A., Calligaris S. 2011. Accelerated shelf life testing (ASLT) of oils by light and temperature exploitation. *Journal of the American Oil Chemists Society*, 89(4), 577-583.

Anese M., Manzocco L., Panozzo A., Beraldo P., Foschia M., Nicoli M.C. Effect of radiofrequency assisted freezing on meat microstructure and quality. *Food Research International*, 46(1), 50-54.

Manzocco L., Spilimbergo S., Ignat A., Ferrentino G., Panozzo A., Mirolo G., Anese M., Nicoli M.C. 2013. Effect of dense phase-CO2 on polyphenoloxidase in model solutions. *International Journal of Food Science*. Accepted.

**Contributions to national and international conferences**

Calligaris S., Da Pieve S., Panozzo A., Nicoli M.C. Effect of organogel structure on oxidative stability of polyunsaturated fatty acids. Delivery of Functionality in Complex Food Systems, Physically-Inspired Approaches from the Nanoscale to the Microscale, 4th International Symposium, August 21-24 2011, Guelph, Ontario, Canada.

Panozzo A. Biomolecule engineering by unconventional technological strategies. In Proc.s of the 16th Workshop on the Developments in the Italian PhD Research on Food Science Technology and Biotechnology, University of Milano e Piacenza, Lodi, 21-23 September 2011.

Manzocco L., Panozzo A., Nicoli M.C. Light induced structural changes of proteins: effect on egg white immunoreactivity. EFFoST Annual Meeting, Berlin, 9-11 November 2011.

Anese M., Manzocco L., Panozzo A., Beraldo P., Foschia M., Nicoli M.C. Effect of radiofrequency assisted freezing on meat microstructure and quality. EFFoST Annual Meeting, Berlin, 9-11 November 2011.

Panozzo A. Effect of pulsed light on selected food proteins. In Proc.s of the 17th Workshop on the Developments in the Italian PhD Research on Food Science Technology and Biotechnology, Cesena (Italy), 19-21 September, 2012.

Panozzo A. Biomolecule engineering by unconventional technological strategies. In Proc.s of the 18th Workshop on the Developments in the Italian PhD Research on Food Science Technology and Biotechnology, Conegliano (Italy), 25-27 September, 2013.

Manzocco L., Panozzo A., Nicoli M.C. Effect of UV and pulsed light on the immunoreactivity of food proteins. EFFoST Annual Meeting, Bologna, 12-15 November 2013.